2023

Evaluation of SpliceAI for Improved Genetic Variant Classification in Inherited Ophthalmic Disease Genes

Melissa Reeves
Virginia Commonwealth University

Evaluation of SpliceAI for Improved Genetic Variant Classification in Inherited Ophthalmic Disease Genes

A dissertation submitted in partial fulfillment of the requirements for the degree of Doctor of Philosophy at Virginia Commonwealth University.

By Melissa Jean Reeves

Bachelor of Science, Virginia Commonwealth University, May 1999

Master of Science, George Washington University, August 2006

Dissertation Chair: Melissa Jamerson, PhD, MLS(ASCP)

Associate Professor

Department of Medical Laboratory Sciences

Virginia Commonwealth University

Richmond, Virginia

July 12, 2023

Acknowledgment

The author would like to thank the Committee members, Drs. Melissa Jamerson, VCU major director, Robert Hufnagel, NEI/NIH mentor, Teresa Nadder, VCU, and Natario Couser, VCU, for their time and expertise in guiding this project. I am also thankful for the support of Dr. Tyler Corson, VCU. Dr. Corson challenged me as a student, especially in my writing, and she was thoughtful and intentional with her support of students in general, years after her class ended. I would also like to thank Dr. Bin Guan, and other members of the NEI Ophthalmic Genomics Laboratory, Chelsea Bender, Amelia Naik, Nia Moore, and Ranya Al Rawi for their technical expertise and guidance along the way. Thank you to the members of the NEI Medical Genetics and Ophthalmic Genomics Unit for their support and feedback on this project. I am also thankful to Dr. Santa Tumminia and Kerry Goetz for their support throughout my dissertation journey. A big thanks to the PhD Squad for all their support along the way; how wonderful to have others who truly understand your struggle. And finally, I would like to thank my husband, Rich, and children, Zachary, and Rebecca. Thank you for always praying for me. Thank you to my best friend, Nyree Adams, for being my biggest cheerleader. Thank you to my family and friends for their unending support and prayers. I couldn't have done this without you.

"For I know the plans I have for you," says the Lord. "They are plans for good and not for disaster, to give you a future and a hope." Jeremiah 29:11

Table of Contents

LIST OF TABLES

LIST OF FIGURES

ABSTRACT

EVALUATION OF SPLICEAI FOR IMPROVED GENETIC VARIANT CLASSIFICATION
IN INHERITED OPHTHALMIC DISEASE GENES

By Melissa Jean Reeves, Ph.D.

A dissertation submitted in partial fulfillment of the requirements for the degree of Doctor of
Philosophy at Virginia Commonwealth University.

Virginia Commonwealth University, 2023

Major Director: Melissa Jamerson, PhD, MLS(ASCP)

Associate Professor, Department of Medical Laboratory Sciences

Inherited ophthalmic diseases impact individuals around the globe. Inherited retinal
diseases (IRDs) are the leading cause of blindness in individuals aged 15 to 45. The personal,
social, and economic impact of vision loss is profound. Due to individual differences, symptoms
can be variable, and it may be difficult to diagnose some diseases based on phenotype alone.
Clinicians often seek out genetic testing to confirm clinical diagnoses when other avenues have
failed.   Clinical laboratories use all available data, such as frequency, population, or
computational data, to evaluate genetic variants and determine their classification. Clinical
laboratories may not have enough evidence to classify a genetic variant as pathogenic or benign
when testing is performed, so variants may be classified of uncertain significance. Because
inherited retinal diseases are considered rare, there are limited treatments available, and most
treatment is offered through clinical trials. Clinical trials often have stringent inclusion and
exclusion criteria to ensure the most optimum outcome for the study. Due to constraints of a
study, patients often must have definitive genetic results to qualify for a trial. A variant of
uncertain significance would likely disqualify an individual for a clinical trial.

Functional assays, such as the minigene assay, have been used extensively across
multiple genes and diseases with ease. This study aimed to investigate a novel methodology for

the minigene assay and establish the sensitivity of SpliceAI for predicting synonymous splice effects in variants with a SpliceAI change (Δ) score ≥ 0.8 in inherited ophthalmic disease genes.

This study used the "P" or process component of the Structure-Process-Outcome (SPO) Donabedian model to evaluate the addition of the minigene assay to the clinical testing workflow. This study also highlights the importance of using a well-validated framework, such as Donabedian, in conjunction with clinical laboratory quality improvements.

Of the 617 synonymous variants in 20 ophthalmic disease genes targeted in the database, 86 synonymous variants in 14 genes were scored ≥ 0.8. Twenty synonymous variants in two ophthalmic disease genes (*ABCA4* and *CHD7*) were selected for this preliminary study. Twenty wildtype and variant pairs were assessed using the novel minigene test to review splice outcomes. This study established that this novel minigene test could be used in a clinical laboratory as a part of the clinical testing pipeline.

Of the 20 variants targeted, 14 variants could be evaluated by minigene. Six variants did not produce high-quality data and will need to be repeated. Eleven of the 14 variants reviewed showed aberrant splice effects through the minigene assay, matching the SpliceAI prediction. Three variants matched the wildtype transcript and were therefore considered discordant.

Based on these results, the sensitivity of SpliceAI for predicting splice effects in synonymous variants in inherited ophthalmic diseases is approximately 79%, slightly less than the expected 80%. The shift in sensitivity is likely due to the small sample size in this study. A Fisher's exact test was performed to evaluate the concordance rate between minigene outcomes and SpliceAI predictions with a p value of 0.2222, indicating no statistical difference between SpliceAI predictions and minigene outcomes.

The results of this study indicate that SpliceAI has a predictive efficiency in ophthalmic disease genes of 79%, which is well below what would be needed (> 95%) for a clinical laboratory to rely solely for variant classification. Though the predictive efficiency is less than expected, this preliminary study offers insight into the predictive value of SpliceAI for synonymous variants in inherited ophthalmic disease genes. This study also introduces a novel minigene method that other clinical laboratories across other diseases and genes can reliably use.

INDEX WORDS: SpliceAI, splice, variant, ophthalmic disease, inherited retinal disease, Stargardt disease, Leber congenital amaurosis, Cone rod dystrophy, macular dystrophy, CHARGE, Achromatopsia, Aniridia, Congenital stationary night blindness, Coucher-Neuhauser, Oliver-McFarlane, Gordon Holmes, retinitis pigmentosa, Usher syndrome, quality improvement, minigene, CLIA, Donabedian, clinical laboratory

Chapter 1

Introduction

Problem Statement

Inherited retinal diseases (IRDs) encompass various diagnoses, including retinitis pigmentosa, Leber congenital amaurosis, Stargardt disease, and others. (ASGCT, 2020). IRDs have an incidence of 1:2,000 and are the leading cause of blindness in individuals aged 15 to 45 (Rattner, Sun, & Nathans, 1999; Cremers, Boon, Bujakowska, & Zeitz, 2018). IRDs are classified as rare diseases, so treatment options are few (Gong et al., 2021). Because many of these diseases manifest early in life, individuals often face lifelong challenges. It is estimated that IRDs cost over $61 million based on socioeconomic impact in the United States (US) (Gong et al., 2021). Patients affected by IRDs often have comorbidities such as an increased risk of anxiety and depression (Gong et al., 2021; Mayro et al., 2020).

Diagnosing patients based on phenotype (symptoms) alone can be difficult, so genetic testing is often sought to confirm or refute a patient's diagnosis. Due to variable expressivity, sufficient evidence may not be available to clinical laboratories to classify a variant (an alteration in the DNA nucleotide sequence) as either pathogenic (disease-causing) or benign (Richards, et al., 2015; NCI, 2021b). To report genetic results more accurately, additional avenues to gather evidence for variant classification must be explored.

Though most pathogenic variants are missense, where a single nucleotide change causes a change in the protein, synonymous variants can also be pathogenic (Miosge, et al., 2015). Synonymous variants (a variant that does not change the amino acid coded in the protein) have traditionally been considered benign as they have no impact on the amino acid composition of the protein; however, it has been discovered that synonymous changes can impact several

1

mechanisms, including 1) mRNA splicing stability, 2) Splicing regulation, 3) mRNA binding with regulatory elements, and 4) translational kinetics impacting ribosomal functions (Sarkar, et al., 2022; Vihinen, 2022). Though uncertain, it has been postulated that splice variants may account for approximately 9% to 62% of disease-causing variants (Fraile-Bethencourt, 2019; López-Bigas, 2005; Keegan, et al., 2022; Stenson, et al., 2017)

Diagnostic testing does not traditionally include RNA analysis as a part of a testing pipeline, so many splice variants could be missed and account for missing heritability when a single heterozygous variant is found in an autosomal recessive disease (Wai, et al., 2019; Girirajan, 2017). Variants in the splice donor (at 5' exon/intron junction, beginning of intron, denoted by a "GT" sequence) or the splice acceptor (at 3' intron/exon junction, end of intron, denoted by "AG" sequence) region often leads to "exon skipping," either partial or whole, where the next neighboring exon is not incorporated into the mRNA sequence during transcription (Wai, 2019; Baten, 2006). Splice variants can also lead to partial exon loss, inclusion of a cryptic or pseudoexon, or inclusion of an intron fragment (Abramowicz & Gos, 2018). Splice variants most commonly affect +1 and +2 residues at the 5' donor site and -1 and -2 residues at the 3' acceptor site (Abramowicz & Gos, 2018). Though it was assumed that larger genes with larger introns would have a higher likelihood of splicing defects, a significant number of variants in smaller genes also cause aberrant splicing (Abramowicz & Gos, 2018; Chen & Manley, 2009)

Predictive software packages are routinely used to predict the effects of a variant on the resulting protein; however, the majority of these programs were initially designed for new gene discovery and were not designed to predict the consequences of variants (Spurdle, et al., 2008). When predicting splice variants, no single prediction program is expected to operate at 100% efficiency (Wai, et al., 2019; Spurdle, et al., 2008). Thus, most researchers use multiple

predictive packages to compare results and determine variant classifications as outlined by the American College of Medical Genetics and Genomics and the Association of Molecular Pathology (ACMG/AMP) (Spurdle, et al., 2008; Richards et al., 2015). It was recently suggested that the score intervals defined by predictive software developers in conjunction with ACMG/AMP guidelines requiring consensus of multiple predictors lack quantitative support (Pejaver, et al., 2022). Because many methods utilized by predictive software packages overlap and standards for concordance between packages are unavailable, variability between laboratory interpretations has been observed (Pejaver, et al., 2022; Harrison, et al., 2017). Further, Pejaver et al. (2022) discusses that these "*in silico* predictors" cannot classify a variant's pathogenicity individually; however, they can provide a valuable contribution to classification with proper validation and calibration. It was recommended that a single tool be used for evidence of pathogenicity to avoid bias in "cherry-picking" the best-scoring predictive packages for any given variant (Pejaver, et al., 2022).

Functional assays are performed to determine the variant's effect on the resulting protein and are necessary to add weighted evidence for variant classification (Wai, et al., 2019). Minigene is a commonly used approach for assessing splicing effects in a cell-based assay (Wai, et al., 2019). Most pre-mRNA splicing elements were also discovered through minigene (Smith & Lynch, 2014). Minigenes are relatively simple to perform and widely apply to nearly any cell type and splice event (Smith & Lynch, 2014). Briefly, the minigene is designed, sequences are transfected to a cell line, RNA is harvested, and splice effects are analyzed through reverse transcription polymerase chain reaction (RT PCR) (Smith & Lynch, 2014). A study by Deng et al., (2022) mentioned that multiple cell lines, such as HEK293 and HeLa cells, be used to avoid false negative results; however, the study by Rossanti, et al. (2021) saw variations in splice

patterns between HEK293 and HeLa cells even though the same minigene construct was used. Additionally, the study showed concordant results between the HEK293 minigene assay and *in vivo* experiments (Rossanti, et al., 2021). Establishing a test's sensitivity and specificity and understanding assay limitations is essential when using new technology.

Though various function tests, such as the minigene assay, have recently become more widely used in clinical diagnostics, they add cost and time for reagents and clinical laboratory personnel (Singer & Bagnall, 2022). Additionally, validated functional tests are uncommon within a clinical laboratory (Richards, et al., 2015). Splice variant predictive packages, such as SpliceAI, were initially developed due to the challenges related to functional testing (Abramowicz & Gos, 2018).

SpliceAI is a recently developed software package with a 32-layer deep neural network to predict splice variants from pre-mRNA sequences. SpliceAI predicts splice effects for genetic variants in four categories and provides a change (Δ) score from 0 – 1 in each category: (1) donor loss, (2) donor gain, (3) acceptor loss, (4) acceptor gain (Jaganathan et al., 2019). This score is based on the type and location of the mutation that occurs in reference to canonical splice sites (two nucleotides that flank the outer edge of the exon: donor and acceptor regions) and related splicing elements (Lord & Baralle, 2021). SpliceAI uses 10,000 nucleotides of the surrounding sequence for each variant position to predict whether a particular position is a splice donor, splice acceptor, or neither (Jaganathan et al., 2019). SpliceAI then calculates the increased or decreased probability that a position is used as a splice donor or acceptor. A change score ≥ 0.8 is considered a high precision score (Chen et al., 2020). For example, if genomic position 38958362-2 in chromosome 19 (19:38958362-2) has a mutation that changes the nucleotide from C (cytosine) to T (thymine) and is given a donor gain score of 0.91, the probability that position

19:38958362-2 is used as a splice donor increases by 0.91 (SpliceAI, 2023). A reliable predictive software that has been validated against a clinical function test would allow a clinical laboratory to evaluate a genetic variant's risk of pathogenicity without the need for functional testing.

Purpose

When variants cannot be classified as pathogenic or benign, they are deemed "variants of uncertain significance" or VUS. Large gene panels have spurred more VUS reported in a patient's genetic result (Chiang & Trzupek, 2015). The number of VUS reported per gene and patient is highly variable, though the number of VUS detected per patient in retinal disease testing is estimated to be 7% to 45% (Chiang & Trzupek, 2015; Ellingford et al., 2016). Forty-eight percent of variants listed in the ClinVar database, a freely accessible public variant archive, are categorized as VUS (He, et al., 2022; Wai, et al., 2020; Landrum, et al., 2018). Patients with genetic results reported as VUS will most often not qualify to participate in clinical trials, limiting treatment options otherwise unavailable.

Of late, antisense oligonucleotide (ASO) drugs are being developed to treat diseases caused by splice effects. Most notably, Spinraza® (nusinersen) has been marketed to those affected with spinal muscular atrophy (SMA) (Wai, et al., 2019). Spinraza® is a type of ASO that binds to a specific sequence within pre-mRNA transcripts of the SMN2 gene and can restore inclusion of exon 7 (where previously lost) in a mature mRNA compound. EXONDYS 51 (eteplirsen) is another type of ASO that has been marketed for the treatment of Duchenne muscular dystrophy (DMD) (Wai, et al., 2019). Traditional treatments are not widely available for patients affected by retinal degeneration, and most treatment is sought out through a clinical trial (Vázquez-Domínguez, et al., 2019). Clinical trials are often gene or variant-specific, so accurate genetic results are essential to determine if a patient qualifies for trial participation.

Previously, each clinical laboratory developed its standards and methods for variant interpretation. In 2015, the ACMG/AMP developed standards and guidelines for variant interpretation (Richards et al., 2015). Current standards for variant interpretation utilize prediction software packages to predict the variant's impact on the related protein and function. Literature and population database review determine the frequency of each variant within various populations. A quantitative cumulative scoring technique based on Bayes' theorem (prior vs. posterior probability) is used to evaluate and provide a final classification for individual variants (Tavtigian, 2018). Many variants do not have enough quantitative evidence to classify them into one of five categories: (1) Benign, (2) Likely Benign, (3) Variant of Uncertain Significance, (4) Likely Pathogenic, and (5) Pathogenic (Richards, et al., 2015). Functional tests to review protein function have not been routinely used in clinical laboratories due to reproducibility and reliability issues (Richards, et al., 2015). Thus, clinical validation of test methodologies is essential.

A clinically validated function test that provides additional evidence to classify VUS as pathogenic or benign will impact the community by offering knowledge to inform patient care, thereby improving the test's clinical utility (usefulness). Insights into variant functions can also inform further research and clinical trial development. The main objective of this study is to improve variant classification for patients affected with inherited ophthalmic diseases. This study aims to investigate a novel methodology for the minigene assay and the sensitivity of the SpliceAI software to predict splice effects in synonymous variants with a change (Δ) score ≥ 0.8. This study will primarily focus on diseases under the "retinal degenerations" category and associated genes and proteins.

Theoretical Framework

Frameworks help establish assessments of new methodologies and guide the researcher in assessing quality improvement measures quantitatively. The Donabedian model has often been used in healthcare research to evaluate healthcare quality (Ayanian & Markel, 2016; Lighter, 2015). The Structure-Process-Outcomes (S-P-O) framework provides classifications to measure quality; however, the process is often the focus in diagnostic testing. Three main facets are highlighted in the diagnostic testing process assessment: (1) Personnel technical competence, (2) Appropriateness and completeness of results, and (3) Successful result communication (Donabedian, 2005; Meier, Badrick & Sikaris, 2018). In this study, a change to the process (genetic testing with functional test vs. software prediction alone) will impact the outcome (synonymous variant classification).

Research Question

> *RQ1:* What is the sensitivity of SpliceAI to predict synonymous variants with a
>
> SpliceAI Δ score ≥ 0.8 in inherited ophthalmic disease genes?

Hypotheses

> *H1:* There will be no statistically significant difference between predicted
>
> SpliceAI outcomes and the minigene assay as measured by Fisher's exact testing.
>
> *H2:* SpliceAI will have a high sensitivity ($> 80\%$) to predict splice effects from
>
> ophthalmic disease gene synonymous variants scored ≥ 0.8.

Significance

Vision health is an important aspect of an individual's life. When vision is lost, it significantly impacts the individual, their families, and society (NASEM, 2016). Only about 50% of patients with retinal disorders have a known genetic cause of disease, so there is a significant disparity in access to treatment for those with unknown causes (Chiang & Trzupek, 2015). Because most retinal degenerations are progressive, treatment timing is critical to slowing, stopping, or potentially reversing vision loss (Sahel, Marazova, & Audo, 2014).

Improved variant classification could significantly and positively impact stakeholders across the inherited ophthalmic genetics community by providing more accurate test results, clinical trial development opportunities, and increased patient trial enrollment. Though mainly focused on retinal degenerations, it is hoped that this study will provide insight into the accuracy of SpliceAI and could lead to future studies in other genes and proteins and improved clinical function testing in clinical genetics laboratories.

Definition of Terms

Acceptor gain (AG) – A new splice acceptor site is created after a mutation occurs (Spurdle, et al., 2008).

Acceptor loss (AL) – A splice acceptor site is lost after a mutation occurs (Spurdle, et al., 2008).

Autosomal dominant (AD) – A way that a genetic trait or condition can be inherited; a genetic condition occurs when a variant is present on only one allele (copy) of a given gene (NCI, 2023a).

Autosomal recessive (AR) – A way that a genetic trait or condition can be inherited; a genetic condition occurs when a variant is present on both alleles (copies) of a given gene (NCI, 2023b).

Benign – Having no significant effect; harmless (Merriam-Webster, 2021).

Clinical utility – The ability of a screening or diagnostic test to prevent or ameliorate adverse health outcomes through the adoption of efficacious treatments conditioned on the test results (Grosse & Khoury, 2006).

Deoxyribonucleic acid (DNA) – Any of various nucleic acids that are usually the molecular basis of heredity, are constructed of a double helix held together by hydrogen bonds between purine and pyrimidine bases which project inward from two chains containing alternate links of deoxyribose and phosphate (Merriam-Webster, 2021).

Donor gain (DG) – A splice donor site is created after a mutation occurs (Spurdle, et al., 2008).

Donor loss (DL) – A splice donor site is lost after a mutation occurs (Spurdle, et al., 2008).

Exon – The part of the RNA that codes for a protein (NHGRI, 2022a).

Expressivity – The degree to which a trait is expressed in individuals with the same genotype (Miko, 2008).

Gene – A specific sequence of nucleotides in DNA or RNA that is located on a chromosome and is the functional unit of inheritance controlling the transmission and expression of one or more traits by specifying the structure of a particular protein (Merriam-Webster, 2021).

Genome – The genetic material of an organism (Merriam-Webster, 2021).

Genotype – All or part of the genetic constitution of an individual or group (Merriam-Webster, 2021).

HEK293 cells – Kidney cells that are commercially available for purchase and can be cultured in the lab (ATCC, 2023a).

HeLa cells – The first immortalized cell line; epithelial cells that are commercially available for purchase and can be cultured in the lab (ATCC, 2023b).

Intron – A region of a gene that is excised from the final mature mRNA molecule following gene transcription and does not code for amino acids (NHGRI, 2022b).

Leber congenital amaurosis (LCA) – An eye disorder that primarily affects the retina, which is the specialized tissue at the back of the eye that detects light and color (MedlinePlus, 2020a).

Messenger ribonucleic acid (mRNA) – Single-stranded RNA involved in protein synthesis (NHGRI, 2022c).

Mutation – A permanent and heritable change in genetic material which can result in altered protein structure or function and lead to changes in the phenotype (Durland & Ahmadian-Moghadam, 2022)

Mutagenesis – A process by which an organism's DNA changes resulting in a genetic mutation (Durland & Ahmadian-Moghadam, 2022).

OddsPath – Odds of pathogenicity; References a calculated estimate of the magnitude of strength for a given assay in the absence of rigorous statistical analysis (Brnich, 2020).

Pathogenic – Causing or capable of causing disease (Merriam-Webster, 2021).

Phenotype – The physical expression of one or more genes (Merriam-Webster, 2021).

Retinal degeneration – References a progressive, debilitating disease that can lead to blindness; Can be caused by pathogenic variants in genes that are critical to retinal function which lead to photoreceptor cell death and associated vision loss (Duncan, et al., 2018).

Retinitis pigmentosa – Any of several hereditary progressive degenerative diseases of the eye marked by night blindness in the early stages, atrophy, and pigment changes in the retina, constriction of the visual field, and eventual blindness (Merriam-Webster, 2021).

Ribonucleic acid (RNA) – Single-stranded nucleic acid present in all living cells (NHGRI, 2022d).

Sanger sequencing – "Gold standard" technology; A low throughput methodology used to determine a portion of the nucleotide sequence of an individual genome, using polymerase chain reaction (PCR) amplification and sequencing techniques (NCI, 2021).

Stargardt disease – Stargardt macular degeneration; A progressive genetic eye disorder that affects a small area near the center of the retina causing blindness (MedlinePlus, 2020b).

Synonymous variant – A variant that does not change the amino acid coded in the protein (Vihinen, 2022).

Transcription – The process of making mRNA from a gene's DNA sequence (NHGRI, 2022e).

Translation – Information encoded in the mRNA directs the addition of amino acids during protein synthesis (NHGRI, 2022f).

Variant – An alteration in the DNA nucleotide sequence that may be benign, pathogenic, or of unknown significance (NCI, 2021b).

Variant of uncertain significance (VUS) – A variation in a genetic sequence for which the association with disease risk is unclear (NCI, 2021b).

X-linked (XL) – Traits or characteristics that are influenced by genes on the X chromosome (NHGRI, 2023).

Study Organization

The study is outlined in five additional chapters, a bibliography, and appendices. Chapter 2 reviews the literature regarding clinical variant interpretation, SpliceAI, and minigene. Chapter 3 outlines the theoretical framework used in this study. Chapter 4 describes the research design, methodologies, samples, and procedures. The data analysis and results are presented in Chapter 5. Chapter 6 outlines the discussion, conclusions, and future directions. A bibliography and appendices conclude the study.

<center>**Chapter 2**</center>

<center>**Literature Review**</center>

Introduction

Before beginning this project, an extensive literature review on inherited ophthalmic disease, functional study methodologies, and splice analysis software was performed. The literature review search strategy, along with the rationale and background on genes and ophthalmic diseases, *in silico* analyses, synonymous variants, quality improvement, minigene, and new clinical assay development, are presented here.

Search Strategy

The literature search began with a review of protein function technologies and variant interpretation techniques. Keywords included, but were not limited to, *clinical*, *testing*, *protein*, *function*, *genetic*, *variant*, *synonymous*, *classification*, *minigene*, *midigene*, *pseudoexon*, *SpliceAI*, *assay*, *mRNA*, *retinal*, *degeneration*, *inherited*, *validity*, *reliability*, *ACMG*, and *interpretation*. Most searches were performed in PubMed/MEDLINE; however, EBSCOhost and Google Scholar were also utilized. Main sources include peer-reviewed journal articles and books primarily published within the last ten years. Primary research dated back to the 1960s was included for a historical perspective. Hundreds of sources were identified as relevant to the research and were tracked and managed through EndNote software.

Rationale

Ophthalmic Genes and Diseases Background

The following ophthalmic genes were targeted in this study: *ABCA4*, *CDHR1*, *CHD7*, *CNGB1*, *CNGB3*, *EYS*, *PAX6*, *PDE6A*, *PDE6B*, *PDE6C*, *PNPLA6*, *RHO*, *RP1*, and *USH2A*. All

<center>13</center>

of the genes are primarily associated with retinal degenerations, except for *PAX6* and *CHD7,*

which are more systemic and developmentally related. *ABCA4* is located on chromosome 1, is

autosomal recessive (AR), and is associated with Stargardt disease, macular dystrophy, retinitis

pigmentosa, cone-rod dystrophy, and fundus flavimaculatus (RetNet, 2023). Clinical features

range from mild to severe, with disease onset from childhood to mid-60's and is characterized by

a central lesion and surrounding lipofuscin flecks (Sung, et al., 2020). *ABCA4* accounts for 30 –

60% of AR CRD cases in European populations (Ducroq, et al., 2002).

 CDHR1 is located on chromosome 10, AR, associated with cone-rod dystrophy (RetNet,

2023). Cone-rod dystrophy symptoms usually occur in the first or second decade of life. They

are characterized by central vision loss, light sensitivity, and night blindness, followed by more

severe peripheral vision later in life (Sobolewska, et al., 2023). *CDHR1*-related disease tends to

be variable in disease onset and severity (Malechka, et al., 2022).

 CHD7 is located on chromosome 8, is autosomal dominant (AD), and is related to

CHARGE (Coloboma, Heart, Atresia, Retardation, Genitourinary, Ear) syndrome (OMIM,

2023). Symptoms are variable and present at birth, though all diagnosed with CHARGE have

dyspnea (labored breathing) present, with a range of other symptoms, which may include eye

coloboma (key-hole shaped pupil), impaired eye movement, nasal cavity abnormalities, ear

abnormalities, heart malformation, esophagus malformation, hypothalamic-pituitary deficiency,

and intellectual disability (Qin, 2020).

 CNGB1, *EYS*, and *PDE6A* are associated with AR retinitis pigmentosa (RP) (RetNet,

2023). RP is characterized by night blindness, attenuated retinal vessels, pigment spicules, and

loss of peripheral vision (Hull, et al., 2017). *CNGB1* is AR located on chromosome 16

accounting for approximately 4% of AR RP cases (RetNet, 2023). *EYS* is located on

chromosome 6 and is one of the largest human genes (RetNet, 2023). *EYS* variants account for 10 – 20% of AR RP cases in Spain, and 12% in France and are a common cause of RP in China (Gao, et al., 2022). The function of the EYS protein is still unknown, but evidence suggests it may help to maintain photoreceptor cell integrity (Suvannaboon, et al., 2022; Messchaert, et al., 2018). *PDE6A* is on chromosome 5 and accounts for less than 4% of AR RP cases in North America (RetNet, 2023; Kuehlewein, et al., 2020).

CNGB3 is located on chromosome 8 and is associated with AR achromatopsia and cone dystrophy (RetNet, 2023). Achromatopsia symptoms include reduced visual acuity, nystagmus (rapid eye movements), light sensitivity, and total color blindness (Khan, et al., 2007). *CNGB3*-related cone dystrophy is progressive and is characterized by color vision defects, macular atrophy, normal rod cell responses and reduced cone cell responses (Michaelides, et al., 2004). *CNGB3* variants account for half of all AR achromatopsia (Kohl, et al., 2005).

PAX6 is located on chromosome 11 and is considered the "master regulator of the eye" as mutations in *PAX6* can cause a wide range of eye abnormalities (Lima Cunha, et al., 2019, p.1). Aniridia is recessive and is the most common disease associated with the *PAX6* gene. A small or absent iris, nystagmus, foveal hypoplasia, cataracts, glaucoma, and corneal damage characterize Aniridia. Aniridia has a prevalence of 1 in 40,000 to 1 in 100,000 and may show variable expressivity (Lima Cunha, et al., 2019).

PDE6B, located on chromosome 4, is associated with AR RP and AD congenital stationary night blindness (CSNB) (RetNet, 2023). CSNB is non-progressive and is characterized by night blindness and visual acuity loss (Manes, et al., 2014). No photoreceptor cell death is associated with CSNB (Manes, et al., 2014).

PDE6C is associated with recessive cone dystrophy and achromatopsia, on chromosome 10 (RetNet, 2023). *PDE6C* accounts for just over 2% of achromatopsia cases (Black, et al., 2022). These patients present with severe cone dysfunction and typical achromatopsia but do not have foveal hypoplasia (Georgiou, et al., 2019).

PNPLA6, located on chromosome 19, is related to recessive conditions such as Coucher-Neuhauser, Oliver-McFarlane, and Gordon Holmes syndromes (RetNet, 2023). Though retinal degeneration may be a part of *PNPLA6*-related disease, this gene is associated with various systemic abnormalities, including ataxia, hair anomalies, hypogonadism, hypopituitarism, neuropathy, short stature, or impaired cognitive functioning. These symptoms may be present in distinct clusters and help to classify the syndrome present (Synofzik, et al., 2014).

RHO is associated with both autosomal dominant and recessive RP and dominant CSNB, and is located on chromosome 3 (RetNet, 2023). The *RHO* gene accounts for 30 to 40% of AD RP cases, with the P23H *RHO* variant responsible for 10% of AD RP in US Caucasians (RetNet, 2023; Ferrari, et al., 2011).

RP1, located on chromosome 8, is associated with AD and AR RP, accounting for 5 – 10% of AD RP cases (RetNet, 2023; Ferrari, et al., 2011). One study found that *RP1* variants found in the beginning and end portions of the gene (N- and C- terminus) were related to AR RP, while variants found in the middle of the gene (c.1981 – c.2749) were associated with AD RP; however, there were a handful of variants that did not fit this model (Wang, et al., 2021).

USH2A is associated with recessive Usher syndrome and RP and is located on chromosome 1 (RetNet, 2023). *USH2A*-associated Usher syndrome (Type II) is characterized by RP, with or without bilateral sensorineural hearing loss (Koenekoop, et al., 1999). *USH2A* is

responsible for 50 to 80% of Usher syndrome Type II cases and 10 to 15% of AR RP (RetNet, 2023). The C759F mutation is found in 4 to 5% of AR RP cases without hearing loss (RetNet, 2023).

Treatment Options

Thus far, treatment options have been limited for retinal degenerations and especially treatments targeting splice variants. Adeno-associated viruses (AAV) are often used in gene-targeted therapies with some success. In six patients with Choroideremia, AAV-delivered therapy was shown to be effective and safe (Garanto, et al., 2016). AAV therapies are limited due to the gene package size they can carry (less than 5 kb), and even native genes with only three exons (*PRPH2*) are too large for AAV therapy (Riedmayr, et al., 2018; Garanto, et al., 2016). Additionally, AAVs carry the risk of increased toxicity because it is difficult to regulate expression levels.

Antisense oligonucleotide (AON or ASO) therapies have been used recently in clinical trials due to their small size and ease of delivery (Garanto, et al., 2016). Through intravitreal injections, AONs can penetrate and reach photoreceptor cells much more easily than AAVs subretinally (Garanto, et al., 2016). Additionally, while ASOs are typically administered through intravenous, percutaneous, or intrathecal (through the spine) methods, small molecules can be dispensed orally (Yamamura, et al., 2022). Specifically, AONs have been used to target splice variants successfully. In the study by Tomkiewicz et al. (2021), they used AONs to rescue 15 pathogenic variants in *ABCA4*. In one case, an AON eliminated nearly all of an aberrant pseudoexon produced by aberrant splicing; in another, the AON obtained 100% normal transcript (Tomkiewicz, et al., 2021). Though AONs have been successfully administered, they have a limited lifespan as they have limited stability, so using "naked" AONs would require life-

long, repeated injections (Garanto, et al., 2016). New sub-classes of AAVs are in development to allow more effective targeting of the retina and could work in tandem with AONs for improved efficacy (Garanto, et al., 2016; Dalkara, et al., 2013; Kay, et al., 2013).

Other therapies, such as those using helicases, small molecules, and monovalent ions, are being explored to target aberrant post-splicing modifications, such as those associated with abnormal secondary structures (Georgakopoulos-Soares, et al., 2022). The currently FDA-approved drug, Spinraza®, is a type of SMA treatment targeting splicing modulation (Georgakopoulos-Soares, et al., 2022).

Predictive Software

Many *in silico* predictors are freely available that can predict genetic variant outcomes; however, the reliability and accuracy of these predictors are variable. Most predictors available rely on genetic homology information which evaluates protein function across species, and generally, this information aligns with expected outcomes; nevertheless, predictors often do not agree (Katsonis, et al., 2022). The Katsonis et al. (2022) study mentioned that other studies have attempted to assess variant impact prediction methodologies; however, previous studies review a limited set of methods in each study, making it challenging to assess the methods independently. Cubak et al. (2021) evaluated 44 *in silico* tools against functional studies in cancer susceptibility genes. At least six tools focus on predictive outcomes for synonymous variants alone (Katsonis, et al., 2022). SpliceAI is one of 5 tools mentioned in the Katsonis et al. (2022) study, which uses pre-mRNA transcript sequence, though it is the most newly developed tool.

The predictive tool landscape is vast and continually changing. SpliceAI was trained on the GENCODE dataset, with splice predictions that are based on 10,000 nucleotides of sequence

18

which flank each pre-mRNA position to predict whether a position will be a splice donor, splice acceptor, or neither (Jaganathan, et al., 2019; Harrow, et al., 2012). Though no predictor is expected to work with 100% accuracy, SpliceAI can potentially provide valuable predictive insight for the clinical laboratory.

"Not Silent" Synonymous Variants

Synonymous variants (variants that do not change the amino acid but impact gene expression and protein production) have been found to impact several processes in the mRNA pathway related to translation, splicing, regulation, and function.

The study by Rossanti et al. (2021) evaluated suspecting synonymous variants in Alport syndrome and saw concordant results from minigene performed in HEK293 cells and *in vivo* experiments. Another study confirmed by minigene and *in vivo* experiments found a synonymous variant caused exon skipping and may have been related to intrafamilial variability in Neuronal Ceroid Lipofuscinosis (Reith, et al., 2022). The H. Zhang et al. (2022) study performed minigene on 14 synonymous variants to assess splice effects in hemophilia B expression. Another study used minigene to evaluate a homozygous synonymous variant discovered in a Han Chinese infant in the *PLOD1* gene, associated with Kyphoscoliotic Ehlers-Danlos syndrome (Yan, et al., 2022). Furthermore, a study by Cui et al. (2022) used minigene to investigate a novel compound heterozygous variation, which included a missense and synonymous variant in the *COL7A1* gene and was able to confirm the pathogenicity of the synonymous variant for a child with dystrophic epidermolysis bullosa.

Though generally, synonymous variants are expected to have a minimal effect on genes and proteins, some studies have suggested that they may be as pathogenic as nonsynonymous

variants and can account for 1% of disease (Rossanti, et al., 2021). One study showed that 5 –

10% of human genes contain at least one region where synonymous variants could be damaging

(Deng, et al., 2022). Synonymous variants should be evaluated as bad actors in disease

pathology, but they are not consistently assessed in the clinical laboratory.

Quality Improvement

Clinical Laboratory Improvement Amendments, CLIA, is the governmental certifying

body for clinical laboratories in the US. As a part of laboratory certification, laboratories are

expected to maintain a high level of quality for testing in three phases: (1) Pre-analytic (sample

accessioning and processing), (2) Testing (test/assay performed), and (3) Post-analytic (result

interpretation and reporting). To ensure testing is performed at the highest quality, laboratories

monitor testing performance and stay abreast of technological changes in the field (CDC, 2018).

Tests must undergo a validation procedure before patient samples can be tested clinically. To

change a test methodology, laboratories evaluate new technologies as a part of a Quality

Improvement process.

New assay development

Many functional studies have been performed at the research level to understand gene

and protein function (Kanavy, et al., 2019). To meet the stringent requirements of clinical test

validation, test methodologies were evaluated for complexity, cost, repeatability, reliability, and

establishment in the research community. One primary test methodology will be the focus of this

study: minigene assay.

Minigene is an extensively used assay to test splicing effects and is widely applicable

across multiple genes and diseases. Minigene has been used in conjunction with HEK293 cells

and is reliable compared to other common cell lines, such as HeLa cells (Rossanti, et al., 2021).

Minigene experiments and HEK293 cells have been shown to be comparable to *in vivo* patient

RNA experiments (Reith, et al., 2022; Rossanti, et al., 2021). Additionally, the minigene assay

does not require a patient's RNA, which can be difficult to acquire (Giorgi, et al., 2015).

The Giorgi et al. (2015) study used minigene to evaluate intronic variants in the *CFTR*

gene for cystic fibrosis and found the assay was sensitive to detect < 1% of correctly spliced

fragments. Another study used minigene to evaluate splicing from variants in the *DSP* gene

associated with cardiocutaneous syndrome and found that direct testing of a patient's cells did

not show any splice effect; however, minigene testing showed that alternative transcripts were

being produced, indicating that normal transcript (and protein levels) could be reduced in this

disease and related to variable phenotypes (Vermeer, et al., 2022). The Stingl et al. (2022) study

evaluated minigene for variants in the *OPN1LW* and *OPN1MW* genes which are related to

dyschromatopsia and Blue Cone Monochromacy and were able to observe specific haplotypes

related to incomplete splicing. Another study used minigene to review variant splice effects in

the *BTK* gene, which is associated with X-linked agammaglobulinemia (Zhou, et al., 2022). Zhou

et al. (2022) determined that a single base deletion resulted in a 35-base pair skipping in exon 18

of the *BTK* gene. Another study used minigene to detect nonsense-mediated decay triggered by

premature termination codons in SMA (Zhang, M., et al., 2022). The study by Steffensen et al.

(2014), described the importance of establishing sensitivity and specificity through test

validation and tested minigene on *BRCA1* gene variants in breast cancer. This study also found a

discrepancy between predicted variant splice effects versus minigene outcomes, emphasizing

that predictive programs alone are often not sufficient (Steffensen, et al., 2014).

The assay was tested for sensitivity at detection of known pathogenic and benign variants according to recently developed guidelines on variant interpretation established by the Clinical Genome Resource (ClinGen) Sequence Variant Interpretation (SVI) Working Group (Brnich et al., 2019).

The OddsPath, or odds of pathogenicity, is a calculation that estimates the strength for any given functional test:

OddsPath = [P2 x (1-P1)]/[1-P2) x P1]

Where P1 is prior probability based upon modeled data and P2 is the posterior probability or proportion of pathogenic variants in groups with functionally normal or functionally abnormal results.

When the OddsPath is utilized, it provides the most robust functional test evidence so that a variant's functional impact can be described as "functionally normal" or "functionally abnormal" (Brnich et al., 2019).

The additional evidence from function testing allows VUS to be reclassified as pathogenic or benign. Variants that do not meet the ACMG/AMP standards for reclassification will remain of uncertain significance. Splice outcomes from minigene will be compared to splice outcomes as predicted by SpliceAI, and a Fisher's exact test will be performed.

Summary

Having the ability to classify a VUS as pathogenic or benign could directly impact a patient's care. A benign classification would indicate that the VUS was likely not the cause of the patient's disease and, therefore, might prompt the patient's clinician to order additional or expanded genetic testing to continue to seek out the cause. On the other hand, a pathogenic or

likely pathogenic classification could allow a clinician to make directive decisions about a patient's care and determine if they are eligible for clinical trials. Patients can also join patient registries, where their known genetic information is shared with researchers. For a clinical researcher, knowledge of pathogenic variants helps determine which genes and variants should be targeted in clinical trials. Variant classification helps to establish a background for clinical trial development toward providing specific, targeted therapies.

Chapter 3

Theoretical Framework

Background

Quality is the cornerstone of the clinical laboratory and an essential part of patient care. Avedis Donabedian developed the S-P-O model as a framework for healthcare providers to evaluate and measure quality in healthcare (Donabedian, 2005). Quality itself is challenging to define and changes over time, so it is essential to have benchmarks to measure quality (Donabedian, 2005). As such, the Donabedian model has been used multiple times across multiple disciplines; it has shown that it is a quality framework used to evaluate quality improvement programs and establish quality metrics.

Donabedian has been used across multiple disciplines of the healthcare field. Some examples include:

- A study used the Donabedian model to evaluate quality indicators for dispensing drugs in a pediatric hospital (Bermúdez-Camps, et al., 2021).

- In 2019, the Donabedian model was used to operationalize the collaborative competencies of the Interprofessional Education Collaborative (Breitbach, et al., 2019).

- Secondary data analysis was performed using the Donabedian model to evaluate maternal mortality and quality of care in the US (Wong & Kitsantas, 2019).

- Pfaff and Markaki (2017) used the Donabedian model to review and analyze data in a secondary analysis of palliative and end-of-life care.

- In 2014, a study using the Donabedian model evaluated the safety and quality of nurse practitioner service (Gardner, Gardner, & O'Connell, 2014).

These examples are just a handful of studies showing an applied use of the Donabedian model.

In genetics, the Donabedian model was used to systematically evaluate quality assurance metrics in medical and public health genetics services (Chou, Norris, Williamson, Garcia, Baysinger, & Mulvihill, 2009). The Donabedian framework was used to categorize quality metrics in a pediatric cardiac catheterization laboratory (O'Byrne, et al., 2020). Donabedian's S-P-O model was also used in a cross-sectional study design to evaluate the quality of patient care for HIV patients in a referral hospital in Ethiopia (Alemayehu, Bushen, & Muluneh, 2009). Donabedian's framework is appropriate for use in healthcare generally, as well as clinical laboratories.

Application

The S-P-O Donabedian model is ideal for any study evaluating quality metrics in healthcare. In this study, the Donabedian framework will be used to review the "P" or process of quality improvement. Specifically, the process of genetic testing and variant classification will be reviewed against a new method that adds a dimension of functional testing which will be compared to a recently developed predictive software. Functional testing is expected to provide additional evidence to classify genetic variants of uncertain significance, specifically synonymous variants which may be considered benign. This quality improvement is expected to enhance the clinical utility, or usefulness, of the genetic test results for inherited ophthalmic diseases. The workflow will be clinically validated using "gold standard" methodologies, and the study uses the Donabedian model, a well-tested theory. This work will be replicable and can be used as a standard for other genetic diseases.

Historical Relevance

Literature Search

The literature was searched extensively to gather support for this study. Since the Donabedian model has been used across multiple disciplines and industries, many citations establish it as a well-researched, well-supported theoretical model. Genetic variant classification and laboratory techniques being reviewed do not have the same rich history nor the general use of the Donabedian model. Additionally, the genes and related diseases evaluated in this study are considered rare, so the literature available is limited compared to other disease models. Therefore, the literature search to support using the Donabedian model was far more expansive than a typical search, though the literature related to the Donabedian model and genetics was limited.
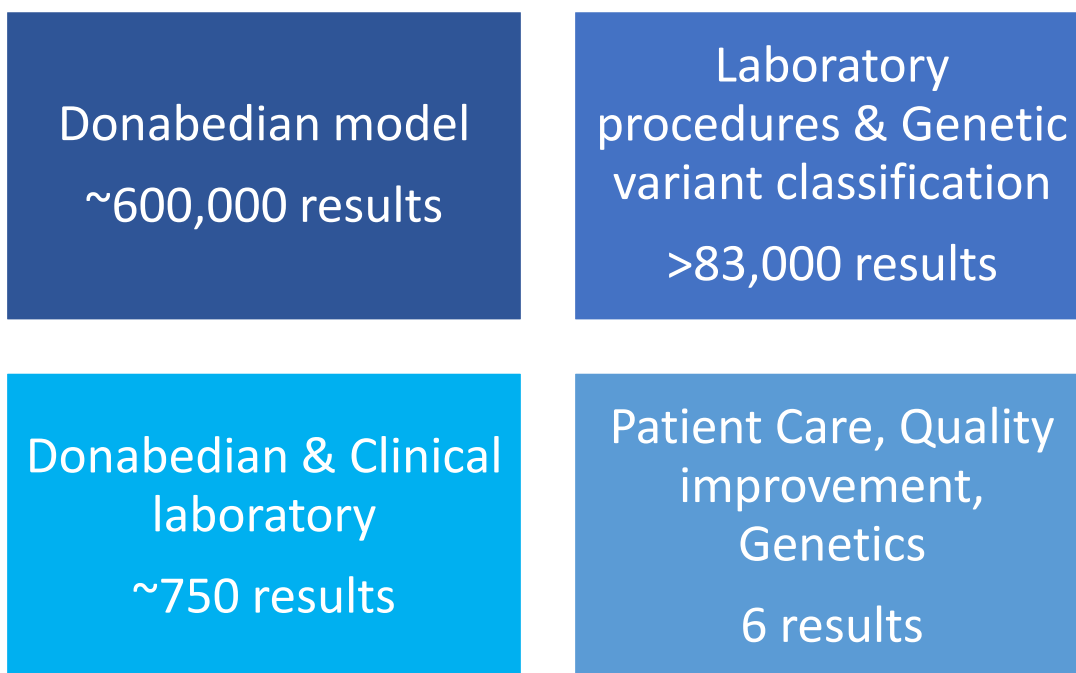
National Library of Medicine Database Search

Several terms were used to review the Donabedian model: Donabedian, model, theory, framework, quality improvement, laboratory, patient care, and genetics. This search strategy differed from the literature review because both a general and particular use of the Donabedian model were reviewed. The literature review is much more specific to the background and specialty of the clinical and research laboratories. A generalized search of the Donabedian model returned over 600,000 results, whereas a more specific search of specialized laboratory procedures and genetic variant classification returned just over 80,000 results. When reviewing the Donabedian model with the laboratory, the literature dwindled to about 750 results. When looking specifically at patient care, quality improvement, and genetics, there were only six related articles (Figure 1). One article focuses on quality improvement standards for colposcopy (Mayeaux, et al., 2017), another on quality of life for patients diagnosed with a brain tumor

(Langegård, et al., 2019), a third on pneumonia (Mattila, et al., 2014), two articles on breast care and quality measures (Landercasper, et al., 2017; Edge, 2013), and the last on managing clinical risk and participant perceptions of clinical research (Lee, et al., 2012). These articles are across multiple disciplines, but none of which directly apply to this study.

Figure 1

Donabedian and Clinical Genetics Laboratory Literature Search

Donabedian model ~600,000 results	Laboratory procedures & Genetic variant classification >83,000 results
Donabedian & Clinical laboratory ~750 results	Patient Care, Quality improvement, Genetics 6 results

Because theories are often not mentioned concerning clinical laboratory work, it was not surprising that there has not been extensive use of the Donabedian model in the clinical genetics laboratory. This research helps to build this background and emphasize the usefulness of a framework when performing quality improvement in the clinical laboratory.

Avedis Donabedian is the "father of quality assurance" (Best & Neuhauser, 2004). His passion for quality patient care led him to develop a framework to evaluate quality measures

used across disciplines consistently and effectively. Though there is no widespread use of theories and frameworks in the clinical genetics field, this study highlights the importance of using a theory to perform quality improvement in the clinical laboratory.

Chapter 4

Methods

Measures

A portion of the genetic sequence of DNA, or gene, is translated into a protein the human body uses in various functions. A single change, or variant, in the sequence, can disrupt the shape or function of the related protein. Unless a functional test is performed, the variant impact is estimated based on currently known information. Evidence to determine variant pathogenicity is collected from many different sources, including (1) Population databases, (2) Computational and predictive software, (3) Segregation (or how a variant is transmitted through families) data, (4) *De novo* (novel) data, (5) Allelic (or how often a variant is seen on its own independent chromosome with another disease-causing variant on the opposite sister chromosome) data, and (6) Laboratory and public variant databases (Richards et al., 2015). For many variants, there is not enough evidence to classify the variant definitively as "pathogenic," disease-causing, or "benign," no effect, so the variants are of uncertain significance (VUS). A genetic test with a functional test component helps to determine the impact on the related protein and improves variant classification, thereby improving clinical utility; however, a reliable predictive software that aligns with the results of a functional assay could impact clinical laboratory functions with significant cost and time savings. This study will evaluate variant splice effects through a functional assay compared to predictive software outcomes to identify the likelihood of a genetic change in causing a disease phenotype (symptoms).

ACMG/AMP provided guidelines in 2015 to determine the different "weight" of different evidence types, including functional evidence, and additional guidance was provided in 2019 by

29

the Clinical Genome Resource (ClinGen) Sequence Variant Interpretation (SVI) Working Group (Richards, et al., 2015; Brnich, et al., 2019). Functional tests that are "well-established" and demonstrate if a variant has normal or abnormal protein function can be labeled as either PS3 (pathogenic strong, level 3) or BS3 (benign strong, level 3), which are the highest possible classifications for functional testing. Currently, it is not recommended that predictive software be used as a sole source of evidence; however, this study could provide evidence supporting the use of SpliceAI as a sole source in specific circumstances (Richards, et al., 2015).

Research Design

This study utilized a quantitative, one-group pre-posttest design. Eighty-six synonymous splice variants with a SpliceAI Δ score ≥0.8 were queried from a public, open database hosted by Illumina in selected ophthalmic genes (Illumina, 2021). A subset of these variants (20) from two genes (*ABCA4* and *CHD7*) were evaluated by minigene (pre-test) to demonstrate proof of concept for this project. The Illumina database includes SpliceAI scores and variant annotations for all possible substitutions, single base insertions, and 1 – 4 base deletions within genes (Illumina, 2021). Though the downloaded variants are classified as synonymous, the high SpliceAI scores imply that these variant changes will impact splicing. The minigene assay is expected to show whether a variant alters the expected mRNA sequence. If the mRNA sequence is altered, this could impact any mRNA-related activities and the final protein, though the amino acid is not altered post-mutation. Once all evidence is weighed, synonymous variants initially expected to be benign may be reclassified to pathogenic or likely pathogenic. After evaluating minigene results, the number of variants showing expected splice effects as predicted by SpliceAI were counted (post-test). Any variants with inconclusive evidence from minigene testing remained classified as VUS and were excluded from the final analysis. Minigene

30

evidence was evaluated against SpliceAI change scores and predictions: Donor gain, donor loss, acceptor gain, and acceptor loss (DG, DL, AG, AL). The outcomes were evaluated by a Fisher's exact test to determine if SpliceAI accurately predicted splice effects.

The "intervention" in this study is a genetic test that includes a component to determine the impact of a change (variation) on the related protein. Six variants have been previously published; two were previously tested by minigene and were used as control samples. The independent variable is the splice effect analysis method (minigene assay vs. SpliceAI). Table 1 summarizes the dependent and independent variables.

Table 1

Measurement Summary

Variable	Type	Data Source	Measure	Construct
Splice Outcomes	DV	Minigene assay results SpliceAI predictions	Categorical (splice effects vs. no splice effects)	Variant splice outcomes as assayed by minigene vs. predicted by SpliceAI
Splice Variant Analysis Method	IV	SpliceAI (Illumina) Minigene	Categorical (predictive vs. functional)	Quality improvement (standard variant analysis w/function test vs. standard variant analysis w/predictive software only)

Note. IV=independent variable, DV=dependent variable

Analysis Methods

One primary splicing function test, minigene, was approached by a novel methodology (NEB HiFi DNA Assembly), and the splice outcomes were evaluated against SpliceAI splice predictions (Jaganathan et al., 2019; NEB, 2023a). Primers were designed using Primer3 and the NEBuilder assembly tool (Untergasser, et al., 2012, NEB, 2023b). Next, primer mixes were prepared, and a polymerase chain reaction (PCR) was performed to amplify the targeted wildtype (unchanged) sequence from template DNA. The variant was incorporated into the PCR product

through primer sequences. The DNA fragments with wildtype or variant sequences were then inserted into the RHCglo plasmid pre-digested with the SalI and XbaI restriction enzymes using the NEB Hifi assembly kit. (NEB, 2023a; Singh & Cooper, 2006). A second PCR was performed to amplify the mutant and wildtype assembled product, including the RSV promoter, minigene exons, and polyA signal (PCR expression cassette). The PCR product was purified by columns and transfected to HEK293 cells. After a 24-hour incubation, the cells were lysed, and RNA was extracted using the XTRACT16+ automated extraction machine (Autogen, 2023). The extracted RNA was converted to complementary DNA (cDNA) through RT PCR, followed by gel electrophoresis to visualize the product, and Sanger sequencing using the Big Dye Direct kit (BIO-RAD, 2023, ThermoFisher Scientific, 2023a). The sequencing product was purified using Performa DTR plates, and samples underwent capillary electrophoresis on the SeqStudio analyzer (EdgeBio, 2023; ThermoFisher, 2023b). Sequencing analysis was performed using SnapGene (SnapGene software, 2023). See Figure 2 below for a graphic of the generalized workflow. Figure 3 details the procedural overview. Detailed protocols are listed in Appendix A. A list of variants and primer sequences is listed in a table in Appendix B.

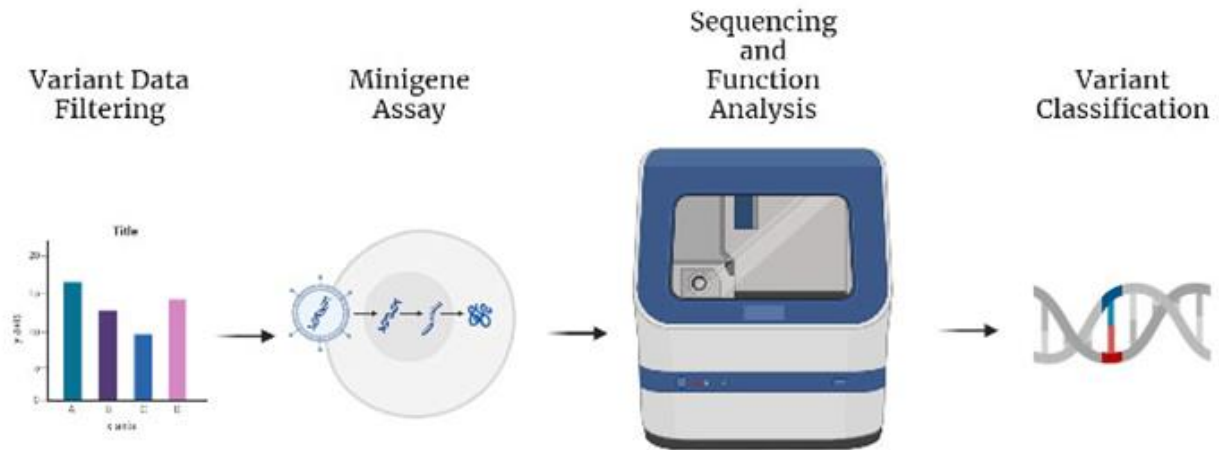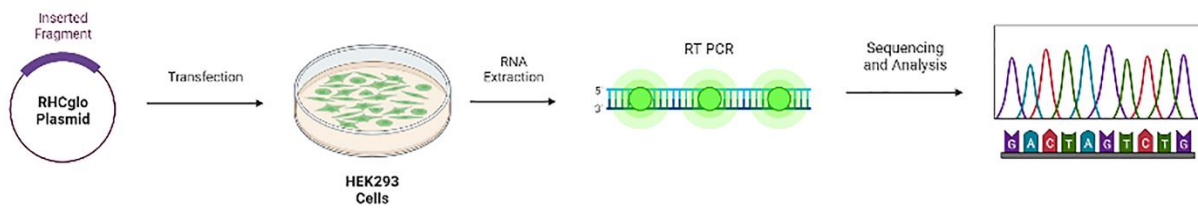**Figure 2**

Generalized Workflow

Figure 3

Minigene Overview

This study was performed as a collaborative effort between Virginia Commonwealth University (VCU) and the National Eye Institute, National Institutes of Health (NEI/NIH) as an intramural study in the Ophthalmic Genomics Laboratory (OGL) under the Ophthalmic Genetics and Visual Function Branch (OGVFB).

IRB Submission

This study (HM20027006) was reviewed by VCU IRB Panel A and was deemed not human subjects research; therefore, further IRB review and approval to proceed with this study was not required.

Target Population

The majority of the population of interest in this study are those affected by inherited retinal degenerations (IRDs), though generally, the population consists of those affected by inherited ophthalmic diseases. The National Ophthalmic Genotyping and Phenotyping Network (eyeGENE®) is a genomic medicine initiative of the NEI that includes a DNA repository and participant registry of nearly 6,500 participants (eyeGENE, 2021). eyeGENE® is open to researchers through controlled access and could be used to dictate future studies built upon this study. Genes of interest were targeted based on noted instances of pathogenic variants in the eyeGENE® database, as well as frequencies of synonymous single nucleotide variants (sSNVs) cited in the gnomAD database (eyeGENE, 2021; gnomAD, 2021).

Data Collection and Evaluation

Data were downloaded from the public Illumina splice database into Excel and filtered by genes associated with eye-related disease (Blueprint Genetics, 2021; Illumina, 2021). The data was further filtered for the targeted genes (*ABCA4, CDHR1, CHD7, CNGA1, CNGA3, CNGB1, CNGB3, EYS, PAX6, PDE6A, PDE6B, PDE6C, PDE6H, PNPLA6, PRPH2, RHO, RP1, RP2, RS1, USH2A*) with a SpliceAI Δ score ≥ 0.8 in at least a single category (DG, DL, AG, AL) and subsequently sub-filtered for synonymous variants (*ABCA4* [12 variants], *CDHR1* [8], *CHD7* [6], *CNGB1* [6], *CNGB3* [1], *EYS* [7], *PAX6* [4], *PDE6A* [3], *PDE6B* [7], *PDE6C* [5], *PNPLA6*

[9], *RHO* [2], *RP1* [2], *USH2A* [14]) (Figure 4). *CNGA1*, *CNGA3*, *PDE6H*, *PRPH2*, *RP2*, and

RS1 did not have synonymous variants with a SpliceAI Δ score ≥ 0.8.

Figure 4

Variant Data Filtering Strategy
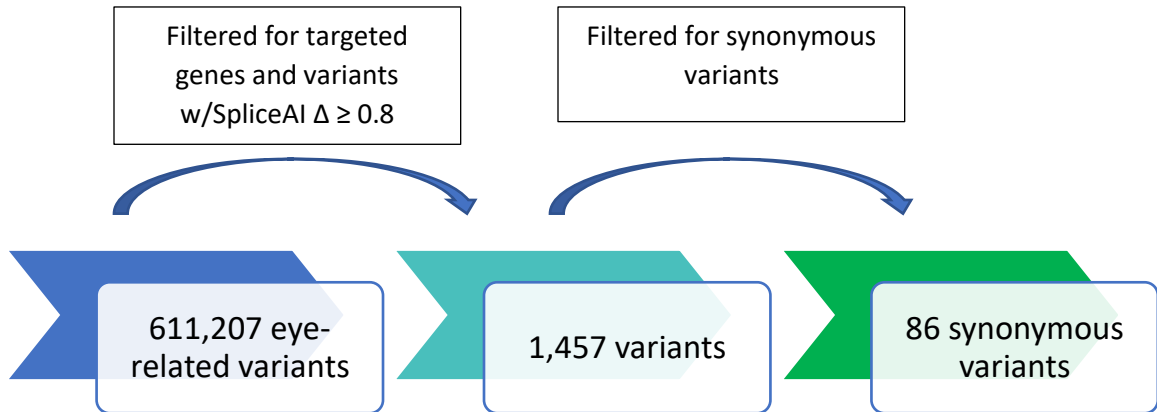
Sequencing data were analyzed using SnapGene (SnapGene Software, 2023). Sequences

were compared to the original sequence downloaded from USCS Genome Browser to determine

specific intron/exon breakpoints (Kent, et al., 2002). Variant classifications will be re-evaluated

through OGL's data pipeline to determine if a variant's current classification can be changed

with the additional functional data. Any VUS that are reclassified as pathogenic or benign will be

reported to ClinVar (Landrum, et al., 2018). Samples that fail to meet stringent analysis

standards will be repeated or marked as "inconclusive" for this study.

Data Security and Management

Data was kept on secure servers behind an NIH firewall and was backed up daily on NIH servers. Any printed data was kept locked and secure.

Limitations

Each assay has technical limitations. Clinical test validation is thorough and establishes the accuracy of the test through controls and duplicate samples, multiple samples and variant review, and the investigator's expertise. This study focuses on genes and proteins related to inherited ophthalmic diseases, so the techniques established and applied in this study may not apply to all inherited diseases. Functional assay utility, or generalizability, will be related to the accuracy of the test and functionality of the proteins evaluated in this study.

Chapter 5

Results

Six-hundred and seventeen synonymous variants were found in the Illumina database in the fourteen selected ophthalmic genes: 86 with a SpliceAI Δ score ≥ 0.8, 173 variants with a Δ score 0.5 – 0.79, 225 variants with a Δ score 0.21 – 0.49, and 133 variants with a Δ score < 0.2 (Illumina, 2021). In the ≥ 0.8 category, most variants were predicted to have at least a donor gain impact (64). SpliceAI predicted changes for the 86 variants in the ≥ 0.8 category are outlined below (Table 2).

Table 2

SpliceAI Predicted Effects in Synonymous Variants Scored ≥ 0.8

Gene	AG	AL	DG	DL	DG/DL
ABCA4	1		9		2
CDHR1	3	1	4		
CHD7	2	5			1
CNGB1	1		5		
CNGB3			1		
EYS	1		4	1	1
PAX6	1		3		
PDE6A			3		
PDE6B	1		5		1
PDE6C	2		3		

PNPLA6	1	7	1
RHO		2	
RP1		1	1
USH2A	1	12	1

Notes. AG = acceptor gain, AL = acceptor loss, DG = donor gain, DL = donor loss, DG/DL = both donor gain and donor loss in a single variant

As a preliminary study to evaluate the novel minigene assay, a subset of the 86 variants with a SpliceAI Δ score ≥ 0.8 were reviewed. Twenty synonymous variants were assayed using the minigene workflow (*ABCA4* [12 variants] and *CHD7* [6]). The genes, variants (c. and p. designations), SpliceAI Δ scores, minigene outcomes, and SpliceAI vs. minigene concordance are listed below in Table 3. Figures outlining the variant information, genomic position, predicted donor and acceptor sites and SpliceAI scores are available in Appendix C. Additional figures with a gel image depicting the minigene results from the wildtype and mutant variant, a schematic of the splice outcome, and the sequencing tracings from successful runs are also shown in Appendix C.

The research question (*RQ1*) stipulated in this study states, "What is the sensitivity of SpliceAI to predict synonymous variants with a SpliceAI Δ score of ≥ 0.8 in inherited ophthalmic disease genes?" Hypothesis 1 (*H1*) states that it is expected that SpliceAI predicted outcomes will not be statistically significant from minigene assay outcomes. Hypothesis 2 (*H2)* states that it is expected that SpliceAI would have a high sensitivity (>80%) to predict splice effects from ophthalmic disease gene synonymous variants scored ≥ 0.8.

Table 3

Genes, Variants, and SpliceAI-Minigene Comparison

Gene	Variant (c.)	Variant (p.)	SpliceAI Δ Scores	Minigene Outcome	SpliceAI vs. Minigene Concordance
ABCA4	c.1299A>G	p.E433=	DG 0.94	Partial e10 loss (57b)	+
	c.2226T>A	p.T742=	AG 0.97	Partial e15 loss (67b)	+
	c.264A>T	p.G88=	DG 0.82	Inconclusive	?
	c.2736A>T	p.G912=	DG 0.92	No splice effect	-
	c.2904G>T	p.G968=	DG 0.85	Partial e19 loss (16b)	+
	c.3018C>T	p.G1006=	DG 0.97	Partial e20 loss (34b)	+
	c.3462C>T	p.G1154=	DG 0.88	Partial e23 loss (62b)	+
	c.4446C>A	p.V1482=	DG 0.89	Partial e30 loss (96b)	+
	c.6000C>T	p.G2000=	DG 0.83	No splice effect	-

	c.6207C>T	p.G2069=	DG 0.97	Total e45 loss	+
	c.6345C>T	p.S2115=	DL 0.87	Inconclusive	?
	c.6360G>T	p.G2120=	DG 1.00, DL 0.87	Inconclusive	?
CHD7	c.3747G>T	p.R1249=	DG 0.82	Inconclusive	?
	c.4512G>T	p.G1504=	DG 1.00, DL 0.89	Partial e19 loss (23b)	+
	c.4641G>T	p.G1547=	DG 0.82	Inconclusive	?
	c.5454G>A	p.L1818=	AG 0.92	No splice effect	-
	c.5841A>G	p.G1947=	DG 0.92	Partial e29 loss (53b)	+
	c.7738C>T	p.L2580=	DG 0.89	Inconclusive	?
	c.7965G>T	p.G2655=	AG 0.96	Partial e36 loss (8b)	+
	c.8115T>A	p.T2705=	AG 0.96	Inconclusive	?

Notes. c. denotes the cDNA position and nucleotide change, p. denotes the protein position and expected amino acid, > indicates the nucleotide from and to, = indicates no amino acid change, variants in italics are classified as VUS in the Human Gene Mutation Database (HGMD), DG = donor gain, AG = acceptor gain, DL = donor loss, AL = acceptor loss, e = exon, b = base, + indicates concordance, - indicates discordance

Both the wildtype and the mutant were assayed for each variant listed above so that the minigene results from the mutant could be compared to the wildtype. Of the 20 variants that

were assayed, 14 of the wildtype and variant pairs had acceptable results that could be evaluated. Six wildtype-variant pairs had results below the quality threshold and could not be evaluated in this study (Figure 5). These variants will be repeated in future assays. Of the 14 variant pairs analyzed, 11 of the variants showed splice effects by minigene (79.0%) (Figure 6). Three variants did not show a difference between the wildtype and mutant (21.0%).
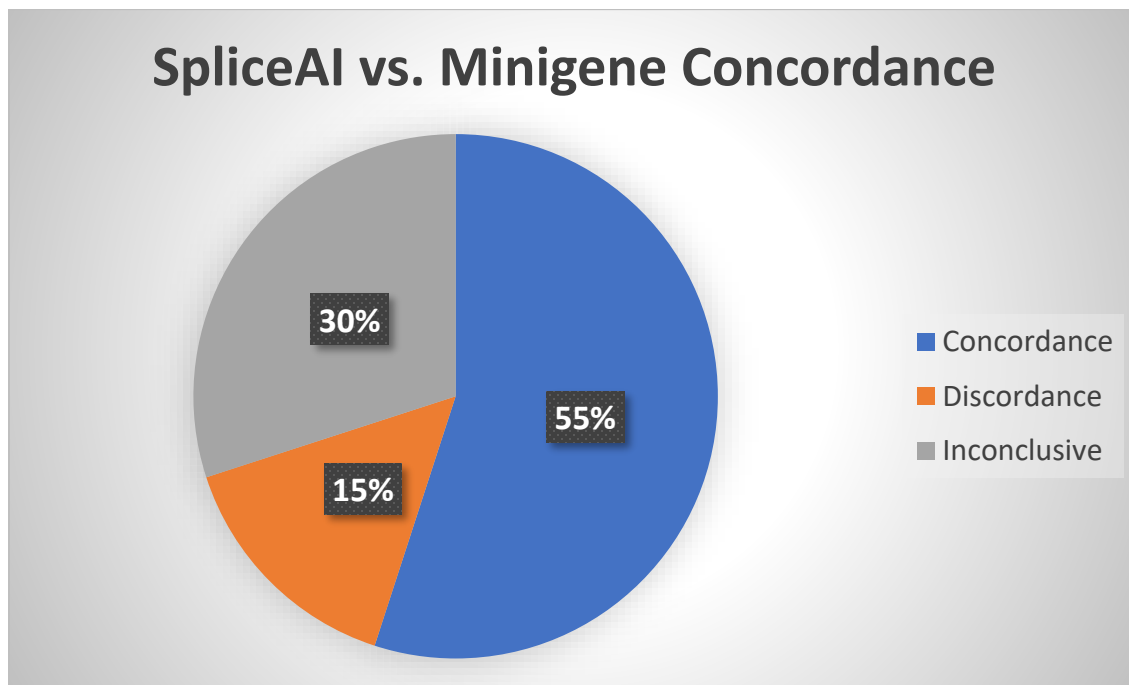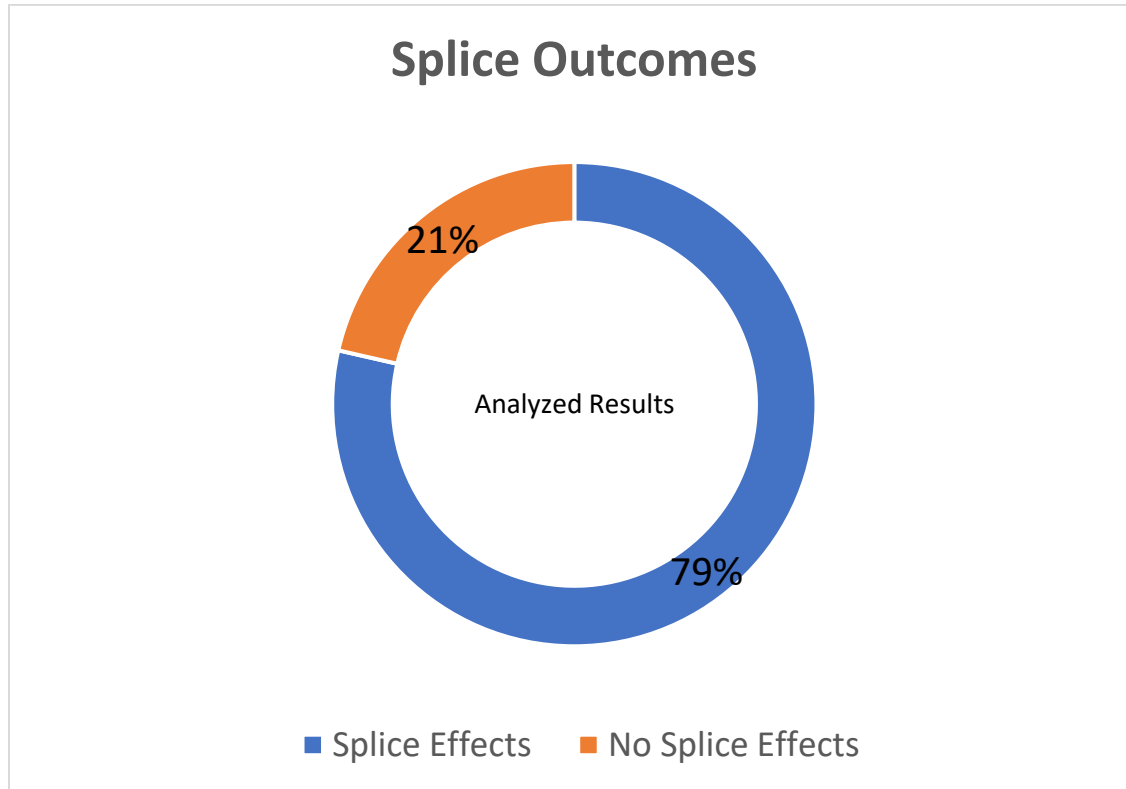
Figure 5

Minigene Concordance

Figure 6

Minigene Splice Outcomes

Specifically, seven of the 12 *ABCA4* variants assayed showed a range of exon loss, from 16 bases to total exon loss. Nine of the *ABCA4* variants were expected to show a donor gain. The ABCA4:c.2226T>A variant was expected to show an acceptor gain. The ABCA4:c.6345C>T was expected to show a donor loss. The ABCA4:c.6360G>T variant was expected to show both a donor gain and donor loss at two different positions, two bases downstream (3') of the variant and -26 bases upstream (5') of the variant, respectively. Five of eight *CHD7* variants assayed also showed a range of exon loss, though less severe, from 8 to 53 bases. Four of the *CHD7* variants were expected to show a donor gain. Two variants, CHD7:c.5454G>A and CHD7:c.8115T>A, were expected to show an acceptor gain. The CHD7:c.4512G>T variant was

expected to show both a donor gain and donor loss, -2 bases upstream of the variant and 21 bases downstream of the variant, respectively.

A Fisher's exact test was performed using Fisher's Exact Test Calculator to evaluate the SpliceAI prediction against the minigene assay outcome (Fisher's Exact Test Calculator, 2018). A 2x2 contingency table was created to plot SpliceAI predicted and minigene assay results, splice effects, or no splice effects. The p value was calculated as 0.2222, indicating no statistical difference between the SpliceAI prediction and the minigene outcome. This result supports *H1* that there would be no statistically significant difference between SpliceAI predicted and minigene assay outcomes. Because three of 14 wildtype-variant pair minigene results did not match as expected, this result does not support *H2*, that SpliceAI's sensitivity would be >80% to predict splice effects from ophthalmic disease gene synonymous variants scored ≥ 0.8. Based on these results, the sensitivity of SpliceAI to predict synonymous variants with a SpliceAI Δ score ≥ 0.8 in inherited ophthalmic disease genes is 79.0%.

Chapter 6

Conclusion

Discussion

Inherited ophthalmic diseases, though often rare, impact thousands of people worldwide. Vision health can significantly impact an individual's wellbeing, in addition to those around them and society as a whole (NASEM, 2016). Because of long-term health and economic impacts, it is estimated that IRDs cost the US over $61 million in economic and wellbeing costs (Gong, et al., 2021). Since IRDs are considered rare, and diagnosis can be difficult due to disease presentation, treatment is often very limited (Gong et al., 2021; Richards, et al., 2015). A confirmed genetic diagnosis is frequently necessary for an individual to qualify for a clinical trial. Variants that cannot be classified as either pathogenic or benign are classified as of uncertain significance; however, a patient will likely not qualify to participate in a clinical trial without a more definite classification that verifies their diagnosis. Most treatments for IRDs are through a clinical trial, so an individual must have an established diagnosis with verified genetic results.

Most disease-causing variants are missense variants, but synonymous variants have been found to impact several mechanisms that routinely cause disease (Miosge, et al., 2015). Synonymous variants (sSNVs), previously overlooked, may provide a pivotal piece to the diagnostic puzzle. RNA studies are not routinely performed in the clinical laboratory, so it is possible that many patients are considered "unsolved" after genetic testing is performed (Wai, et al., 2019; Girirajan, 2017). Functional assays have been more widely used in diagnostic pipelines but add cost in reagents and personnel time (Singer & Bagnall, 2022). Over the long term, these costs can become significant and would most likely be passed along to the consumer, increasing

the overall cost of genetic testing. Since insurance coverage for inherited ophthalmic disease is variable, even for those with the same insurance plan, it is important to reduce genetic testing disparities by keeping overall costs down (Zhao, et al., 2021). A predictive software that could accurately predict variant outcomes would save a clinical laboratory hours of labor and thousands of dollars that could reduce the overall cost of testing to consumers.

SpliceAI is a recently developed neural network-based software trained to predict variant splice effects from pre-mRNA sequences. Since most previous algorithms were designed for novel gene discovery and were not trained to predict variant consequences, they were not accurate at predicting splice variant outcomes (Spurdle, et al., 2008). SpliceAI is one of a handful of recently developed software that can predict splice variant outcomes more accurately than previous software; however, the majority of researchers still use multiple packages to predict variant outcomes (Spurdle, et al., 2008). This is problematic as there is often a lack of consensus between algorithms and a lack of structure for synthesizing scoring across multiple programs, which can lead to bias and potential "cherry picking" of the most desirable algorithm predictions (Pejaver, et al., 2022). Additionally, issues arise when multiple laboratories upload their variant classifications to public databases, such as ClinVar, and the interpretations between laboratories are discordant (Pejaver, et al., 2022; Landrum, et al., 2018; Harrison, et al., 2017). Because no algorithm is expected to operate at 100% efficiency, it is not enough to use algorithm predictions alone, though they can provide valuable insight into expected variant outcomes (Pejaver, et al., 2022).

Functional assays, which provide experimental evidence to support predicted outcomes, are necessary to add weighted evidence for variant classification (Wai, et al., 2019). The minigene assay is relatively easy to perform, is versatile with various cell types, and has been

used across multiple disease models (Smith & Lynch, 2014). Additionally, minigene assays capture various splice events, including partial exon loss, whole exon loss, pseudoexon gain, and intron retention (Abramowicz & Gos, 2018; Smith & Lynch, 2014).

The Donabedian model was used to evaluate the addition of the novel minigene assay to the clinical testing pipeline. The "P" or process component of the Structure-Process-Outcome (SPO) Donabedian model was used as the framework for this clinical laboratory quality improvement. Because the Donabedian model is so widely used in quality improvement in healthcare, it is an ideal model for use in the clinical laboratory (Bermúdez-Camps, et al., 2021; Wong & Kitsantas, 2019; Gardner, Gardner, & O'Connell, 2014; Chou, Norris, Williamson, Garcia, Baysinger, & Mulvihill, 2009). The majority of clinical laboratories have innately established high standards of quality based on tenets set by CLIA for clinical laboratory certification (CDC, 2022). For new clinical laboratories who are just beginning to establish these standards, the Donabedian model provides a blueprint for quality improvement across the entire organization (the structure of the laboratory, clinical processes, and related clinical outcomes). With the emphasis on quality improvement in the clinical laboratory, it is vital to highlight the importance of using well-established models when working towards the highest quality standards.

This preliminary study aimed to show "proof of concept" for a novel minigene assay in the clinical laboratory. Since the minigene assay has been previously extensively tested in clinical and diagnostic settings, it seemed like an ideal system to use here. Additionally, this study reviewed minigene results against the predictions of a highly trained algorithm, SpliceAI, on a rarely evaluated variant, sSNVs. The results of this study indicate that SpliceAI can predict splice effects for synonymous variants within ophthalmic disease genes, as evidenced by

minigene assay results; however, it may not predict as well as would be needed to replace the minigene assay entirely.

Though only 20 wildtype and variant pairs were tested, overall, the results were fairly positive. Based on previous research, it was expected that SpliceAI would have a sensitivity of at least 80%, and these results showed a 79% predictive rate, just shy of the expected 80% (Bryen, et al., 2022; Chen et al., 2020; Jaganathan, et al., 2019). Even with the small cohort, the concordance rate between minigene and SpliceAI was over 50% (79% with the inconclusive results excluded). The Fisher's exact test showed there was no statistical difference (p >0.05), so the outcomes between SpliceAI and minigene were fairly well matched, with only three discordant results (no difference between wildtype and mutant variant splice effects). It is expected that testing of additional variants would elucidate the accuracy of SpliceAI further.

Based on these results, SpliceAI provides valuable information for a clinical laboratory to investigate splice effects further through functional assays; however, an accuracy of 79% would not be enough for a laboratory to use to classify a variant alone. Moreover, according to current variant classification standards, predictive software results cannot be used individually to classify a variant, likely due to the variabilities in splice predictions and discordance between algorithms. Unless further testing shows an accuracy greater than 95%, the requirements surrounding variant classification will likely remain the same. Developers need to continue to test and refine current algorithms and utilize artificial intelligence to develop new and improved predictive software packages. Clinical laboratories will continue to use reliable, functional assays, such as minigene, to confirm variant outcome predictions.

These results also showed that this novel minigene assay is consistent for use in the clinical laboratory. While some of the procedures in the minigene pipeline are automated, such

as the RNA extraction, other procedures were performed manually. Increased automation will improve the minigene pipeline by reducing personnel time and cost. Though only two genes were targeted in this preliminary study, this minigene assay is expected to work well across multiple genes and diseases. Further testing would promote this presumption and provide a broader scope of the minigene outcomes compared to predicted SpliceAI scores.

There were several previous studies published that evaluated the predictive efficiency of SpliceAI as compared to other predictive software packages, but there were few studies that used SpliceAI to evaluate synonymous variants (Ha, et al., 2021; Strauch, et al., 2022; Zeng, et al., 2021). Additionally, many studies have highlighted the minigene assay to evaluate synonymous variants. Still, there have been a small number of studies that focus on inherited ophthalmic disease genes. Those studies centered on inherited ophthalmic diseases evaluated variants in single genes related to specific patient cases where the genetic diagnosis was confirmed by minigene (Qian et al., 2021; Zeitz, et al., 2021; Zou, et al., 2019).

This study is novel because the minigene assay used in this study has not been previously published. This study evaluated SpliceAI predictions across 20 inherited ophthalmic disease genes and 86 synonymous variants in the ≥ 0.8 category. Moreover, this study focused on experimentally generated data to evaluate a predictive software package that has previously shown promising predictive value. IRB approval was unnecessary and there was less risk of bias as these results are not specifically tied to patient outcomes. The minigene assay presented here comprises several smaller procedures across the pipeline (PCR, purification, cell culture, transfection, RNA extraction, and Sanger sequencing), each with individual limitations. These assay limitations are controlled by establishing the sensitivity and specificity of the testing

pipeline through the clinical validation procedure, and through the use of validated controls and duplicates.

Future Studies

The additional 66 variants previously queried from the Illumina database will be assayed through the minigene workflow, and the outcomes will be compared to SpliceAI Δ scores for further analysis. The concordant SpliceAI and minigene results will be evaluated against ACMG/AMP guidelines for variant classification to determine if any of the variants' current classifications can be updated. Once verified, this data can be uploaded to ClinVar.

Because this study only evaluated synonymous variants with SpliceAI scores ≥ 0.8, reviewing other synonymous variants from the Illumina database that fell below this scoring threshold to determine the accuracy of SpliceAI's splicing predictions with lower scores may be beneficial. Other studies which have explored minigene along with SpliceAI have found splice effects with SpliceAI scores as low as 0.01 (Torrado, et al., 2022).

Additionally, because the minigene assay only measures the presence or absence of splice effects, testing each variant on a quantitative assay would be helpful so that wildtype and mutant transcript could be measured. Because it is nearly impossible to distinguish band intensity on an agarose gel, a quantitative assay could determine whether a normal transcript is present but in reduced quantity in the mutant compared to the wildtype transcript. The discordant results seen in this study could indeed be concordant if the normal transcript is found to be reduced in the mutant as compared to the wildtype, thereby increasing the accuracy of SpliceAI predictions. Phenotype-genotype studies could be established based on amounts of normal transcript present and could lead to further discoveries related to disease pathology.

Finally, it would be useful to query the eyeGENE® database to determine if any of the sSNVs found to be likely disease-causing are present in participants in the eyeGENE® database. This information could be helpful to participants if they currently have a single pathogenic variant in an autosomal recessive disease and could provide the missing heritability for an individual, thereby offering a definitive genetic diagnosis that could be used towards future therapies.

References

Abramowicz, A., & Gos, M. (2018). Splicing mutations in human genetic disorders: examples, detection, and confirmation. *Journal of applied genetics*, *59*(3), 253–268. https://doi.org/10.1007/s13353-018-0444-7

Alemayehu, Y. K., Bushen, O. Y., & Muluneh, A. T. (2009). Evaluation of HIV/AIDS clinical care quality: the case of a referral hospital in North West Ethiopia. *International journal for quality in health care: journal of the International Society for Quality in Health Care*, *21*(5), 356–362. https://doi.org/10.1093/intqhc/mzp030

American Society of Gene & Cell Therapy (ASGCT). (2020). *Inherited Retinal Diseases.* http://patienteducation.asgct.org/disease-treatments/inherited-retinal-diseases

ATCC. (2023a). *HEK293 cells*. https://www.atcc.org/products/crl-1573

ATCC. (2023b). *HeLa cells.* https://www.atcc.org/products/ccl-2

Autogen. (2023). *XTRACT16+*. https://autogen.com/product/xtract-16/

Ayanian, J. Z., & Markel, H. (2016). Donabedian's Lasting Framework for Health Care Quality. *New England Journal of Medicine, 375*(3), 205-207. doi:10.1056/NEJMp1605101

Baten, A. K., Chang, B. C., Halgamuge, S. K., & Li, J. (2006). Splice site identification using probabilistic parameters and SVM classification. *BMC bioinformatics*, *7 Suppl 5*(Suppl 5), S15. https://doi.org/10.1186/1471-2105-7-S5-S15

Best, M., & Neuhauser, D. (2004). Avedis Donabedian: father of quality assurance and poet. *Quality & safety in health care*, *13*(6), 472–473. https://doi.org/10.1136/qhc.13.6.472

Bermúdez-Camps, I. B., Flores-Hernández, M. A., Aguilar-Rubio, Y., López-Orozco, M., Barajas-Esparza, L., Téllez López, A. M., García-Pérez, M. E., Fegadolli, C., & Reyes-Hernández, I. (2021). Design and validation of quality indicators for drug dispensing in a pediatric hospital. *Journal of the American Pharmacists Association : JAPhA*, S1544-3191(21)00090-X. Advance online publication. https://doi.org/10.1016/j.japh.2021.02.018

BIO-RAD. (2023). *iScript reverse transcription supermix for RT-qPCR*. https://www.bio-rad.com/en-us/product/iscript-reverse-transcription-supermix-for-rt-qpcr?ID=M87EVMKG4

Black, C. M., Ashworth, J. L., & Sergouniotis, P. I. (2022). Genetic disorders causing non-syndromic retinopathy. *Clinical ophthalmic genetics and genomics* (pp. 161-265). Academic Press.

Blueprint Genetics. (2021). https://blueprintgenetics.com/tests/panels/ophthalmology/

Breitbach, A., Lockeman, K., Gunaldo, T., Pardue, K., Eliot, K., Goumas, A., Kettenbach, G., Lanning, S., & Mills, B. (2019). Utilizing Shared Expertise Across Contexts to Engage in Multi-institutional Interprofessional Scholarship. *Journal of allied health*, *48*(3), e95–e100.

Brnich, S. E., Abou Tayoun, A. N., Couch, F. J., Cutting, G. R., Greenblatt, M. S., Heinen, C. D., Kanavy, D. M. . . . Group, C. G. R. S. V. I. W. (2019). Recommendations for application of the functional evidence PS3/BS3 criterion using the ACMG/AMP sequence variant interpretation framework. *Genome Medicine*, *12*(1), 3. https://doi.org/10.1186/s13073-019-0690-2

Bryen, S. J., Yuen, M., Joshi, H., Dawes, R., Zhang, K., Lu, J. K., Jones, K. J., Liang, C., Wong, W. K., Peduto, A. J., Waddell, L. B., Evesson, F. J., & Cooper, S. T. (2022). Prevalence, parameters, and pathogenic mechanisms for splice-altering acceptor variants that disrupt the AG exclusion zone. *HGG advances*, *3*(4), 100125. https://doi.org/10.1016/j.xhgg.2022.100125

Centers for Disease Control & Prevention (CDC). (2018). *Individualized Quality Control Plan.* https://www.cdc.gov/labquality/iqcp.html

Centers for Disease Control & Prevention (CDC). (2022). *CLIA Law & Regulations*. https://www.cdc.gov/clia/law-regulations.html

Chen, J. M., Lin, J. H., Masson, E., Liao, Z., Férec, C., Cooper, D. N., & Hayden, M. (2020). The Experimentally Obtained Functional Impact Assessments of 5' Splice Site GT'GC Variants Differ Markedly from Those Predicted. *Current genomics*, *21*(1), 56–66. https://doi.org/10.2174/1389202921666200210141701

Chen, M., & Manley, J. L. (2009). Mechanisms of alternative splicing regulation: insights from molecular and genomics approaches. *Nature reviews. Molecular cell biology*, *10*(11), 741–754. https://doi.org/10.1038/nrm2777

Chiang, J. P., & Trzupek, K. (2015). The current status of molecular diagnosis of inherited retinal dystrophies. *Current Opinion in Ophthalmology, 26*(5), 346-351. doi:10.1097/ICU.0000000000000185

Chou, A. F., Norris, A. I., Williamson, L., Garcia, K., Baysinger, J., & Mulvihill, J. J. (2009). Quality assurance in medical and public health genetics services: a systematic review. *American journal of medical genetics. Part C, Seminars in medical genetics*, *151C*(3), 214–234. https://doi.org/10.1002/ajmg.c.30219

Cremers, F. P. M., Boon, C. J. F., Bujakowska, K., & Zeitz, C. (2018). Special issue

introduction: Inherited retinal disease: Novel candidate genes, genotype-phenotype correlations, and inheritance models. *Genes (Basel), 9*(4). doi:10.3390/genes9040215

Cubuk, C., Garrett, A., Choi, S., King, L., Loveday, C., Torr, B., Burghel, G. J., Durkie, M., Callaway, A., Robinson, R., Drummond, J., Berry, I., Wallace, A., Eccles, D., Tischkowitz, M., Whiffin, N., Ware, J. S., Hanson, H., Turnbull, C., & CanVIG-Uk (2021). Clinical likelihood ratios and balanced accuracy for 44 in silico tools against multiple large-scale functional assays of cancer susceptibility genes. *Genetics in medicine : official journal of the American College of Medical Genetics*, *23*(11), 2096–2104. https://doi.org/10.1038/s41436-021-01265-z

Cui, L. M., Jiang, J. Y., Hu, N. N., Zou, H. E., Zhao, B. Z., Han, C. Y., Yang, K., Wang, Y. P., & Xing, H. X. (2022). Whole exome sequencing identified a novel compound heterozygous variation in COL7A1 gene causing dystrophic epidermolysis bullosa. *Molecular genetics & genomic medicine*, *10*(5), e1907. https://doi.org/10.1002/mgg3.1907

Dalkara, D., Byrne, L. C., Klimczak, R. R., Visel, M., Yin, L., Merigan, W. H., Flannery, J. G., & Schaffer, D. V. (2013). In vivo-directed evolution of a new adeno-associated virus for therapeutic outer retinal gene delivery from the vitreous. *Science translational medicine*, *5*(189), 189ra76. https://doi.org/10.1126/scitranslmed.3005708

Deng, H., Zhang, Y., Ding, J., & Wang, F. (2022). Presumed *COL4A3/COL4A4* Missense/Synonymous Variants Induce Aberrant Splicing. *Frontiers in medicine*, *9*, 838983. https://doi.org/10.3389/fmed.2022.838983

Donabedian A. (2005). Evaluating the quality of medical care. 1966. *The Milbank quarterly*, *83*(4), 691–729. https://doi.org/10.1111/j.1468-0009.2005.00397.x

Ducroq, D., Rozet, J. M., Gerber, S., Perrault, I., Barbet, D., Hanein, S., Hakiki, S., Dufier, J. L., Munnich, A., Hamel, C., & Kaplan, J. (2002). The ABCA4 gene in autosomal recessive cone-rod dystrophies. *American journal of human genetics*, *71*(6), 1480–1482. https://doi.org/10.1086/344829

Duncan, J. L., Pierce, E. A., Laster, A. M., Daiger, S. P., Birch, D. G., Ash, J. D., Iannaccone, A., Flannery, J. G., Sahel, J. A., Zack, D. J., Zarbin, M. A., & and the Foundation Fighting Blindness Scientific Advisory Board (2018). Inherited Retinal Degenerations: Current Landscape and Knowledge Gaps. *Translational vision science & technology*, *7*(4), 6. https://doi.org/10.1167/tvst.7.4.6

Durland, J., & Ahmadian-Moghadam, H. (2022). Genetics, Mutagenesis. In *StatPearls*. StatPearls Publishing.

Edge S. B. (2013). The challenge of quality in breast care: beyond accreditation. *Journal of oncology practice*, *9*(2), e71–e72. https://doi.org/10.1200/JOP.2012.000792

EdgeBio. (2023). *Performa DTR ultra plates*. https://www.edgebio.com/products/performa

Ellingford, J. M., Barton, S., Bhaskar, S., O'Sullivan, J., Williams, S. G., Lamb, J. A., . . . Black, G. C. M. (2016). Molecular findings from 537 individuals with inherited retinal disease. *Journal of Medical Genetics, 53*(11), 761-767. doi:10.1136/jmedgenet-2016-103837

Ferrari, S., Di Iorio, E., Barbaro, V., Ponzin, D., Sorrentino, F. S., & Parmeggiani, F. (2011). Retinitis pigmentosa: genes and disease mechanisms. *Current genomics*, *12*(4), 238–249. https://doi.org/10.2174/138920211795860107

Fisher's Exact Test Calculator. (2018). *Easy Fisher Exact Test Calculator*. https://www.socscistatistics.com/tests/chisquare2/default2.aspx

Fraile-Bethencourt, E., Valenzuela-Palomo, A., Díez-Gómez, B., Caloca, M. J., Gómez-Barrero, S., & Velasco, E. A. (2019). Minigene Splicing Assays Identify 12 Spliceogenic Variants of *BRCA2* Exons 14 and 15. *Frontiers in genetics*, *10*, 503. https://doi.org/10.3389/fgene.2019.00503

Gao, F. J., Wang, D. D., Hu, F. Y., Xu, P., Chang, Q., Li, J. K., Liu, W., Zhang, S. H., Xu, G. Z., & Wu, J. H. (2022). Genotypic spectrum and phenotype correlations of EYS-associated disease in a Chinese cohort. *Eye (London, England)*, *36*(11), 2122–2129. https://doi.org/10.1038/s41433-021-01794-6

Garanto, A., Chung, D. C., Duijkers, L., Corral-Serrano, J. C., Messchaert, M., Xiao, R., Bennett, J., Vandenberghe, L. H., & Collin, R. W. (2016). In vitro and in vivo rescue of aberrant splicing in CEP290-associated LCA by antisense oligonucleotide delivery. *Human molecular genetics*, *25*(12), 2552–2563. https://doi.org/10.1093/hmg/ddw118

Gardner, G., Gardner, A., & O'Connell, J. (2014). Using the Donabedian framework to examine the quality and safety of nursing service innovation. *Journal of clinical nursing*, *23*(1-2), 145–155. https://doi.org/10.1111/jocn.12146

Genome Aggregation Database (gnomAD). (2021). https://gnomad.broadinstitute.org/

Georgakopoulos-Soares, I., Parada, G. E., Wong, H. Y., Medhi, R., Furlan, G., Munita, R., Miska, E. A., Kwok, C. K., & Hemberg, M. (2022). Alternative splicing modulation by G-quadruplexes. *Nature communications*, *13*(1), 2404. https://doi.org/10.1038/s41467-022-30071-7

Georgiou, M., Robson, A. G., Singh, N., Pontikos, N., Kane, T., Hirji, N., Ripamonti, C., Rotsos, T., Dubra, A., Kalitzeos, A., Webster, A. R., Carroll, J., & Michaelides, M. (2019). Deep Phenotyping of PDE6C-Associated Achromatopsia. *Investigative ophthalmology & visual science*, *60*(15), 5112–5123. https://doi.org/10.1167/iovs.19-27761

Giorgi, G., Casarin, A., Trevisson, E., Donà, M., Cassina, M., Graziano, C., Picci, L., Clementi, M., & Salviati, L. (2015). Validation of CFTR intronic variants identified during cystic fibrosis population screening by a minigene splicing assay. *Clinical chemistry and*

laboratory medicine, *53*(11), 1719–1723. https://doi.org/10.1515/cclm-2014-1047

Girirajan S. (2017). Missing heritability and where to find it. *Genome biology*, *18*(1), 89. https://doi.org/10.1186/s13059-017-1227-x

Gong, J., Cheung, S., Fasso-Opie, A., Galvin, O., Moniz, L. S., Earle, D., Durham, T., Menzo, J., Li, N., Duffy, S., Dolgin, J., Shearman, M. S., Fiorani, C., Banhazi, J., & Daly, A. (2021). The Impact of Inherited Retinal Diseases in the United States of America (US) and Canada from a Cost-of-Illness Perspective. *Clinical ophthalmology (Auckland, N.Z.)*, *15*, 2855–2866. https://doi.org/10.2147/OPTH.S313719

Grosse, S. D., & Khoury, M. J. (2006). What is the clinical utility of genetic testing?. *Genetics in medicine*, *8*(7), 448–450. https://doi.org/10.1097/01.gim.0000227935.26763.c6

Ha, C., Kim, J. W., & Jang, J. H. (2021). Performance Evaluation of SpliceAI for the Prediction of Splicing of *NF1* Variants. *Genes*, *12*(9), 1308. https://doi.org/10.3390/genes12091308

Harrison, S. M., Dolinsky, J. S., Knight Johnson, A. E., Pesaran, T., Azzariti, D. R., Bale, S., Chao, E. C., Das, S., Vincent, L., & Rehm, H. L. (2017). Clinical laboratories collaborate to resolve differences in variant interpretations submitted to ClinVar. *Genetics in medicine : official journal of the American College of Medical Genetics*, *19*(10), 1096–1104. https://doi.org/10.1038/gim.2017.14

Harrow, J., Frankish, A., Gonzalez, J. M., Tapanari, E., Diekhans, M., Kokocinski, F., Aken, B. L., Barrell, D., Zadissa, A., Searle, S., Barnes, I., Bignell, A., Boychenko, V., Hunt, T., Kay, M., Mukherjee, G., Rajan, J., Despacio-Reyes, G., Saunders, G., Steward, C., … Hubbard, T. J. (2012). GENCODE: the reference human genome annotation for The ENCODE Project. *Genome research*, *22*(9), 1760–1774. https://doi.org/10.1101/gr.135350.111

He, W. B., Xiao, W. J., Dai, C. L., Wang, Y. R., Li, X. R., Gong, F., Meng, L. L., Tan, C., Zeng, S. C., Lu, G. X., Lin, G., Tan, Y. Q., Hu, H., & Du, J. (2022). RNA splicing analysis contributes to reclassifying variants of uncertain significance and improves the diagnosis of monogenic disorders. *Journal of medical genetics*, *59*(10), 1010–1016. https://doi.org/10.1136/jmedgenet-2021-108013

Hull, S., Attanasio, M., Arno, G., Carss, K., Robson, A. G., Thompson, D. A., Plagnol, V., Michaelides, M., Holder, G. E., Henderson, R. H., Raymond, F. L., Moore, A. T., & Webster, A. R. (2017). Clinical Characterization of CNGB1-Related Autosomal Recessive Retinitis Pigmentosa. *JAMA ophthalmology*, *135*(2), 137–144. https://doi.org/10.1001/jamaophthalmol.2016.5213

Illumina. (2021) Splice Variants VCF. https://support.illumina.com/help/BS_App_TruSightTumor170_OLH_1000000028435/Content/Source/Informatics/Apps/SpliceVariantsOutputRNA_appT170.htm

Jaganathan, K., Kyriazopoulou Panagiotopoulou, S., McRae, J. F., Darbandi, S. F., Knowles, D., Li, Y. I., Kosmicki, J. A., Arbelaez, J., Cui, W., Schwartz, G. B., Chow, E. D., Kanterakis, E., Gao, H., Kia, A., Batzoglou, S., Sanders, S. J., & Farh, K. K. (2019). Predicting Splicing from Primary Sequence with Deep Learning. *Cell*, *176*(3), 535–548.e24. https://doi.org/10.1016/j.cell.2018.12.015

Kanavy, D. M., McNulty, S. M., Jairath, M. K., Brnich, S. E., Bizon, C., Powell, B. C., & Berg, J. S. (2019). Comparative analysis of functional assay evidence use by ClinGen Variant Curation Expert Panels. *Genome medicine*, *11*(1), 77. https://doi.org/10.1186/s13073-019-0683-1

Katsonis, P., Wilhelm, K., Williams, A., & Lichtarge, O. (2022). Genome interpretation using in silico predictors of variant impact. *Human genetics*, *141*(10), 1549–1577. https://doi.org/10.1007/s00439-022-02457-6

Kay, C. N., Ryals, R. C., Aslanidi, G. V., Min, S. H., Ruan, Q., Sun, J., Dyka, F. M., Kasuga, D., Ayala, A. E., Van Vliet, K., Agbandje-McKenna, M., Hauswirth, W. W., Boye, S. L., & Boye, S. E. (2013). Targeting photoreceptors via intravitreal delivery using novel, capsid-mutated AAV vectors. *PloS one*, *8*(4), e62097. https://doi.org/10.1371/journal.pone.0062097

Keegan, N. P., Wilton, S. D., & Fletcher, S. (2022). Analysis of Pathogenic Pseudoexons Reveals Novel Mechanisms Driving Cryptic Splicing. *Frontiers in genetics*, *12*, 806946. https://doi.org/10.3389/fgene.2021.806946

Kent, W. J., Sugnet, C. W., Furey, T. S., Roskin, K. M., Pringle, T. H., Zahler, A. M., & Haussler, D. (2002). The human genome browser at UCSC. *Genome research*, *12*(6), 996–1006. https://doi.org/10.1101/gr.229102

Khan, N. W., Wissinger, B., Kohl, S., & Sieving, P. A. (2007). CNGB3 achromatopsia with progressive loss of residual cone function and impaired rod-mediated function. *Investigative ophthalmology & visual science*, *48*(8), 3864–3871. https://doi.org/10.1167/iovs.06-1521

Kohl, S., Varsanyi, B., Antunes, G. A., Baumann, B., Hoyng, C. B., Jägle, H., Rosenberg, T., Kellner, U., Lorenz, B., Salati, R., Jurklies, B., Farkas, A., Andreasson, S., Weleber, R. G., Jacobson, S. G., Rudolph, G., Castellan, C., Dollfus, H., Legius, E., Anastasi, M., … Wissinger, B. (2005). CNGB3 mutations account for 50% of all cases with autosomal recessive achromatopsia. *European journal of human genetics : EJHG*, *13*(3), 302–308. https://doi.org/10.1038/sj.ejhg.5201269

Kuehlewein, L., Zobor, D., Andreasson, S. O., Ayuso, C., Banfi, S., Bocquet, B., Bernd, A. S., Biskup, S., Boon, C. J. F., Downes, S. M., Fischer, M. D., Holz, F. G., Kellner, U., Leroy, B. P., Meunier, I., Nasser, F., Rosenberg, T., Rudolph, G., Stingl, K., Thiadens, A. A. H. J., … RD-CURE Consortium (2020). Clinical Phenotype and Course of PDE6A-

Associated Retinitis Pigmentosa Disease, Characterized in Preparation for a Gene
Supplementation Trial. *JAMA ophthalmology*, *138*(12), 1241–1250.
https://doi.org/10.1001/jamaophthalmol.2020.4206

Landercasper, J., Bailey, L., Buras, R., Clifford, E., Degnim, A. C., Thanasoulis, L., Fayanju, O.
M., Tjoe, J. A., & Rao, R. (2017). The American Society of Breast Surgeons and Quality
Payment Programs: Ranking, Defining, and Benchmarking More Than 1 Million Patient
Quality Measure Encounters. *Annals of surgical oncology*, *24*(10), 3093–3106.
https://doi.org/10.1245/s10434-017-5940-1

Landrum, M. J., Lee, J. M., Benson, M., Brown, G. R., Chao, C., Chitipiralla, S., Gu, B., Hart, J.,
Hoffman, D., Jang, W., Karapetyan, K., Katz, K., Liu, C., Maddipatla, Z., Malheiro, A.,
McDaniel, K., Ovetsky, M., Riley, G., Zhou, G., Holmes, J. B., … Maglott, D. R. (2018).
ClinVar: improving access to variant interpretations and supporting evidence. *Nucleic
acids research*, *46*(D1), D1062–D1067. https://doi.org/10.1093/nar/gkx1153

Langegård, U., Ahlberg, K., Fransson, P., Johansson, B., Sjövall, K., Bjork-Eriksson, T.,
Ohlsson-Nevo, E., & Proton Care Study Group (2019). Evaluation of quality of care in
relation to health-related quality of life of patients diagnosed with brain tumor: a novel
clinic for proton beam therapy. *Supportive care in cancer : official journal of the
Multinational Association of Supportive Care in Cancer*, *27*(7), 2679–2691.
https://doi.org/10.1007/s00520-018-4557-7

Lee, L. M., Yessis, J., Kost, R. G., & Henderson, D. K. (2012). Managing Clinical Risk and
Measuring Participants' Perceptions of the Clinical Research Process. *Principles and
Practice of Clinical Research*, 573–587. https://doi.org/10.1016/B978-0-12-382167-
6.00039-4

Lighter, D. E. (2015). How (and why) do quality improvement professionals measure
performance? *International Journal of Pediatrics and Adolescent Medicine, 2*(1), 7-11.
doi:10.1016/j.ijpam.2015.03.003

Lima Cunha, D., Arno, G., Corton, M., & Moosajee, M. (2019). The Spectrum of PAX6
Mutations and Genotype-Phenotype Correlations in the Eye. Genes, 10(12), 1050.
https://doi.org/10.3390/genes10121050

López-Bigas, N., Audit, B., Ouzounis, C., Parra, G., & Guigó, R. (2005). Are splicing mutations
the most frequent cause of hereditary disease?. *FEBS letters*, *579*(9), 1900–1903.
https://doi.org/10.1016/j.febslet.2005.02.047

Lord, J., & Baralle, D. (2021). Splicing in the Diagnosis of Rare Disease: Advances and
Challenges. *Frontiers in genetics*, *12*, 689892. https://doi.org/10.3389/fgene.2021.689892

Malechka, V. V., Cukras, C. A., Chew, E. Y., Sergeev, Y. V., Blain, D., Jeffrey, B. G., Ullah, E.,
Hufnagel, R. B., Brooks, B. P., Huryn, L. A., & Zein, W. M. (2022). Clinical Phenotypes
of *CDHR1*-Associated Retinal Dystrophies. *Genes*, *13*(5), 925.

https://doi.org/10.3390/genes13050925

Manes, G., Cheguru, P., Majumder, A., Bocquet, B., Sénéchal, A., Artemyev, N. O., Hamel, C. P., & Brabet, P. (2014). A truncated form of rod photoreceptor PDE6 β-subunit causes autosomal dominant congenital stationary night blindness by interfering with the inhibitory activity of the γ-subunit. *PloS one*, *9*(4), e95768. https://doi.org/10.1371/journal.pone.0095768

Mattila, J. T., Fine, M. J., Limper, A. H., Murray, P. R., Chen, B. B., & Lin, P. L. (2014). Pneumonia. Treatment and diagnosis. *Annals of the American Thoracic Society*, *11 Suppl 4*(Suppl 4), S189–S192. https://doi.org/10.1513/AnnalsATS.201401-027PL

Mayeaux, E. J., Jr, Novetsky, A. P., Chelmow, D., Garcia, F., Choma, K., Liu, A. H., Papasozomenos, T., Einstein, M. H., Massad, L. S., Wentzensen, N., Waxman, A. G., Conageski, C., Khan, M. J., & Huh, W. K. (2017). ASCCP Colposcopy Standards: Colposcopy Quality Improvement Recommendations for the United States. *Journal of lower genital tract disease*, *21*(4), 242–248. https://doi.org/10.1097/LGT.0000000000000342

Mayro, E. L., Murchison, A. P., Hark, L. A., Silverstein, M., Wang, O. Y., Gilligan, J. P., Leiby, B. E., Pizzi, L. T., Casten, R. J., Rovner, B. W., & Haller, J. A. (2021). Prevalence of depressive symptoms and associated factors in an urban, ophthalmic population. *European journal of ophthalmology*, *31*(2), 740–747. https://doi.org/10.1177/1120672120901701

Meier, F. A., Badrick, T. C., & Sikaris, K. A. (2018). What's to Be done about laboratory quality? Process indicators, laboratory stewardship, the outcomes problem, risk assessment, and economic value: Responding to contemporary global challenges. *American Journal of Clinical Pathology*, *149*(3), 186–196. https://doi.org/10.1093/ajcp/aqx135

Merriam-Webster Dictionary. (2021). https://www.merriam-webster.com/

Messchaert, M., Haer-Wigman, L., Khan, M. I., Cremers, F. P. M., & Collin, R. W. J. (2018). EYS mutation update: In silico assessment of 271 reported and 26 novel variants in patients with retinitis pigmentosa. *Human mutation*, *39*(2), 177–186. https://doi.org/10.1002/humu.23371

Michaelides, M., Aligianis, I. A., Ainsworth, J. R., Good, P., Mollon, J. D., Maher, E. R., Moore, A. T., & Hunt, D. M. (2004). Progressive cone dystrophy associated with mutation in CNGB3. *Investigative ophthalmology & visual science*, *45*(6), 1975–1982. https://doi.org/10.1167/iovs.03-0898

Miko, I. (2008). Phenotype variability: penetrance and expressivity. *Nature Education*, *1*(1), 137.

Miosge, L. A., Field, M. A., Sontani, Y., Cho, V., Johnson, S., Palkova, A., Balakishnan, B.,

Liang, R., Zhang, Y., Lyon, S., Beutler, B., Whittle, B., Bertram, E. M., Enders, A., Goodnow, C. C., & Andrews, T. D. (2015). Comparison of predicted and actual consequences of missense mutations. *Proceedings of the National Academy of Sciences of the United States of America*, *112*(37), E5189–E5198. https://doi.org/10.1073/pnas.1511585112

National Academies of Sciences, Engineering, and Medicine (NASEM), Health and Medicine Division, Board on Population Health and Public Health Practice, Committee on Public Health Approaches to Reduce Vision Impairment and Promote Eye Health, Welp, A., Woodbury, R. B., McCoy, M. A., & Teutsch, S. M. (Eds.). (2016). *Making Eye Health a Population Health Imperative: Vision for Tomorrow*. National Academies Press (US).

National Cancer Institute (NCI), National Institutes of Health. (2021a). *Sanger sequencing*. https://www.cancer.gov/publications/dictionaries/genetics-dictionary/def/sanger-sequencing

National Cancer Institute (NCI), National Institutes of Health. (2021b). *Variant*. https://www.cancer.gov/publications/dictionaries/genetics-dictionary/search/variant

National Cancer Institute (NCI), National Institutes of Health. (2023a). *Autosomal dominant inheritance*. https://www.cancer.gov/publications/dictionaries/genetics-dictionary/def/autosomal-dominant-inheritance

National Cancer Institute (NCI), National Institutes of Health. (2023b). *Autosomal recessive inheritance*. https://www.cancer.gov/publications/dictionaries/genetics-dictionary/def/autosomal-recessive-inheritance

National Human Genome Research Institute (NHGRI). (2022a). *Exon*. https://www.genome.gov/genetics-glossary/Exon

National Human Genome Research Institute (NHGRI). (2022b). *Intron*. https://www.genome.gov/genetics-glossary/Intron

National Human Genome Research Institute (NHGRI). (2022c). *Messenger ribonucleic acid (mRNA)*. https://www.genome.gov/genetics-glossary/messenger-rna

National Human Genome Research Institute (NHGRI). (2022d). *Ribonucleic acid (RNA)*. https://www.genome.gov/genetics-glossary/RNA-Ribonucleic-Acid

National Human Genome Research Institute (NHGRI). (2022e).*Transcription*. https://www.genome.gov/genetics-glossary/Transcription

National Human Genome Research Institute (NHGRI). (2022f). *Translation*. https://www.genome.gov/genetics-glossary/Translation

National Human Genome Research Institute (NHGRI). (2023). *X-Linked*.

https://www.genome.gov/genetics-glossary/X-Linked

National Ophthalmic Genotyping and Phenotyping Network (eyeGENE). (2021). https://eyegene.nih.gov

New England Biolabs (NEB). (2023a). *NEBuilder assembly tool*. https://nebuilder.neb.com/#!/

New England Biolabs (NEB). (2023b). *NEBuilder hifi dna assembly.* https://www.neb.com/applications/cloning-and-synthetic-biology/dna-assembly-and-cloning/nebuilder-hifi-dna-assembly

O'Byrne, M. L., Huang, J., Asztalos, I., Smith, C. L., Dori, Y., Gillespie, M. J., Rome, J. J., & Glatz, A. C. (2020). Pediatric/Congenital Cardiac Catheterization Quality: An Analysis of Existing Metrics. *JACC. Cardiovascular interventions*, *13*(24), 2853–2864. https://doi.org/10.1016/j.jcin.2020.09.002

Online Mendelian Inheritance of Man (OMIM). (2023). CHARGE syndrome. https://www.omim.org/entry/214800

Pejaver, V., Byrne, A. B., Feng, B. J., Pagel, K. A., Mooney, S. D., Karchin, R., O'Donnell-Luria, A., Harrison, S. M., Tavtigian, S. V., Greenblatt, M. S., Biesecker, L. G., Radivojac, P., Brenner, S. E., & ClinGen Sequence Variant Interpretation Working Group (2022). Calibration of computational tools for missense variant pathogenicity classification and ClinGen recommendations for PP3/BP4 criteria. *American journal of human genetics*, *109*(12), 2163–2177. https://doi.org/10.1016/j.ajhg.2022.10.013

Pfaff, K., & Markaki, A. (2017). Compassionate collaborative care: an integrative review of quality indicators in end-of-life care. *BMC palliative care*, *16*(1), 65. https://doi.org/10.1186/s12904-017-0246-4

Qian, X., Wang, J., Wang, M., Igelman, A. D., Jones, K. D., Li, Y., Wang, K., Goetz, K. E., Birch, D. G., Yang, P., Pennesi, M. E., & Chen, R. (2021). Identification of Deep-Intronic Splice Mutations in a Large Cohort of Patients With Inherited Retinal Diseases. *Frontiers in genetics*, *12*, 647400. https://doi.org/10.3389/fgene.2021.647400

Rattner, A., Sun, H., & Nathans, J. (1999). Molecular genetics of human retinal disease. *Annual Review of Genetics, 33*, 89-131. doi:10.1146/annurev.genet.33.1.89

Reith, M., Zeltner, L., Schäferhoff, K., Witt, D., Zuleger, T., Haack, T. B., Bornemann, A., Alber, M., Ruf, S., Schoels, L., Stingl, K., & Weisschuh, N. (2022). A Novel, Apparently Silent Variant in *MFSD8* Causes Neuronal Ceroid Lipofuscinosis with Marked Intrafamilial Variability. *International journal of molecular sciences*, *23*(4), 2271. https://doi.org/10.3390/ijms23042271

RetNet. (2023). *Retinal information network*. https://web.sph.uth.edu/RetNet/home.htm

Richards, S., Aziz, N., Bale, S., Bick, D., Das, S., Gastier-Foster, J., . . . Committee, A. L. Q. A. (2015). Standards and guidelines for the interpretation of sequence variants: A joint consensus recommendation of the American College of Medical Genetics and Genomics and the Association for Molecular Pathology. *Genetics in Medicine, 17*(5), 405-424. doi:10.1038/gim.2015.30

Riedmayr, L. M., Böhm, S., Michalakis, S., & Becirovic, E. (2018). Construction and Cloning of Minigenes for *in vivo* Analysis of Potential Splice Mutations. *Bio-protocol*, *8*(5), e2760. https://doi.org/10.21769/BioProtoc.2760

Rossanti, R., Horinouchi, T., Yamamura, T., Nagano, C., Sakakibara, N., Ishiko, S., Aoto, Y., Kondo, A., Nagai, S., Okada, E., Ishimori, S., Nagase, H., Matsui, S., Tamagaki, K., Ubara, Y., Nagahama, M., Shima, Y., Nakanishi, K., Ninchoji, T., Matsuo, M., … Nozu, K. (2021). Evaluation of Suspected Autosomal Alport Syndrome Synonymous Variants. *Kidney360*, *3*(3), 497–505. https://doi.org/10.34067/KID.0005252021

Sahel, J. A., Marazova, K., & Audo, I. (2014). Clinical characteristics and current therapies for inherited retinal degenerations. *Cold Spring Harbor Perspectives in Medicine*, *5*(2), a017111. https://doi.org/10.1101/cshperspect.a017111

Sarkar, A., Panati, K., & Narala, V. R. (2022). Code inside the codon: The role of synonymous mutations in regulating splicing machinery and its impact on disease. *Mutation research. Reviews in mutation research*, *790*, 108444. https://doi.org/10.1016/j.mrrev.2022.108444

Singer, E. S., & Bagnall, R. D. (2022). Splicing Functional Assays Into the Genetic Testing Pipeline. *Circulation. Genomic and precision medicine*, *15*(6), e003949. https://doi.org/10.1161/CIRCGEN.122.003949

Singh, G., & Cooper, T. A. (2006). Minigene reporter for identification and analysis of cis elements and trans factors affecting pre-mRNA splicing. *BioTechniques*, *41*(2), 177–181. https://doi.org/10.2144/000112208

Smith, S. A., & Lynch, K. W. (2014). Cell-based splicing of minigenes. *Methods in molecular biology (Clifton, N.J.)*, *1126*, 243–255. https://doi.org/10.1007/978-1-62703-980-2_18

SnapGene software. (2023). www.snapgene.com

Sobolewska, M., Świerczyńska, M., Dorecka, M., Wyględowska-Promieńska, D., Krawczyński, M. R., & Mrukwa-Kominek, E. (2023). *CDHR1*-Related Cone-Rod Dystrophy: Clinical Characteristics, Imaging Findings, and Genetic Test Results-A Case Report. *Medicina (Kaunas, Lithuania)*, *59*(2), 399. https://doi.org/10.3390/medicina59020399

SpliceAI. (2023). A deep learning-based tool to identify splice variants. https://github.com/Illumina/SpliceAI

Spurdle, A. B., Couch, F. J., Hogervorst, F. B., Radice, P., Sinilnikova, O. M., & IARC

Unclassified Genetic Variants Working Group (2008). Prediction and assessment of splicing alterations: implications for clinical testing. *Human mutation*, *29*(11), 1304–1313. https://doi.org/10.1002/humu.20901

Stenson, P. D., Mort, M., Ball, E. V., Evans, K., Hayden, M., Heywood, S., Hussain, M., Phillips, A. D., & Cooper, D. N. (2017). The Human Gene Mutation Database: towards a comprehensive repository of inherited mutation data for medical research, genetic diagnosis and next-generation sequencing studies. *Human genetics*, *136*(6), 665–677. https://doi.org/10.1007/s00439-017-1779-6

Stingl, K., Baumann, B., De Angeli, P., Vincent, A., Héon, E., Cordonnier, M., De Baere, E., Raskin, S., Sato, M. T., Shiokawa, N., Kohl, S., & Wissinger, B. (2022). Novel *OPN1LW/OPN1MW* Exon 3 Haplotype-Associated Splicing Defect in Patients with X-Linked Cone Dysfunction. *International journal of molecular sciences*, *23*(12), 6868. https://doi.org/10.3390/ijms23126868

Strauch, Y., Lord, J., Niranjan, M., & Baralle, D. (2022). CI-SpliceAI-Improving machine learning predictions of disease causing splicing variants using curated alternative splice sites. *PloS one*, *17*(6), e0269159. https://doi.org/10.1371/journal.pone.0269159

Suvannaboon, R., Pawestri, A. R., Jinda, W., Tuekprakhon, A., Trinavarat, A., & Atchaneeyasakul, L. O. (2022). Genotypic and phenotypic profiles of EYS gene-related retinitis pigmentosa: a retrospective study. *Scientific reports*, *12*(1), 21494. https://doi.org/10.1038/s41598-022-26017-0

Synofzik, M., Hufnagel, R. B., & Züchner, S. (2014). *PNPLA6* Disorders. In M. P. Adam (Eds.) et. al., *GeneReviews®*. University of Washington, Seattle.

Tavtigian, S. V., Greenblatt, M. S., Harrison, S. M., Nussbaum, R. L., Prabhu, S. A., Boucher, K. M., Biesecker, L. G., & ClinGen Sequence Variant Interpretation Working Group (ClinGen SVI) (2018). Modeling the ACMG/AMP variant classification guidelines as a Bayesian classification framework. *Genetics in medicine : official journal of the American College of Medical Genetics*, *20*(9), 1054–1060. https://doi.org/10.1038/gim.2017.210

ThermoFisher Scientific. (2023a). *BigDye direct cycle sequencing kit*. https://www.thermofisher.com/order/catalog/product/4458687

ThermoFisher Scientific. (2023b). *SeqStudio genetic analyzer*. https://www.thermofisher.com/us/en/home/life-science/sequencing/sanger-sequencing/genetic-analyzers/models/seqstudio.html

Tomkiewicz, T. Z., Suárez-Herrera, N., Cremers, F. P. M., Collin, R. W. J., & Garanto, A. (2021). Antisense Oligonucleotide-Based Rescue of Aberrant Splicing Defects Caused by 15 Pathogenic Variants in *ABCA4*. *International journal of molecular sciences*, *22*(9), 4621. https://doi.org/10.3390/ijms22094621

Torrado, M., Maneiro, E., Lamounier Junior, A., Fernández-Burriel, M., Sánchez Giralt, S., Martínez-Carapeto, A., Cazón, L., Santiago, E., Ochoa, J. P., McKenna, W. J., Santomé, L., & Monserrat, L. (2022). Identification of an elusive spliceogenic MYBPC3 variant in an otherwise genotype-negative hypertrophic cardiomyopathy pedigree. *Scientific reports*, *12*(1), 7284. https://doi.org/10.1038/s41598-022-11159-y

Untergasser, A., Cutcutache, I., Koressaar, T., Ye, J., Faircloth, B. C., Remm, M., & Rozen, S. G. (2012). Primer3--new capabilities and interfaces. *Nucleic acids research*, *40*(15), e115. https://doi.org/10.1093/nar/gks596

U.S. National Library of Medicine, National Institutes of Health, MedlinePlus. (2020a, August 18). *Leber congenital amaurosis*. https://medlineplus.gov/genetics/condition/leber-congenital-amaurosis/

U.S. National Library of Medicine, National Institutes of Health, MedlinePlus. (2020b, August 18). *Stargardt macular degeneration*. https://medlineplus.gov/genetics/condition/stargardt-macular-degeneration/

Vázquez-Domínguez I, Garanto A, Collin RWJ. Molecular Therapies for Inherited Retinal Diseases-Current Standing, Opportunities and Challenges. Genes (Basel). 2019 Aug 28;10(9):654. doi: 10.3390/genes10090654. PMID: 31466352; PMCID: PMC6770110.

Vermeer, M. C. S. C., Andrei, D., Kramer, D., Nijenhuis, A. M., Hoedemaekers, Y. M., Westers, H., Jongbloed, J. D. H., Pas, H. H., van den Berg, M. P., Silljé, H. H. W., van der Meer, P., & Bolling, M. C. (2022). Functional investigation of two simultaneous or separately segregating DSP variants within a single family supports the theory of a dose-dependent disease severity. *Experimental dermatology*, *31*(6), 970–979. https://doi.org/10.1111/exd.14571

Vihinen M. (2022). When a Synonymous Variant Is Nonsynonymous. *Genes*, *13*(8), 1485. https://doi.org/10.3390/genes13081485

Wai, H. A., Lord, J., Lyon, M., Gunning, A., Kelly, H., Cibin, P., Seaby, E. G., Spiers-Fitzgerald, K., Lye, J., Ellard, S., Thomas, N. S., Bunyan, D. J., Douglas, A. G. L., Baralle, D., & Splicing and disease working group (2020). Blood RNA analysis can increase clinical diagnostic rate and resolve variants of uncertain significance. *Genetics in medicine : official journal of the American College of Medical Genetics*, *22*(6), 1005–1014. https://doi.org/10.1038/s41436-020-0766-9

Wai, H., Douglas, A. G. L., & Baralle, D. (2019). RNA splicing analysis in genomic medicine. *The international journal of biochemistry & cell biology*, *108*, 61–71. https://doi.org/10.1016/j.biocel.2018.12.009

Wang, J., Xiao, X., Li, S., Wang, P., Sun, W., & Zhang, Q. (2021). Dominant RP in the Middle While Recessive in Both the N- and C-Terminals Due to *RP1* Truncations: Confirmation,

Refinement, and Questions. *Frontiers in cell and developmental biology*, *9*, 634478. https://doi.org/10.3389/fcell.2021.634478

Wong, P. C., & Kitsantas, P. (2020). A review of maternal mortality and quality of care in the USA. *The journal of maternal-fetal & neonatal medicine : the official journal of the European Association of Perinatal Medicine, the Federation of Asia and Oceania Perinatal Societies, the International Society of Perinatal Obstetricians*, *33*(19), 3355–3367. https://doi.org/10.1080/14767058.2019.1571032

Yamamura, T., Horinouchi, T., Aoto, Y., Lennon, R., & Nozu, K. (2022). The Contribution of COL4A5 Splicing Variants to the Pathogenesis of X-Linked Alport Syndrome. *Frontiers in medicine*, 9, 841391. https://doi.org/10.3389/fmed.2022.841391

Yan, X., Shu, J., Nie, Y., Zhang, Y., Wang, P., Zhou, W., Cui, X., & Liu, Y. (2022). Case Report: Identification and Functional Analysis of a Homozygous Synonymous Variant in the *PLOD1* Gene in a Chinese Neonatal With the Ehlers-Danlos Syndrome. *Frontiers in pediatrics*, *10*, 813758. https://doi.org/10.3389/fped.2022.813758

Zeitz, C., Michiels, C., Neuillé, M., Friedburg, C., Condroyer, C., Boyard, F., Antonio, A., Bouzidi, N., Milicevic, D., Veaux, R., Tourville, A., Zoumba, A., Seneina, I., Foussard, M., Andrieu, C., N Preising, M., Blanchard, S., Saraiva, J. P., Mesrob, L., Le Floch, E., … Audo, I. (2019). Where are the missing gene defects in inherited retinal disorders? Intronic and synonymous variants contribute at least to 4% of CACNA1F-mediated inherited retinal disorders. *Human mutation*, *40*(6), 765–787. https://doi.org/10.1002/humu.23735

Zeng, Z., Aptekmann, A. A., & Bromberg, Y. (2021). Decoding the effects of synonymous variants. *Nucleic acids research*, *49*(22), 12673–12691. https://doi.org/10.1093/nar/gkab1159

Zhang, H., Chen, C., Wu, X., Lou, C., Liang, Q., Wu, W., Wang, X., & Ding, Q. (2022). Effects of 14 F9 synonymous codon variants on hemophilia B expression: Alteration of splicing along with protein expression. *Human mutation*, *43*(7), 928–939. https://doi.org/10.1002/humu.24377

Zhang, M., Lin, Y., Zhang, X., Lan, F., & Zeng, J. (2022). Premature termination codons in SMN1 leading to spinal muscular atrophy trigger nonsense-mediated mRNA decay. *Clinica chimica acta; international journal of clinical chemistry*, *530*, 45–49. https://doi.org/10.1016/j.cca.2022.02.020

Zhao, P. Y., Branham, K., Schlegel, D., Fahim, A. T., & Jayasundera, K. T. (2021). Association of No-Cost Genetic Testing Program Implementation and Patient Characteristics With Access to Genetic Testing for Inherited Retinal Degenerations. *JAMA ophthalmology*, *139*(4), 449–455. https://doi.org/10.1001/jamaophthalmol.2021.0004

Zhou, Q., Teng, Y., Pan, J., Shi, Q., Liu, Y., Zhang, F., Liang, D., Li, Z., & Wu, L. (2022). Identification of four novel mutations in BTK from six Chinese families with X-linked agammaglobulinemia. *Clinica chimica acta; international journal of clinical chemistry*, *531*, 48–55. https://doi.org/10.1016/j.cca.2022.02.019

Zou, G., Zhang, T., Cheng, X., Igelman, A. D., Wang, J., Qian, X., Fu, S., Wang, K., Koenekoop, R. K., Fishman, G. A., Yang, P., Li, Y., Pennesi, M. E., & Chen, R. (2021). Noncoding mutation in *RPGRIP1* contributes to inherited retinal degenerations. *Molecular vision*, *27*, 95–106.

1. Primer Design using Primer3 and NEBuilder:

1. Go to UCSC Genome Browser (https://genome.ucsc.edu/cgi-bin/hgGateway), select the Human Assembly. *GRCh37/hg19* was used for the first 29 variants and verified against the *GRCh38/hg38* assembly to ensure proper coverage. *GRCh38/hg38* was used for the remaining variants. Enter the chromosome and chromosome position for best search accuracy (*eg.* chr6:65057651) in the Position/Search Term field.

2. The variant (highlighted) and surrounding sequence will be visible. The arrow at the top under "Scale" should face right (->). By using the "move" arrows at the top, determine the intron/exon boundaries for the variant region and note the chromosomal positions for each boundary on either side of the variant.

3. Right-click on the gene name (left side of screen) and select "Get DNA for *xxx gene.*" In the "position" field, add/subtract 400 bases to the previously determined intron/exon boundaries, and set the range. Under "Sequence Retrieval Options," "Add extra bases" should be set to 0 in both fields. Under "Sequence Formatting Options," select "All lower case" and "Reverse complement."

    **Note: *For deep intronic variants (variants more than 100 bp from a flanking intron/exon boundary), add 500 bases to the variant site location instead of the intron/exon boundaries. Alternatively, you may include the closest flanking exon sequence +/- at least 250 bases of the intron on both sides where the variant occurs. If a pseudoexon is predicted, add at least 250 bases of the intron sequence on either side of the pseudoexon sequence.*

4. Select "extended color/case options," and select "Underline" for "RepeatMasker" and "Toggle Case" for "NCBI RefSeq." Click "submit" at the top. The "Extended DNA Output" will be visible, and the exon sequence is in ALL CAPS, with the surrounding intron sequence in lower case.

5. Copy and paste this sequence into Primer3 (https://primer3.ut.ee/). To ensure the primers flank the sequence of interest, place a left bracket ([) and right bracket (]) at 250 bases of either end of the exon/intron boundary. Click "Pick Primers."

6. Forward and reverse primers are indicated as (>>>) and (<<<) in the sequence. Starting with the (>>>) forward primer sequence and ending with the (<<<) reverse primer sequence, copy and paste the sequence into NEBuilder (https://nebuilder.neb.com/#!/).

7. Click "New fragment" then paste the sequence from Primer3. You will need to remove all characters copied over (>>>, <<<, line numbers, etc.) and leave only the remaining sequence, then click "Process text."

8. Locate the variant change and manually change the base. *For instance, if the sequence is ...CAGCAGG... and the change is A>T, type in the new base as ...CAGCtGG.*

9. Delete the sequence starting at the variant change through the end. This sequence becomes Fragment 1.

10. Rename the fragment related to the exon or variant (*eg. ABCA4e20frag1*).

11. Click "Add" at the bottom.

12. Follow steps 7-8 again, then delete the sequence starting at the beginning through the variant change. This sequence becomes Fragment 2.

13. Rename the fragment according to convention above (*eg. ABCA4e20frag2*).

14. Add the plasmid sequence for RHCglo (see below) by clicking "Add Fragment," "Process text," check the boxes for "Vector" and "Circular," then rename the fragment (*eg. RHCgloplasmid*).

RHCglo sequence:

ggtacatatcgaattcgagctcgcccggggatcatatggtgcactctcagtacaatctgctctgatgccgcatagttaagccagtat
ctgctccctgcttgtgtgttggaggtcgctgagtagtgcgcgagcaaaatttaagctacaacaaggcaaggcttgaccgacaatt
gcatgaagaatctgcttagggttaggcgttttgcgctgcttcgcgatgtacgggccagatatacgcgtatctgaggggactaggg
tgtgtttaggcgaaaagcggggcttcggttgtacgcggttaggagtcccctcaggatatagtagtttcgcttttgcatagggaggg
ggaaatgtagtcttatgcaatactcttgtagtcttgcaacatggtaacgatgagttagcaacatgccttacaaggagagaaaaagc
accgtgcatgccgattggtggaagtaaggtggtacgatcgtgccttattaggaaggcaacagacgggtctgacatggattggac
gaaccactgaattccgcattgcagagatattgtatttaagtgcctagctcgatacaataaacgccatttgaccattcaccacattggt
gtgcacctccaagctccggactcgggtgagcccttatgcatgtctcttactgaccagcttgctcttaccggggttgcagggaggc
agatttgctcacctgaatgttggggaggtaaatgcttggagagatgggggtgctgataaatccatctctgtcctatgccggtcaga
gggtctgtgcatcgggagctctccctcttcctttcccagctgccttctttgcctttggtttcatcctcacttggttttatgctctgccttcg
tctccctaactcctccctagtaggaaaaagcatcctccgctgtggcaccttgcaattctccccatctgcacccctccctctgcctgct
gcgtgcagcccttcctccccaggttgcccctcagcacctgagtttccgtaactcaaggactggagcccctgttactgaccatac
cccgctatgggggctgatctggcattgctcccccacgcctttgcgctttcagtgagggtgcacggatatgggaacgccagcaaaa
atagctcctgctcctcatccacctgtggtggcttttgcctcgcgtcgcccccaacctccctgagtcacggggcctggctgcgtctga
ggagacagctgcagctccttgtgcagctccccagccattttttagaagcactttccccacccccctccccccccccctcttcccagcaa
tgtgttgtgcccgcacattttccaggataaggtttcctcggggggagcttggccctgcagcctttacctcctcctcaggcaacgacccc
gtcgatcctcactttgtagttcctctgtaggcaaagcagttgtggagtggtgggaggaaagaatgtcccatgacttggctttcctga
tgccttctggagaagaaaggaagggcgagcaaaatcccttttcgcgaagggcctttgctggcagttggatgctttccccctttcctg
cttccctagccggccacgagatggtgctgggaagcgaaagggtcgacaccaatagaaactgggcatgtggagacagagaag
actcttgggtttctgataggcactgactctctctgcctattggtctattttccacccttaggatccatctaccatcgattggcatggct

cgaggttggtatcaaggttacaagacaggtttaaggagaccaatagaaactgggcatgtggagacagagaagactcttgggtct
agactagtcgagctgcccgaacaacttcagggccgcatctcatttgccagcaggggggatgcaaaaaatcccacctatggtgct
gatgttcaatgaatgcattgggtgcccactagcccagtgacccagggaaggctaggaaagcactccgagacaaagtagcacttt
tcagaaggagaataagccctgggcttggagtccttgaggaatctgagcaagattcctctggttaatggtgcacaatatctctaagc
tagaagctgaagctggtttggggaccaaatgtgtgacaagctgtgggattgtgtggggaagaagaaaagatgaaggaatgcat
cgtaacttaccttgttctcatttttccctcctacagaaaaagaggagggcagccaccgcccggcggcagcacctgaagagtgcta
tgctccagcaatcttgtaggttccaggctgctgaggacctgcaccagccatgcaactttctattttgtaacaatttctggttactgttg
ctgcaaagctccatgtgacacagtgtatgtaaagtgtacataaattaatttattttacctcgtttgtttgtttttaaaaccaatgccctgt
ggaaggaaacataaaacttcaagaagcattaaatcatcagtcattctgtcacacccctaatgcagttgtttctgtcatcatttccctgg
gctcttccatctctcgctgacctgggactgggtgctggggctgggagcaggggttggggctctccagggagagatggcatggg
gagagtgatgggatactgctgggggggggggggactcaccctgctgtgggctgcaggaagcccattggtgcagagagcagcct
gggatgcccatgacacgggcacccactgcaccgtgtttctcccatgcccagtagggaaagggttacgagcgccgttcattctca
gcttgtgaaggattttgttgggctcagcctgccagagcagtagccaggcatgcctgtgcagctccgagctgtgatggacagagg
caaggctgcagctagagcggccgccaccgcggtggagctccaattcgccctatagtgagtcgtattacaattcactggccgtcg
ttttacaacgtcgtgactgggaaaaccctggcgttacccaacttaatcgccttgcagcacatccccccttcgccagctggcgtaat
agcgaagaggcccgcaccgatcgcccttcccaacagttgcgtagcctgaatggcgaatgggacgcgccctgtagcggcgcat
taagcgcggcgggtgtggtggttacgcgcagcgtgaccgctacacttgccagcgccctagcgcccgctcctttcgctttcttccc
ttcctttctcgccacgttcgccggctttccccgtcaagctctaaatcggggctccctttagggttccgatttagtgctttacggcacc
tcgaccccaaaaaacttgattagggtgatggttcacgtagtgggccatcgccctgatagacggtttttcgccctttgacgttggagt
ccacgttctttaatagtggactcttgttccaaactggaacaacactcaaccctatctcggtctattcttttgatttataaggggattttgcc
gatttcggcctattggttaaaaaatgagctgatttaacaaaaatttaacgcgaattttaacaaaatattaacgtttacaatttcaggtgg
cactttttcggggaaatgtgcgcggaacccctatttgtttatttttctaaatacattcaaatatgtatccgctcatgagacaataacccg
ataaatgcttcaataatattgaaaaaggaagagtatgagtattcaacatttccgtgtcgcccttattcccttttttgcggcattttgcctt
cctgttttgctcacccagaaacgctggtgaaagtaaaagatgctgaagatcagttgggtgcacgagtgggttacatcgaactgg
atctcaacagcggtaagatccttgagagttttcgccccgaagaacgttttccaatgatgagcacttttaaagttctgctatgtggcgc
ggtattatcccgtattgacgccgggcaagagcaactcggtcgccgcatacactattctcagaatgacttggttgagtactcaccag
tcacagaaaagcatcttacggatggcatgacagtaagagaattatgcagtgctgccataagcatgagtgataacactgcggcca
acttacttctgacaacgatcggaggaccgaaggagctaaccgcttttttttcacaacatggggggatcatgtaactcgccttgatcgtt
gggaaccggagctgaatgaagccataccaaacgacgagcgtgacaccacgatgcctgtagcaatggcaacaacgttgcgca
aactattaactggcgaactacttactctagcttcccggcaacaattaatagactggatggaggcggataaagttgcaggaccactt
ctgcgctcggcccttccggctggctggtttattgctgataaatctggagccggtgagcgtgggtctcgcggtatcattgcagcact
ggggccagatggtaagccctcccgtatcgtagttatctacacgacgggcagtcaggcaactatggatgaacgaaatagacagat
cgctgagataggtgcctcactgattaagcattggtaactgtcagaccaagtttactcatatatactttagattgatttaaaacttcatttt
taatttaaaaggatctaggtgaagatcctttttgataatctcatgaccaaaatcccttaacgtgagttttcgttccactgagcgtcaga
ccccgtagaaaagatcaaaggatcttcttgagatcctttttttctgcgcgtaatctgctgcttgcaaacaaaaaaaccaccgctacc
agcggtggtttgtttgccggatcaagagctaccaactctttttccgaaggtaactggcttcagcagagcgcagataccaaatactg
tccttctagtgtagccgtagttaggccaccacttcaagaactctgtagcaccgcctacatacctcgctctgctaatcctgttaccagt
ggctgctgccagtggcgataagtcgtgtcttaccgggttggactcaagacgatagttaccggataaggcgcagcggtcgggct
gaacggggggttcgtgcacacagcccagcttggagcgaacgacctacaccgaactgagatacctacagcgtgagcattgaga
aagcgccacgcttcccgaagggagaaaggcggacaggtatccggtaagcggcagggtcggaacaggagagcgcacgagg
gagcttccaggggggaacgcctggtatctttatagtcctgtcgggtttcgccacctctgacttgagcgtcgatttttgtgatgctcgt
caggggggccgagcctatggaaaaacgccagcaacgcggcctttttacggttcctggccttttgctggccttttgctcacatgttct
ttcctgcgttatcccctgattctgtggataaccgtattaccgcctttgagtgagctgataccgctcgccgcagccgaacgaccgag
cgcagcgagtcagtgagcgaggaagcggaagagcgcccaatacgcaaaccgcctctccccgcgcgttggccgattcattaat
gcagctggcacgacaggtttcccgactggaaagcgggcagtgagcgcaacgcaattaatgtgagttacctcactcattaggcac

69

cccaggctttacactttatgcttccggctcctatgttgtgtggaattgtgagcggataacaatttcacacaggaaacagctatgacca
tgattacgccaagctcggaattaaccctcactaaagggaacaaaagctg

15. Under "Select method for production of linearized fragment," select "Restriction Digest," select "SalI" for the 5' end of the fragment and "XbaI" for the 3' end of the fragment, then click "Add."

16. Click to edit Fragment 2 by clicking the pencil icon. Scroll down to "Adjust junction properties," under the "Upstream junction," be sure the "Split" option is selected, and enter the variant sequence in the "Custom spacer" textbox. *In the example above, t would be entered.* Click "Update."

17. The primer sequences are displayed at the bottom under "Required oligos."

2. PCR #1 (Wildtype (WT) & Variant (Var)) Amplification:

1. Prepare primer mixes as outlined below for both the wildtype (outer) primer mixes and variants for each variant being testing (*enough for 10 variants*).

PRIMER MIXES:

WT (100 uM stock ea, Primer mix 10+10 uM)

ROW A (of PCR plate):

dH2O   90 uL

WT OutF   5 uL

WT OutR   5 uL

For each Variant (100 uM stock ea, Primer mix 10+10 uM):

ROW B (of PCR plate):

dH2O   90 uL

WT OutF   5 uL

VarR   5 uL

ROW C (of PCR plate):

dH2O   90uL

VarF   5 uL

WT OutR   5 uL

2. Retrieve the template DNA (*any previously tested DNA with wildtype region of interest or CEPH DNA may be used*).

3. Prepare the PCR reaction # 1 master mix as outlined below and add 23.5 uL to each sample well in the sample plate.

PCR Reaction # 1 Master Mix (25 uL rxn, enough for 36 samples):

KOD 2X Master mix 450 uL

dH2O   360 uL

Template DNA   90 uL

4. Add 1.5 uL of each primer mix to the appropriate well as shown in the attached plate map.

5. Seal the plate, spin briefly, and place in the thermocycler to run the protocol as outlined below.

Regular TouchDown PCR protocol:

TouchDown64

96°C	2 min	
94°C	20 sec	
64-61-58°C	20 sec	3x3 cycles
70°C	40 sec	
94°C	20 sec	
57°C	20 sec	31 cycles
70°C	40 sec	
70°C	2min	
10°C	∞	

6. Once PCR is completed, store at 4°C overnight or -20°C.

3. Column PCR product Purification using Qiagen QIAquick PCR Purification:

1. If not done previously, dilute the concentrated Buffer PE by adding 45 ml ethanol (96-100%) to the Buffer bottle. Mark the check box on the bottle to indicate the completed step, initial and date.

2. Label the top of the purification columns and place in a provided 2 ml collection tube.

3. Add 125 uL (5:1 volume) of Buffer PB to each PCR reaction (25 uL rxn). Mix thoroughly by pipetting 2-3 times.

4. Transfer all solution from step above (150 uL total volume) to the center of the purification columns. Centrifuge for 30-60 seconds at 13,000 rpm. Discard the flow-through and place the column back into the collection tube.

5. Add 750 µl of Buffer PE to the column. Centrifuge for 30-60 seconds at 13,000 rpm. Discard the flow-through and place the column back into the collection tube.

6. Centrifuge for 1 minute at 13,000 rpm. Label a set of clean 1.5 ml microcentrifuge tubes.

7. Transfer the empty purification column to a 1.5 ml microcentrifuge tube. Add 50 µl of Buffer EB to the center of the purification column membrane, incubate for 1 min, and centrifuge for 1 min at 13,000 rpm. Pay attention to the orientation of the caps to avoid caps breaking up during spin.

8. Measure DNA concentration using DeNovix. Blank with the Buffer EB.

4. DeNovix DNA or RNA Concentrations (*from NEI OGL SOP "Measuring DNA concentrations using the DeNovix DS11 FX+ Spectrophotometer and Fluorometer"*):

1. Ensure the top arm is down and launch the dsDNA application (for RNA, select the RNA application) on the home screen.

2. Once the machine is initialized, lift the top arm and clean the upper and lower sample surfaces with a Kimwipe.

3. Pipette 1 µl of DNA diluent, or appropriate blanking solution, onto the lower sample surface. Lower the top arm and tap the Blank button.

4. After blank is taken, remove the solution from both sample surfaces using a Kimwipe.

5. Pipette 1 µl of DNA onto the lower sample surface. Lower the top arm and tap the Measure button.

6. Remove the solution from both sample surfaces using a Kimwipe.

7. After the last sample has been measured, pipette 2 µl dH$_2$O onto the pedestal. Lower the arm and let stand for 1 minute, then remove the water from both sample surfaces using a Kimwipe.

5. E-gel Electrophoresis (*from NEI OGL SOP "Site-directed Sequencing Test"*):

1. Add 14 µl water to every well in 2% E-Gel EX, then add 1 µl PCR reaction to each well with a multi-channel pipette.

2. Add 10 µl water and 5 µl ladder mix to Marker wells (*1 kb GeneRuler DNA Ladder used as marker*).

3. Run 15-20 min for mini e-gel. Run 10 min for the 48-well gel. If necessary to resolve the PCR bands better, run another 10-20 min.

4. Take a picture of gel using gel imager.

6. RHCglo Plasmid Preparation for Minigene:

Plasmid Digestion:

1. Pull any RHCglo plasmid (WT or mut) from the -20C OGL Plasmid box and thaw.

2. In a 1.5 mL tube, prepare the following mix. This may be scaled up depending on the amount of plasmid needed.

Plasmid Digestion Mix (50 uL Rxn, ~4 ug)):

RHCglo plasmid (PNPLA6WT or mut) 530 ng/uL	10.0 uL
CutSmart Buffer	5.0 uL
XbaI	0.5 uL
SalI-HF	0.5 uL
dH2O	34.0 uL

3. Place in thermocycler at 37°C for at least 16 hours, and then may stay at 4°C after.

Gel and Purification:

1. After incubation, run the sample on a 1.2% or 2% gel, loading 20 uL/well, watching the separation of bands. The bands may separate well after 20 min, but you may run up to 40 min to obtain good band separation.

2. The bands will separate out into 2 distinct bands (see below):
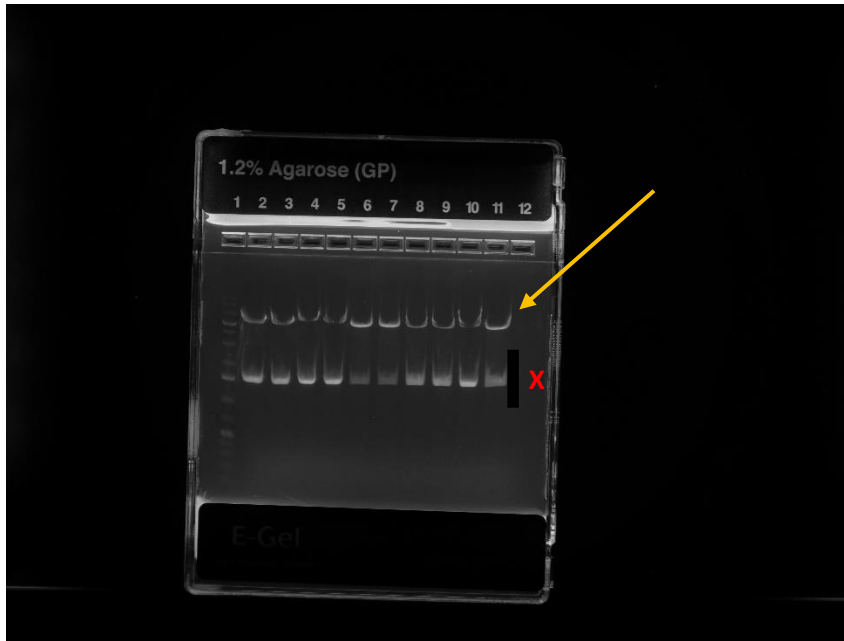
3. Carefully remove the top of the E-gel cassette using the E-gel opener (see below).

   a. Screw or unscrew the long silver screw using the black handle to increase or decrease the distance between the two flat ends so that the E-gel sits between the flat ends.

   b. Ensure that the silver razor edge is aligned with the edge of the E-gel cassette, between the cassette plates, on both sides.

   c. Screw to tighten and place pressure on E-gel cassette – You will need to use some force for this. You should visualize bubbles forming in the top of the gel between the gel and the top plate and hear cracking noises.

   d. Once it appears that the top plate is loose, you can unscrew to relieve pressure and carefully remove the top cassette plate.

SHARP EDGES
WATCH
YOUR FINGERS

Screw/unscrew to place pressure on E-Gel.

Place the E-gel between the two flat ends, carefully. There is a sharp razor edge on either end.

4. Cut out the top bands as indicated by the **orange arrow** in the gel image above. The lower bands (**red** "**X**") can be ignored. Begin gel extraction using the QIAquick Gel Extraction Kit (Qiagen # 28704).

   a. To five 1.5 mL snap cap tubes, add 600 uL of Buffer QG each.

   b. Using a clean, sharp edge and leaving approximately 1 mm edge around the top and bottom of the band, carefully cut around and in between the bands of the top row. Cut each band individually and carefully lift each band onto your cutting tool as it is cut.

   c. Add two cut fragments to each 1.5 mL tube by carefully shaking the gel fragments off of the tool into the Buffer QG. Each gel fragment is approximately 100 mg. *The max amount per spin column is 400 mg.*

5. Once the gel fragments have been added to the tubes, and ensuring the fragments are mixed into the Buffer QG, set the Eppendorf Thermomixer to 50°C.

6. Incubate the tubes at 50°C for 10 min and check to see that the gel has fully digested. Flick the tubes until the solution is clear yellow and quickly spin down. Expect the total volume, with added Buffer QG and gel fragments, to be around 700 uL on average (<750 uL per tube).

7. Place a QIAquick spin column in a provided 2 mL collection tube. **Spin columns may be used more than once, so for 5 sample tubes, you may use 4 spin columns and load 1 spin column twice (after spinning and pouring off the first sample).*

8. Add the entire sample from each sample tube to a separate spin column, directing the tip at the center of the column membrane when adding the sample, and centrifuge for 1 min at 13,000 rpm.

9. Discard the flow-through and place the QIAquick column back into the same tube.

10. Add 500 uL of Buffer QG to each QIAquick column, again directing the tip at the center of the of the column membrane, and centrifuge for 1 min at 13,000 rpm.

11. Discard the flow-through for each sample and place the QIAquick column back into the same tubes.

12. Add 750 uL of Buffer PE to each QIAquick column, incubate the columns at room temperature (RT) for 2 minutes, then centrifuge at 13,000 rpm for 1 min.

13. Discard the flow-through for each sample, place the QIAquick column back into the same tubes, and centrifuge one last time at 13,000 rpm for 1 min to remove any residual buffer.

14. Place each QIAquick column into a clean 1.5 mL microcentrifuge tube.

15. To elute the DNA, add 50 uL of Buffer EB to the center of each QIAquick membrane, incubate the columns at RT for 1 min, and then centrifuge the columns at 13,000 rpm for 1 min.

16. Combine the eluate from each tube into a single tube and measure the concentration on the DeNovix. *A good concentration should be around 85 ng/uL or more.*

7. Site-directed Mutagenesis with HiFi Assembly kit and PCR # 2:

HiFi Assembly:

1. Set up the HiFi assembly reactions *ON ICE/COLD BLOCK*. Prepare the HiFi reaction master mixes as outlined below.

HiFi Assembly Reaction WT [Vector+PCR 1A] Master Mix (10 uL rxn, enough for 25 samples):

HiFi MM   125 uL

dH2O   87.5 uL

RHCglo vector (25 fmol)   25 uL

HiFi Assembly Reaction Var [Vector+PCR 1B+1C] Master Mix (10 uL rxn, enough for 25 samples):

HiFi MM   125 uL

dH2O   75 uL

RHCglo vector (25 fmol)   25 uL

2. Add 9.5 uL of the WT MM to the appropriate sample tubes.

3. Add 9 uL of the Var MM to the appropriate sample tubes.

4. Add 0.5 uL of PCR 1A product (50 fmol) from PCR # 1 to each of the corresponding WT sample tubes.

5. Add 0.5 uL each of PCR 1B product and PCR 1C product (*1 uL total PCR product*) from PCR # 1 to each of the corresponding Var sample tubes.

6. Place the samples in the thermocycler at 50°C for 15 minutes.

PCR Reaction # 2:

7. Set up PCR Reaction # 2 master mix as outlined below and add 24.5 ul to each sample tube.

PCR Reaction # 2 Master Mix (25 uL rxn, enough for 45 samples):

KOD 2X Master mix 562.5 uL

dH2O   472.5 uL

Primer mix SplF + SplR (10 +10)   67.5 uL

4. Add 0.5 uL of HiFi assembly product to each of the corresponding sample tubes.

5. Place the samples in the thermocycler to run the protocol as outlined below.

Regular TouchDown PCR protocol:

TouchDown64

96°C	2 min	
94°C	20 sec	
64-61-58°C	20 sec	3x3 cycles
70°C	40 sec	
94°C	20 sec	
57°C	20 sec	31 cycles
70°C	40 sec	
70°C	2min	
10°C	∞	

6. Once PCR is completed, store at 4°C overnight or -20°C.

8. Setting up HEK293 Cell Culture from Frozen Aliquot

1. Ensure that you have enough premade culture media to begin:

    a. **DMEM Prepared Media**: Gibco DMEM with GlutaMAX and high glucose (ThermoFisher cat # 10566016), Sigma FBS (F0926-500 mL), ATCC PenStrep Solution (cat # 30-2300, 100X)

        i. To one 500 mL bottle of DMEM, add 50 mL of FBS and 5 mL of PenStrep

2. Place the culture media at room temperature (RT) as you prepare your workspace. Media should sit 15-30 min at RT.

3. Prepare your workspace – Clean work surface, bottles, your gloves with 70% ethanol. Be sure to have supplies needed for the culture nearby or set up in the hood to reduce the number of times you will need to go in and out of the culture hood.

4. Label a T-175 flask with the cell name, date, and passage number (i.e., HEK293, 5-31-23, p6). Add 35 mL of DMEM/FBS/PenStrep mix as prepared above to the T-175 flask and place in the 37°C incubator for 10 min to prewarm.

5. Remove the HEK293 cell aliquot from the freezer and place in the 37°C dry bath for 1-2 min.

6. Add the cells from the tube to the prewarmed T-175 flask and place back in the 37°C incubator.

7. Allow to grow for 48 hours and check growth.

8. If continuing culture, split the cells once they are confluent or near confluent. You'll notice the media color will change from red/pink to orange/yellow as the cells become confluent.

    a. Label a new T-175 flask, ensuring that you update the passage number. The prepared media should be brought to RT.

    b. Remove the culture media from the culture flask and discard.

    c. Rinse the cells with 10 mL dPBS (Gibco cat # 10010-023, 1X, pH 7.4), remove and discard.

    d. Add 10 mL TrypLE (Gibco Select CTS cat # A12859-01) and incubate at 37°C for 5 min to detach the cells.

    e. Add 10 mL of DMEM prepared media and pipet up and down to resuspend the cells.

f. Remove 5 mL of cell mixture and place in newly labeled flask. Add 30 mL of DMEM prepared media and place in 37°C incubator.

g. Check cells again for growth/confluency in 2 days if continuing cell culture or planning to freeze down.

Notes:

- Be sure to use aseptic technique! Cleanliness is essential during tissue culture. Wipe any bottles, vials, working hood surface, and your gloves with 70% ethanol. Change your gloves frequently and be sure to clean your workspace both before and after tissue culture.

- If you do not prewarm the media, you will likely stress or shock the cells and many of the cells may die. You want to go directly from the freezer to dry bath to do a quick thaw because it stresses the cells less than a long thaw.

- HEK293 cells are adherent but do become round and detach during expansion. Any floating dark cells visualized are dead cells.

- HEK293 cells grow fast, so you have to monitor the growth and passage as needed. The larger the culture flask, the more room for growth and more cells will grow.

- Check for rod or string-shaped bacteria when viewing cells for contamination. Fungus is often visible to the naked eye (nothing should be floating in your culture). If a culture becomes contaminated, discard, and clean the incubator thoroughly.

- For more information, here is a great guide for HEK293 cells as well as links to videos on general tissue culture techniques: HEK293 Cells: Background, Applications, Protocols, and More (synthego.com)

- This link provides a volume table for various sized culture flasks/plates/dishes: https://www.thermofisher.com/us/en/home/references/gibco-cell-culture-basics/cell-culture-protocols/cell-culture-useful-numbers.html
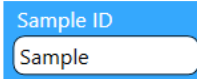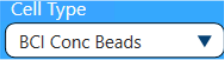
9. Vi-Cell Blu Cell Counting protocol
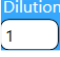
1. Click [☰] and then [⌂ Home] to display the carousel Sample Set.
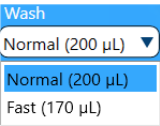
2. Check the Reagent Status to ensure there is enough reagent to complete the sample set. If there are not enough cycles in the reagent pack, the pack should be replaced.

3. Select to create a sample set.
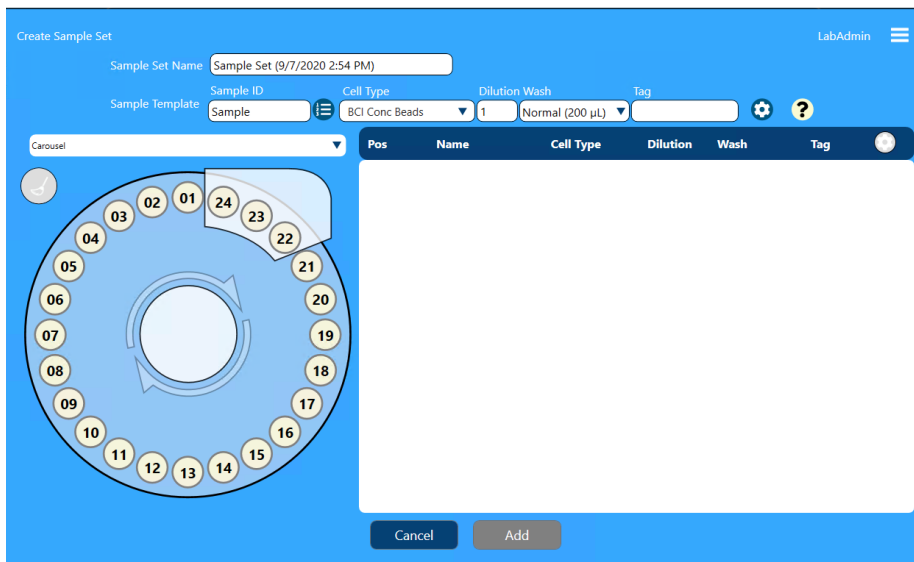
4. Enter a sample name . Optional.

5. Select Cell Type from the dropdown menu . Select BCI Default.
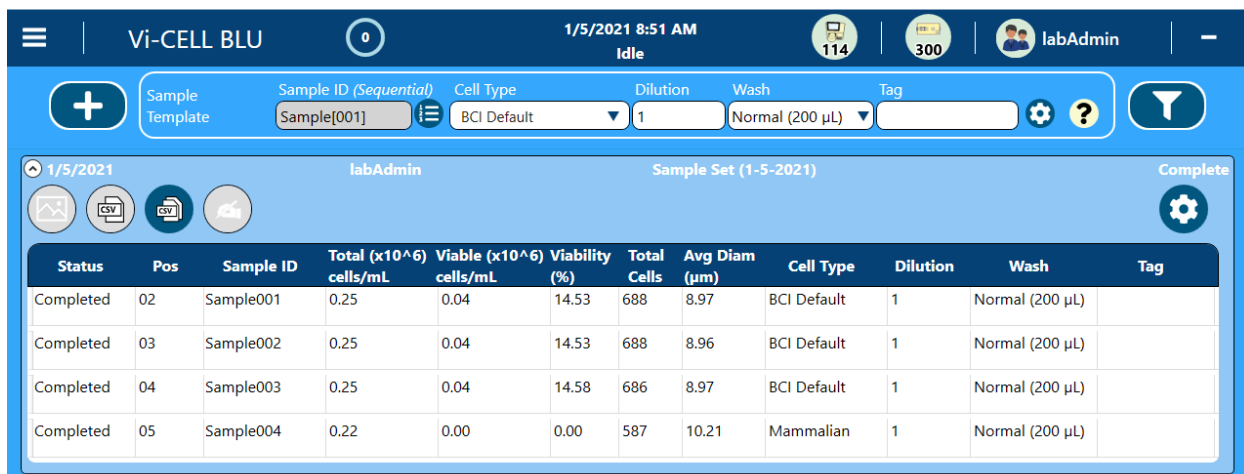
6. Enter a dilution factor (whole number 1 – 9999) [Dilution: 1]. Leave at 1.

7. Select the Normal wash mode setting [Wash: Normal (200 µL) ▼ / Normal (200 µL) / Fast (170 µL)].

8. Select [Add] to create the sample set.

9. Manually rotate the carousel to load the sample tubes onto the carousel to match what was selected on the sample set (if location 5 was selected for a sample, ensure that the sample is placed in location 5).

10. Select [▶] to Run the samples in the carousel. The carousel will rotate to look for tubes and process the samples.

11. When finished, the completed Sample Set screen is displayed.

Status	Pos	Sample ID	Total (x10^6) cells/mL	Viable (x10^6) cells/mL	Viability (%)	Total Cells	Avg Diam (µm)	Cell Type	Dilution	Wash	Tag
Completed	02	Sample001	0.25	0.04	14.53	688	8.97	BCI Default	1	Normal (200 µL)	
Completed	03	Sample002	0.25	0.04	14.53	688	8.96	BCI Default	1	Normal (200 µL)	
Completed	04	Sample003	0.25	0.04	14.58	686	8.97	BCI Default	1	Normal (200 µL)	
Completed	05	Sample004	0.22	0.00	0.00	587	10.21	Mammalian	1	Normal (200 µL)	

12. Note the cell count and % viability for each sample.

10. Transfection:

1. Dilute 200 ng DNA to 50 ul Opti-MEM in each well of a 24 well plate. Refer to DNA concentrations. *The DNA can be added to 50 uL of Opti-MEM at 200 ng. The further dilution in Opti-MEM is negligible.*

2. Prepare Opti-MEM/Lipofectamine 2000 mix. Add 20 uL of Lipofectamine 2000 to 2 mL of Opti-MEM (enough for 40 samples) and incubate at RT for 5 min.

3. Add 50 uL of Opti-MEM/Lipofectamine directly to each well containing DNA. Mix and incubate another 20 min at RT.

4. During incubation, remove culture media from T-175 flask and add 10 mL of PBS to gently rinse. Remove PBS, then add 5 mL of TrypLE and incubate in the incubator for 3 min. Add 7 mL of 10% Complete DMEM (with FBS/Pen Strep) and rinse/pipet up/down 5 times to break up any clumps. Place cells into conical and perform cell count on Vi-Cell Blu using 100 uL of cells for count.

5. The cells should be 0.8 x 10^6 c/mL. Aliquot 400 uL of cells at that concentration to each well. Gently rock plates front and back, left and right to mix. *Do not swirl, which will accumulate cells to the center.*

6. Place plates in incubator overnight.

7. Harvest cells 20-28 hours.

11. Cell Harvest and RNA Extraction (*adapted from NEI OGL SOP "RNA Extraction from Whole Blood"*):

1. Prepare Resuspension Buffer (RB) with β-ME if not done previously:

2. Add 50 µL of β-ME to 5 mL of RB Buffer in a 50 mL conical tube. Alternatively, if the kit is going to be used up in a month, add 600 µL of β-ME to the 60 mL bottle of RB buffer. Record RB+βME, initials, and date on the tube or bottle. Vortex briefly.

** *β-ME is stored at 4C. Work with β-ME in the fume hood, as it has a strong odor and is a dangerous chemical.*

**The RB +βME mix can be stored at room temperature for 1 month.*

3. Remove media from each culture well in the 24-well plate using the vacuum in the tissue culture hood.

4. Add 400 µL RB Buffer mix to each well, incubate at room temperature for 2-3 minutes, swirl and accumulate the sample at the bottom of each well by gently tipping the culture plate.

5. Remove the cell lysis solution for each sample and place in a spin column. *To note, the cell lysis solution will be sticky, so you may consider using a cell scraper to help remove media.*

6. Centrifuge the columns for 2 minutes at 13,000 rpm and place in an XTRACT sample tube or Sarstedt tube (curved bottom). Samples can be stored at -20°C until running on the XTRACT16+. *Samples will become cloudy in appearance once frozen but will become clear when thawed.*

7. Bring the XTRACT 16+ T-rack into the hood.

8. Place the labeled sample and eluate tubes into the T-rack.

9. Place the sample tube in the leftmost column in the W1 position on the T-rack (see image below), moving from left to right for subsequent samples. Place the eluate tube in the W5

position of the same column in the T-rack as its corresponding sample tube. Take care to open and bend the eluate tube caps backward with the cap connector sitting in the slot so that it does not obscure the opening of the tube.
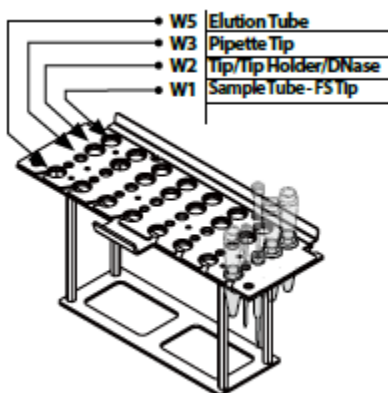
10. Place a pipette tip into the W3 position of each column that contains a sample. Pipette tips need to be removed from the paper and pulled out of the plastic cover.

11. On the XTRACT16+, Select *Set Up Run*.

12. Press *Start* on the home screen.

13. Retrieve the correct number of reagent cartridges and place into the cartridge rack by holding the end with the sticker and inserting the back end into the space below the fixing plate of the cartridge rack. Ensure that the cartridges are seated flat.

14. Insert the T-rack into the instrument. If the T-rack does not sit flush with the cartridge rack, the reagent cartridges may need to be adjusted.

15. Insert the waste bin into the instrument and ensure that it is pushed all the way in.

16. Configure and Start Run: Press *Next* to choose the Cartridge Code. The Cartridge code is located on the sticker of each cartridge (631 for TriXact RNA Kit). Press *No* for DNase treatment. Select 400 µL for the Sample Volume. Select 100 µL for the Elution Volume.

17. Ensure that nothing is obscuring the openings of any sample or eluate tubes, then close the door and press *Start*.

12. RT PCR:

iScript RT-qPCR (10 uL rxn volume; 300 ng of RNA):

1. Set up the RT PCR reactions *ON ICE/COLD BLOCK*.

2. Add 2 uL of the iScript RT Supermix to each sample tube.

3. Water and sample volumes will vary according to individual RNA concentrations. *The table below provides example concentrations and volumes.* Add dH2O to each sample tube according to the table.

4. Add RNA sample to the appropriate sample tube according to the table volumes.

Sample #	RNA Extraction concentrations- Batch 1 (ng/uL)	RNA volume for RT PCR	H_2O volume for RT PCR
1	42.96	7.0	1.0
2	41.79	7.2	0.8
3	40.8	7.4	0.6
4	40.37	7.4	0.6
5	43.25	6.9	1.1
6	45.62	6.6	1.4
7	39.72	7.6	0.4
8	38.86	7.7	0.3
9	44.15	6.8	1.2
10	40.84	7.3	0.7
11	65.62	4.6	3.4
12	66.89	4.5	3.5
13	99.13	3.0	5.0
14	87.71	3.4	4.6
15	118.32	2.5	5.5
16	93.79	3.2	4.8

17	92.42	3.2	4.8
19	99.04	3.0	5.0
20	101.12	3.0	5.0
21	100.79	3.0	5.0
22	110.38	2.7	5.3
23	101.92	2.9	5.1
24	101.48	3.0	5.0
25	109.56	2.7	5.3
26	87.82	3.4	4.6
27	102.42	2.9	5.1
28	93.37	3.2	4.8
29	103.14	2.9	5.1
30	100.28	3.0	5.0
33	101.64	3.0	5.0
34	96.54	3.1	4.9
35	93.17	3.2	4.8
36	110.13	2.7	5.3
37	97.97	3.1	4.9
38	100.94	3.0	5.0
39	110.63	2.7	5.3
40	83.54	3.6	4.4

5. Place the samples in the thermocycler and run the iScript protocol.

iScript

25°C	5 min
46°C	20 min
95°C	1 min

10°C	∞

6. Add 40 ul 1xTE to each sample. Samples may be stored at 4°C overnight or -20°C.

13. Sanger Sequencing (*from NEI OGL SOP "Site-directed Sequencing Test"*):

1. Using a multichannel pipette, split PCR reactions in half by transferring 8 µl PCR reactions to the next column over, according to plate map. The first column will be used for M13 Forward sequencing reaction, and the second column will be used for M13 Reverse sequencing reaction.

2. Create forward and reverse sequencing master mixes according to the table below (example master mix for 14 samples shown below). Record lot numbers and expiration dates.

Reagent	Vol (µl)	14X (µl)
BigDye® Direct Sequencing Master Mix	2	28
BigDye® Direct M13 F OR R primer	1	14
Total volume to add to each reaction	3	

**sequencing reagents (primers & mastermix) may be used up to 5 years following the expiration date on the tube.

3. Using a repeater pipette or multichannel pipette, add 3 µL of sequencing reaction mix to the appropriate Forward or Reverse columns.

4. Use the BigDye-Direct-Seq program shown below on a validated thermocycler, record which cycler was used.

BigDye-Direct-Seq		
37°C	15 min	
80°C	2min	
96°C	1min	
96°C	10 sec	
50°C	5 sec	25 cycles
60°C	4 min	
10°C	∞	

5. Samples can be stored at +4°C overnight or extended time at -20°C.

14. Sanger Product Cleanup (*from NEI OGL SOP "Sanger Cleanup and Capillary Preparation"*): *Reaction Electrophoresis*

1. Sequencing reactions are purified using Edge Bio Performa DTR Ultra plates. Retrieve the Edge plate from the fridge. Peel off the bottom seal and then the top seal slowly.

2. Place on a waste plate, and pre-spin for 5 min at 850 rcf. Check to see if any of the wells of the Edge plate appear abnormal (*wells should all look uniform*). Avoid using any abnormal wells in the Edge plate. Dump pre-spin waste plate contents down the sink, rinse waste plate, then place on drying rack for future use.

3. Place Edge plate on a new collection plate (PCR plate) labeled with EDGE-Initials-date. Load the entire sequencing reaction (12 µl) on to the center of the column and spin 5 min at 850 rcf.

4. Pay close attention to following plate map, as after final spin all the wells will be filled and look identical.

5. Thaw HiDi Formamide and add 10 µl to each well in a new PCR plate labeled with HiDi-Initials-date.*Make sure HiDi is added to all wells that the array tips may occupy (array loads in sets of 4 or 8 per column).*

6. Label wells, columns, or rows if needed as a sample guide. Transfer 3 µl EDGE-eluate to HiDi plate to the correct wells.

7. Spin briefly, and heat for 3 min at 95°C.

8. Immediately transfer to a cold block in 4°C fridge and chill for at least 3 min.

9. Seal the EDGE-eluate plate with foil seal and store at -20°C until all testing is confirmed and finalized.

15. Sanger Sequencing (*from NEI OGL SOP "Operation and Maintenance for the SeqStudio Genetic Analyzer"*):

1. Sample can be run either on a plate or 8-well strips. *Samples are stable for 16-24 hours on the instrument.*

2. Plate setup can be performed on the Cloud (thermofisher.com/cloud), on a PC, or on the instrument. On the preferred platform, open the Plate Manager software.

3. In the Plate Setup screen, create or open a plate setup in PSM or CSV file.

4. In the properties tab, edit the Plate Name (Initials_Date), select Shared in the Plate setup security field, and select Sequencing as the application type.

5. In the Sequencing analysis settings, select Analysis settings 2018 and click Next.

6. In the Plate screen, add the sample names using the plate or line-by-line view.

**Load samples or Hi-Di to all wells in the injection group. Samples should be loaded in duplicate if there are empty wells in the injection group.

7. Select a dye set for the injection group.

8. Select a run module MediumSeq.

9. Click Next and proceed to "Save a plate setup in the Plate Manager" in the cloud or save to a flash drive. *The default injection order is: A1-D1, E1-H1, A2-D2, E2-H2…A12-D12, E12-H12. Injection groups can be skipped using the Plate Manager.*

10. Add HiDi or HiDi mixture according to the specific protocol being performed.

11. Add the appropriate sample volume to the plate according to the protocol.

12. Centrifuge the plate assembly briefly to collect the contents at the bottom of each well.

13. Heat at $95°C$ for 3 minutes.

14. Cool in the metal blocks at $4°C$ for 3 minutes or until loaded onto the instrument.

15. Place a septum on the plate. Align the holes of the septa with the wells and press gently until it is seated flat on the plate. For strips use the following plate assembly:

① Septum
② 96-well retainer
③ 8-tube strip
④ MicroAmp™ 96-well tray
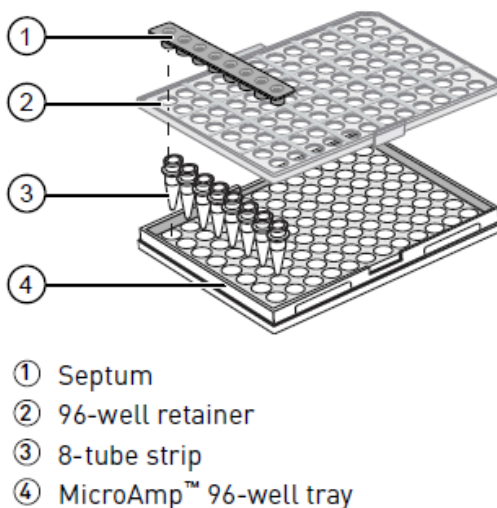
16. Touch Eject plate, then open the instrument door when prompted.

17. Press the release button on the autosampler to open the lid, then remove the cathode buffer container (CBC) on the right side.

18. Ensure that the level of the buffer is above the fill line.

19. Close the autosampler lid. Press down on the center of the lid or press down on both sides of the lid with equal pressure until the lid clicks shut.

20. Touch Retract plate, then close the instrument door.

21. In the instrument home screen, touch Setup run.

22. Import the plate setup file from cloud or flash drive to the SeqStudio.

23. Verify that settings are correct as needed. Specify the Save location to Cloud or USB. Touch Start run.

Appendix B

Variants and Primers

Variant	Gene_exon/intron	Outer_fwd	Outer_rev	Var_fwd	Var_rev
ABCA4:NM _000350.3:c. 1299A>G	ABCA4_E10	ggtgctgggaagcgaaagg GTTCTGTCAGCCCAGGAAG	gttcgggcagctcgactagTACATATTTCTCATCCAAAGTCAGTGAC	cctgggaagagGTAGGGCCCCAGATCTGG	gggccctaccTCTTCCCAGGCTTTGACC
ABCA4:NM _000350.3:c. 2226T>A	ABCA4_E15	ggtgctgggaagcgaaagg GTACTGATGACTGTTAGGAG	gttcgggcagctcgactagTGGTGAGGAGTCACTGTTGC	ctttctccacaGCCACCATCATGCTGTGC	gatggtggctGTGGAGAAAGCCAACAAG
ABCA4:NM _000350.3:c. 264A>T	ABCA4_E3	ggtgctgggaagcgaaaggGATCCGTCTGTCTCCCCAC	gttcgggcagctcgactagTCAAGAAATTTTGTGCACG	caccccaggtGAATCTCCTGGAATTGTG	caggagattcaCCTGGGGTGGGGCTTTGA
ABCA4:NM _000350.3:c. 2736A>T	ABCA4_E18	ggtgctgggaagcgaaaggGATGGCACATTGAGAGGAGG	gttcgggcagctcgactagTTATTTGCTTTCTCCAGGAAATATG	gcacccagatGGAATACACGGTAAAACC	cgtgtattccaTCTGGGTGCTCTGGATCC
ABCA4:NM _000350.3:c. 2904G>T	ABCA4_E19	ggtgctgggaagcgaaaggGAATTTGTGTAAAGCAGTCGAAGCAG	gttcgggcagctcgactagTCACTTCCCCGGCACACAAAAG	tggagctggtAAAACCACCACCTTGTGAGTC	tggtggttttaCCAGCTCCATTGTGGCCC
ABCA4:NM _000350.3:c. 3018C>T	ABCA4_E20	ggtgctgggaagcgaaaggGTTTGAGGCTGGGAATCCCAAAG	gttcgggcagctcgactagTAGGGAGGAGCCCTCAGCT	gagccttggtATGTGTCCACAGCACAACATCC	gtggacacataCCAAGGCTCTGCCGGACT

ABCA4:NM _000350.3:c. 3462C>T	ABCA4_E23	ggtgctgggaa gcgaaaggG AGACACT GTGTGTG GCAATG	gttcgggcagctc gactagTTAA TACTTGCA GACCATTT AAAG	ttggcacaggtT TGTACTTA ACCTTGGT G	taagtacaaaCC TGTGCCAA AGCAGTTC
ABCA4:NM _000350.3:c. 4446C>A	ABCA4_E30	ggtgctgggaa gcgaaaggG GAGATGG TTATTCC CCAG	gttcgggcagctc gactagTAAG CTTTTGGT GAGTGGC	ggacacaggtaA ACCCTTCA CCATCCTG C	tgaagggtttAC CTGTGTCC ATTTCTGC
ABCA4:NM _000350.3:c. 6000C>T	ABCA4_E43	ggtgctgggaa gcgaaaggG ACAATTT CTCGTTG TTTTTAA GTCTTG AATCTTT AC	gttcgggcagctc gactagTAAT CCATCCCA ACAGAGG	cgtagcaggtA AGAGGTGA GTATCCTG C	ctcacctcttaCC TGCTACGG TGGCATCC
ABCA4:NM _000350.3:c. 6207C>T	ABCA4_E45	ggtgctgggaa gcgaaaggG ATGCTGA GCAGGCT GGGC	gttcgggcagctc gactagTAGG ATGTGCGC AGTCCCAA G	cctggctggtAC GTACAGTG GGGGCAAC	cactgtacgtaC CAGCCAGG CAGTCGGC G
ABCA4:NM _000350.3:c. 6345C>T	ABCA4_E46	ggtgctgggaa gcgaaaggG GTGGGCT GAAATGG GCCC	gttcgggcagctc gactagTACA CAGGATCC AGGTGGAT C	catcgtgagtAT CATCAGAG AAGGGAG GG	ctctgatgataCT CACGATGA CGTTCCAC AG
ABCA4:NM _000350.3:c. 6360G>T	ABCA4_E46	ggtgctgggaa gcgaaaggG GTGGGCT GAAATGG GCCC	gttcgggcagctc gactagTACA CAGGATCC AGGTGGAT C	cagagaaggtA GGGCTGTG GTCCTCAC ATC	ccacagccctaC CTTCTCTG ATGATCCT CACGATG
CHD7:NM_0 17780.4:c.37 47G>T	CHD7_E15	ggtgctgggaa gcgaaaggG CCTCTTC TCTATCT TCCC	gttcgggcagctc gactagTAAA GGCAAGGT GAGATTC	tggaattgcgtA AGTGCTGC AATCATCC G	gcagcacttaCG CAATTCCA TCATAGTG

CHD7:NM_0 17780.4:c.45 12G>T	CHD7_E19	ggtgctgggaa gcgaaaggG GCCCAAA CCATTTA TTTATTC	gttcgggcagctc gactagTGGG AAGCAGAT ACAAGGAT G	agtcagaaggtA AAGGTTCC ACATTTGC TAAG	ggaacctttaCC TTCTGACT CAATGGTA ATG
CHD7:NM_0 17780.4:c.46 41G>T	CHD7_E20	ggtgctgggaa gcgaaaggG TTGCTCC CTATCAT TTATC	gttcgggcagctc gactagTACG CCGTGGCT TTGCACA	ccttaaatggtA GGGTGAGT AAGAAGTC CCATTCG	actcaccctaCC ATTTAAGG CATCAATA TC
CHD7:NM_0 17780.4:c.54 54G>A	CHD7_E26	ggtgctgggaa gcgaaaggG GTGGTAA TTCTGAT AATATCC CTGAAGT GTAACTT G	gttcgggcagctc gactagTGAT TGCGGGAA ATGACATT TG	gtgctttctaGA ACGAGTCG GTATGCCT G	cgactcgttctA GAAAGCAC AGCGCGGG G
CHD7:NM_0 17780.4:c.58 41A>G	CHD7_E29	ggtgctgggaa gcgaaaggG AGGACTA ATAAATA ATGTTTT CATCCCC TCTAAGG AGGTAAA AAAG	gttcgggcagctc gactagTGCA TCATACTT CAGGAAA AGAC	ctcgagaggagG TGAGAGCT CTGGAAGC G	agctctcaccTC CTCTCGAG GCCGCCGT
CHD7:NM_0 17780.4:c.77 38C>T	CHD7_E35	ggtgctgggaa gcgaaaggG GCCCACC TCGGCCT CCCA	gttcgggcagctc gactagTTAA CGCGCATC TTCAAATA ACTG	gggactaggtTG GTGGGGGA AGATGCTC	tcccccaccaaC CTAGTCCC ATCTTCAA GATTGATA ACAGGGAT CCG
CHD7:NM_0 17780.4:c.79 65G>T	CHD7_E36	ggtgctgggaa gcgaaaggG TAGATAA AAGGAAA AGCCAAT TC	gttcgggcagctc gactagTCAT AGCTCCAC CCATCTG	aacgaaatggtA AGAAGGTA AACGCTGG G	taccttcttaCCA TTTCGTTT ATTGACAA C

92

CHD7:NM_0 17780.4:c.81 15T>A	CHD7_E38	ggtgctgggaa gcgaaaggG TACCTCA CTGATGA GTAGC	gttcgggcagctc gactagTCTC TCAAATTT CATCTCTC CTAGGGAT AATAAATA ATGCACTG	gccttctcacaG GGCCTGTA GTGCGGGG A	tacaggccctGT GAGAAGGC GGTCAAAC

Notes. E=exon, In=intron, Outer_fwd=Outer forward wildtype primer, Outer_rev=Outer reverse

wildtype primer, Var_fwd=Variant-specific forward primer, Var_rev=Variant-specific reverse prime

Appendix C

Variant Position, SpliceAI Scores, and Minigene Outcomes

Figure C1

Variant Position and SpliceAI Scores

ABCA4:NM_000350.3:exon10:c.1299A>G:p.E433= Splice type: Exonic; Genomic pos: 94,544,203, 59 bases from intron 9, 58 bases from intron 10
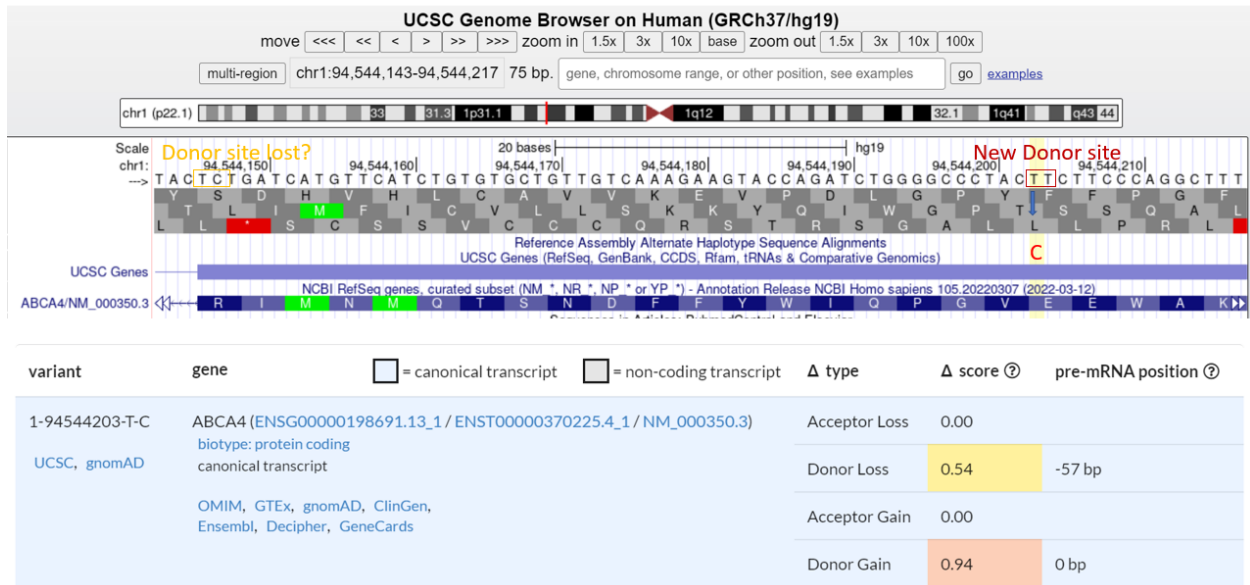
Figure C2

Variant Position and SpliceAI Scores

ABCA4:NM_000350.3:exon15:c.2226T>A:p.T742= Splice type: Exonic; Genomic pos: 94,522,313, 65 bases from intron 14, 156 bases from intron 15
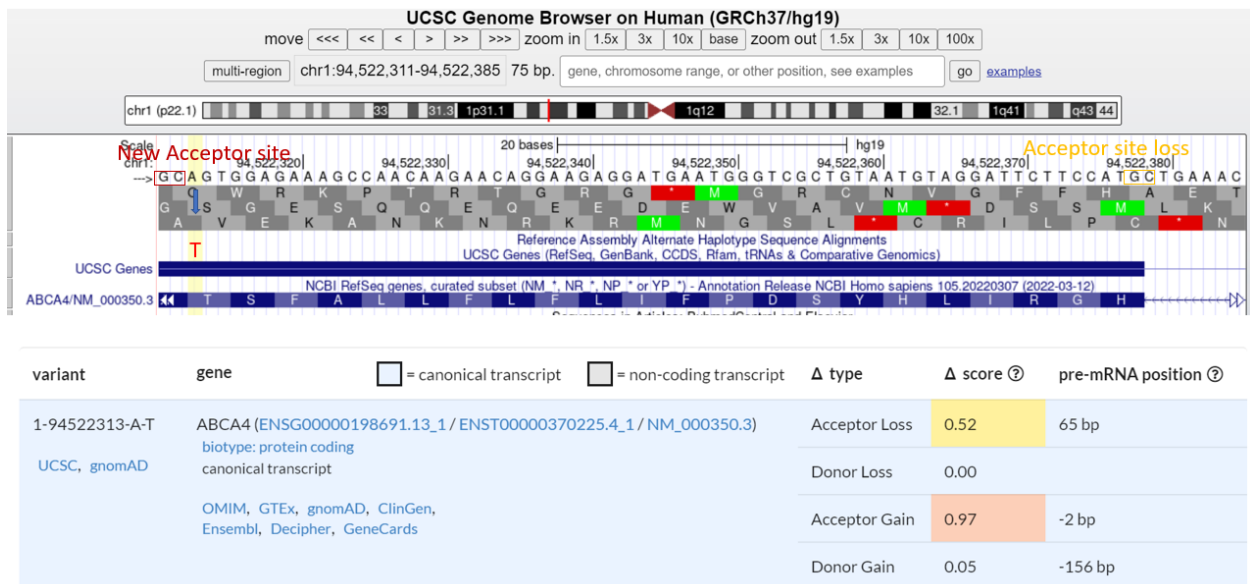
Figure C3

Variant Position and SpliceAI Scores

ABCA4:NM_000350.3:exon3:c.264A>T:p.G88=

Splice type: Exonic; Genomic pos: 94,577,032, 104 bases from intron 2, 40 bases from intron 3

variant	gene			Δ type	Δ score ⊙	pre-mRNA position ⊙
1-94111476-T-A	ABCA4 (ENSG00000198691.13 / ENST00000370225.4 / NM_000350.3)	= canonical transcript	= non-coding transcript	Acceptor Loss	0.00	
UCSC, gnomAD	biotype: protein coding			Donor Loss	0.06	-38 bp
	canonical transcript			Acceptor Gain	0.00	
	OMIM, GTEx, gnomAD, ClinGen, Ensembl, Decipher, GeneCards			Donor Gain	0.82	2 bp
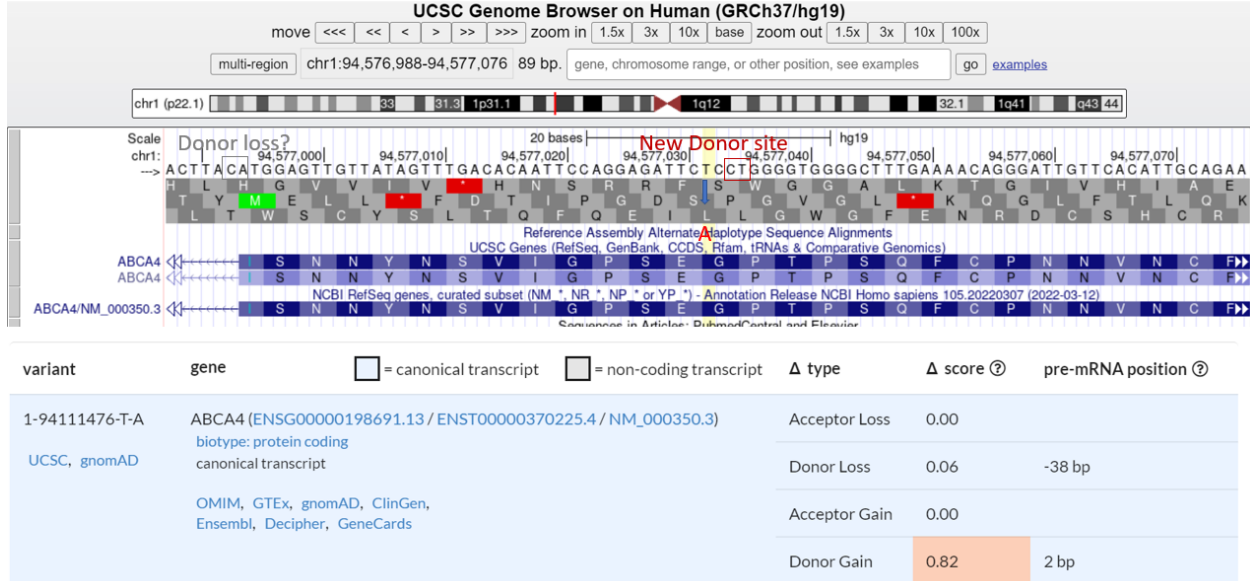
Figure C4

Variant Position and SpliceAI Scores

ABCA4:NM_000350.3:exon18:c.2736A>T:p.G912=

Splice type: Exonic; Genomic pos: 94,514,431, 83 bases from intron 17, 8 bases from intron 18

variant	gene			Δ type	Δ score ⊙	pre-mRNA position ⊙
1-94514431-T-A	ABCA4 (ENSG00000198691.13_1 / ENST00000370225.4_1 / NM_000350.3)	= canonical transcript	= non-coding transcript	Acceptor Loss	0.00	
UCSC, gnomAD	biotype: protein coding			Donor Loss	0.11	-7 bp
	canonical transcript			Acceptor Gain	0.06	122 bp
	OMIM, GTEx, gnomAD, ClinGen, Ensembl, Decipher, GeneCards			Donor Gain	0.92	2 bp
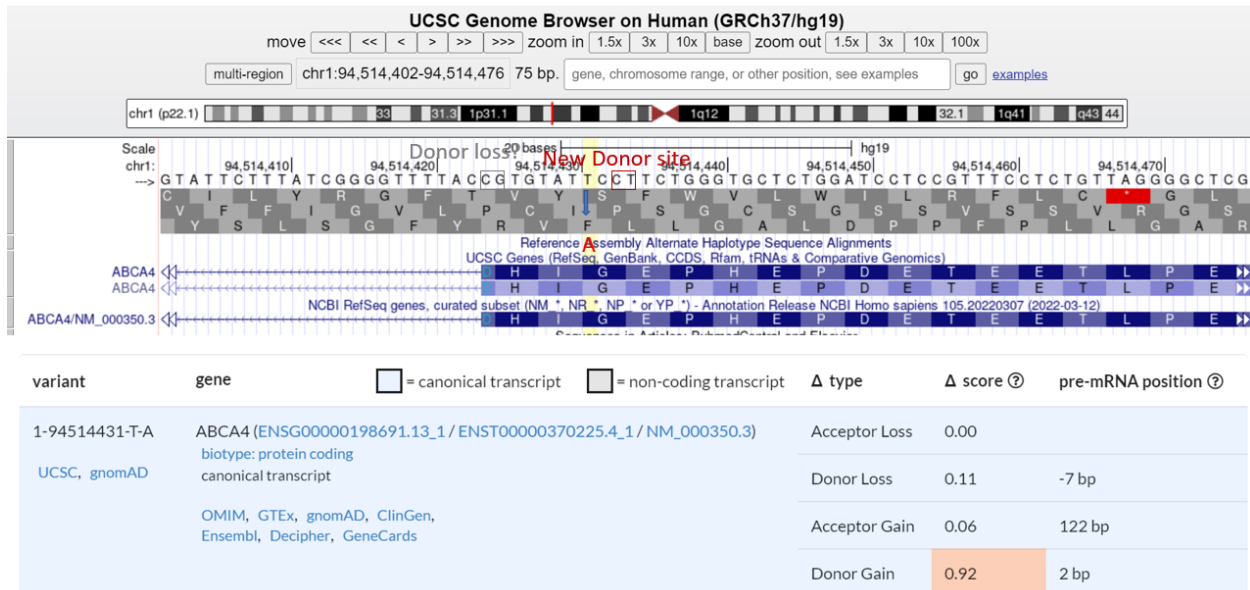
Figure C5

Variant Position and SpliceAI Scores
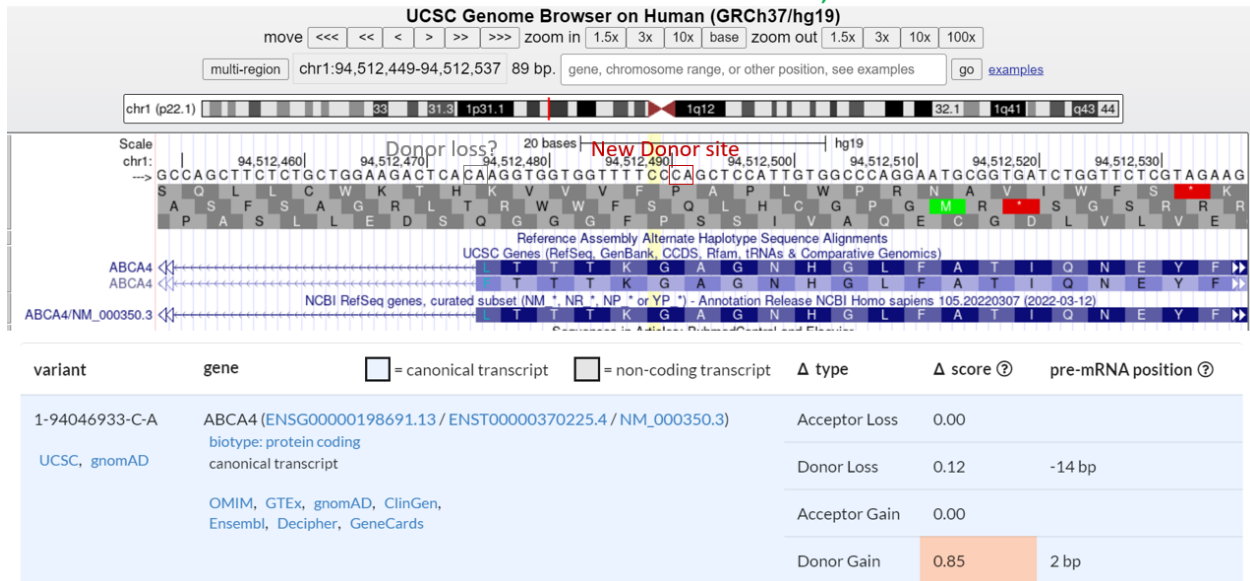
Figure C6

Variant Position and SpliceAI Scores

Figure C7

Variant Position and SpliceAI Scores

96
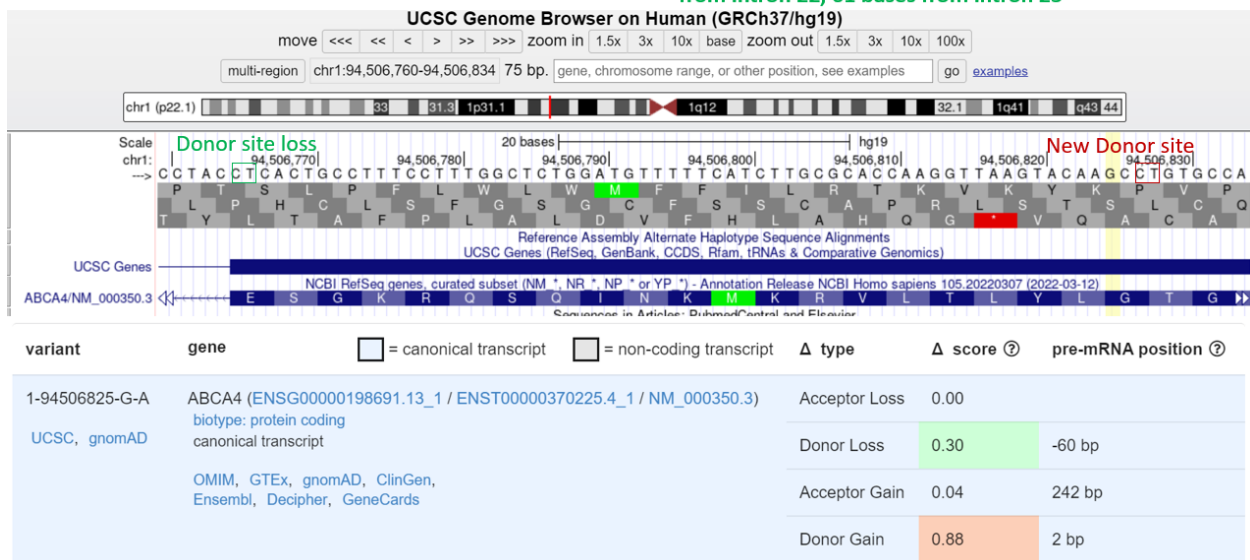
Figure C8

Variant Position and SpliceAI Scores
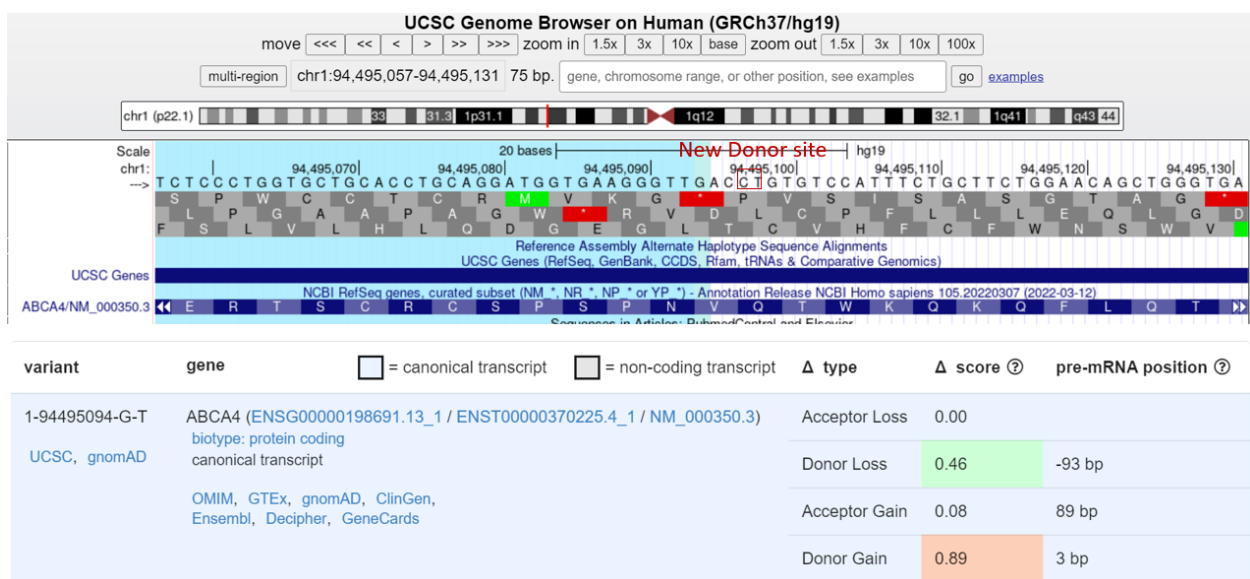
Figure C9

Variant Position and SpliceAI Scores

ABCA4:NM_000350.3:exon43:c.6000C>T:p.G2000=

Splice type: Exonic; Genomic pos: 94,473,195, 102 bases from intron 42, 6 bases from intron 43

variant	gene	= canonical transcript	= non-coding transcript	Δ type	Δ score ⑦	pre-mRNA position ⑦
1-94473195-G-A	ABCA4 (ENSG00000198691.13_1 / ENST00000370225.4_1 / NM_000350.3) biotype: protein coding canonical transcript			Acceptor Loss	0.00	
UCSC, gnomAD				Donor Loss	0.04	-5 bp
	OMIM, GTEx, gnomAD, ClinGen, Ensembl, Decipher, GeneCards			Acceptor Gain	0.01	130 bp
				Donor Gain	0.83	2 bp
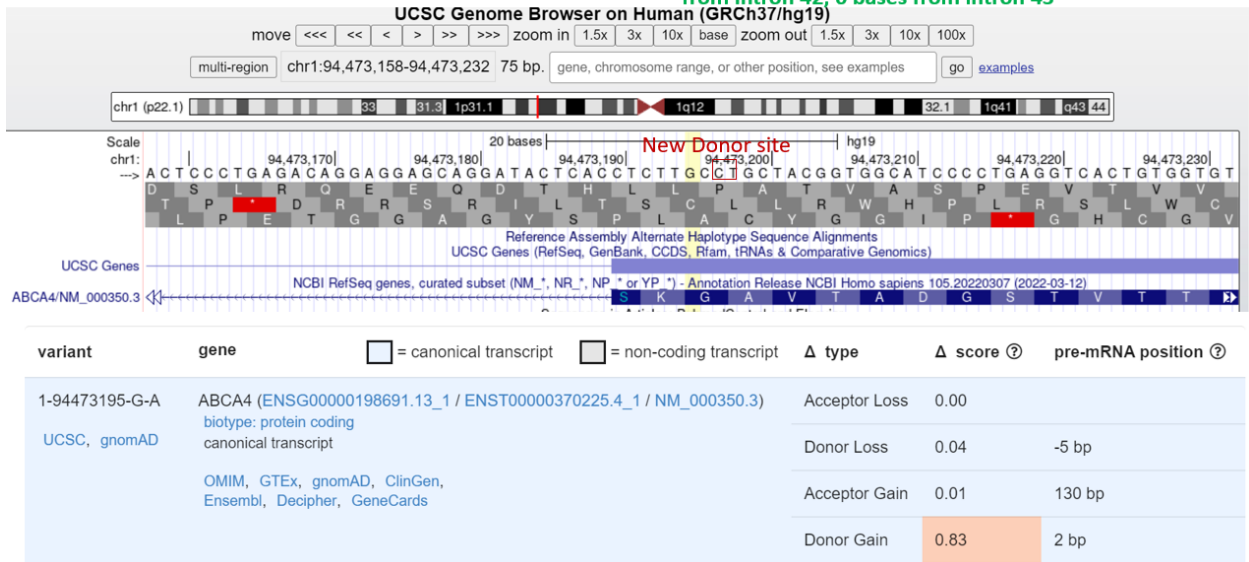
Figure C10

Variant Position and SpliceAI Scores

ABCA4:NM_000350.3:exon45:c.6207C>T:p.G2069=

Splice type: Exonic; Genomic pos: 94,467,489, 60 bases from intron 44, 76 bases from intron 45

variant	gene	= canonical transcript	= non-coding transcript	Δ type	Δ score ⑦	pre-mRNA position ⑦
1-94467489-G-A	ABCA4 (ENSG00000198691.13_1 / ENST00000370225.4_1 / NM_000350.3) biotype: protein coding canonical transcript			Acceptor Loss	0.00	
UCSC, gnomAD				Donor Loss	0.00	
	OMIM, GTEx, gnomAD, ClinGen, Ensembl, Decipher, GeneCards			Acceptor Gain	0.01	-248 bp
				Donor Gain	0.97	2 bp

Figure C11

Variant Position and SpliceAI Scores

Figure C12

Variant Position and SpliceAI Scores

Figure C13

Variant Position and SpliceAI Scores
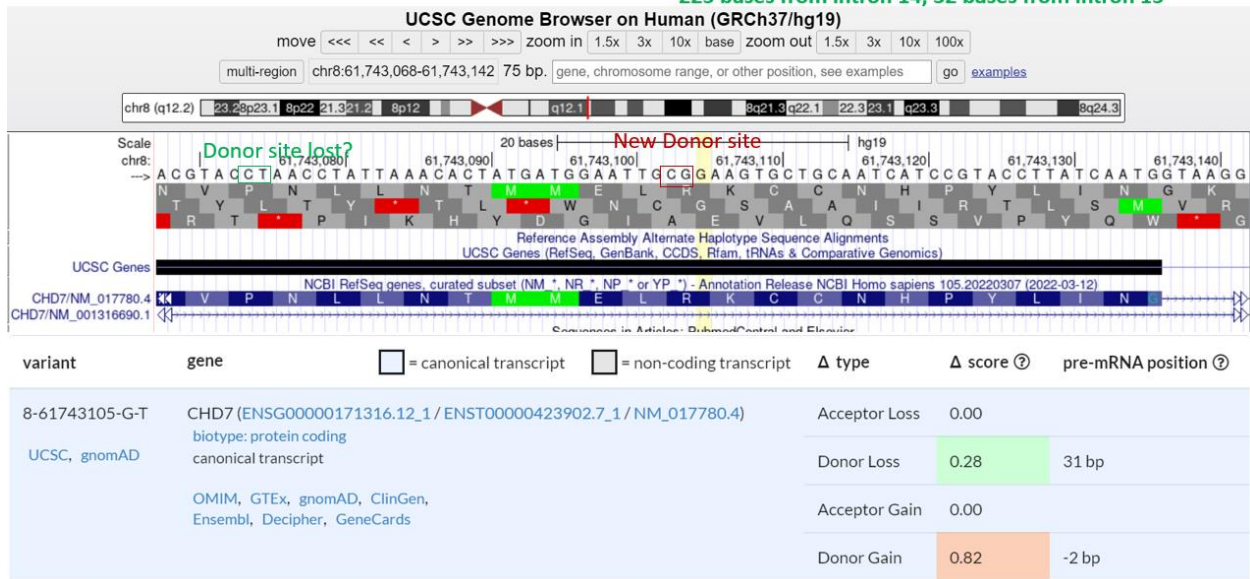
Figure C14

Variant Position and SpliceAI Scores

Figure C15

Variant Position and SpliceAI Scores

Figure C16

Variant Position and SpliceAI Scores

Figure C17

Variant Position and SpliceAI Scores
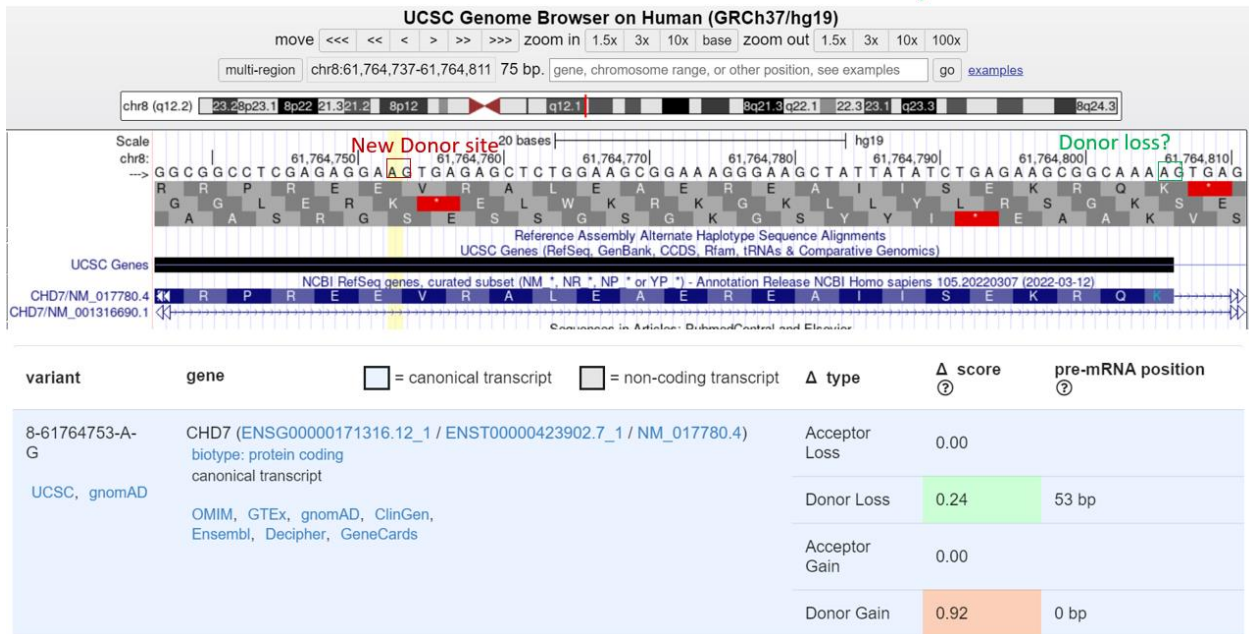
Figure C18

Variant Position and SpliceAI Scores
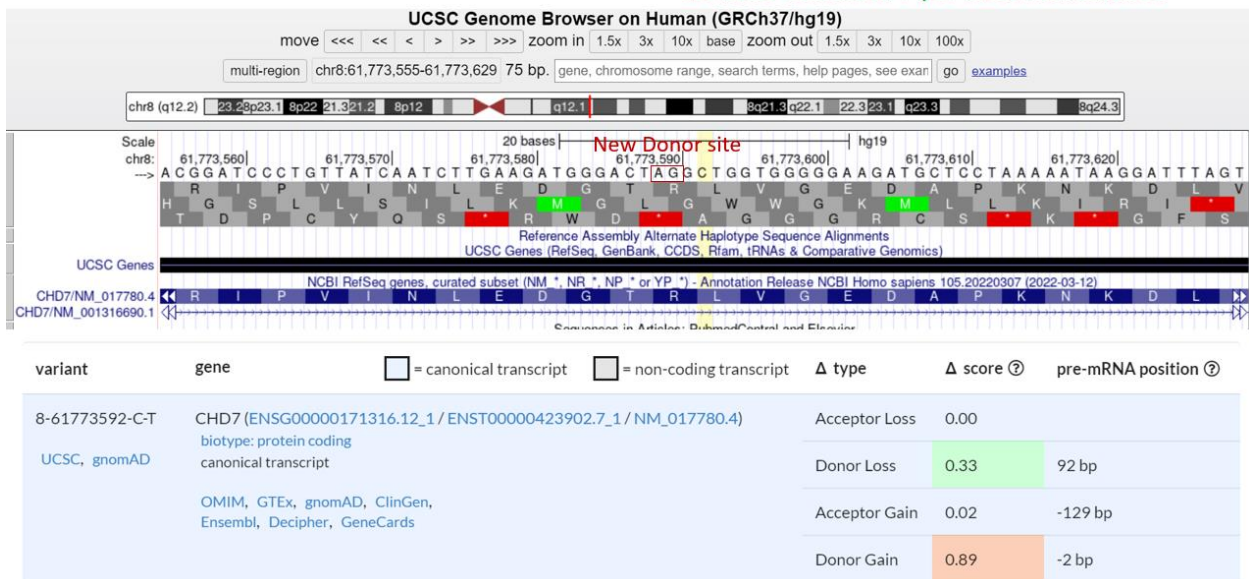
Figure C19

Variant Position and SpliceAI Scores
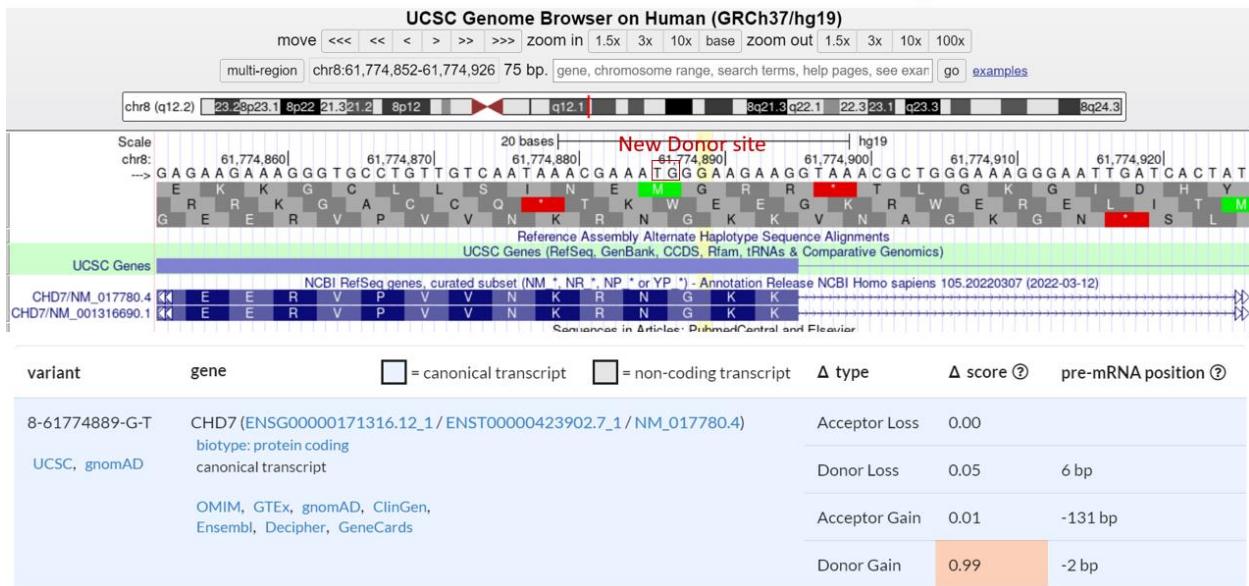
Figure C20

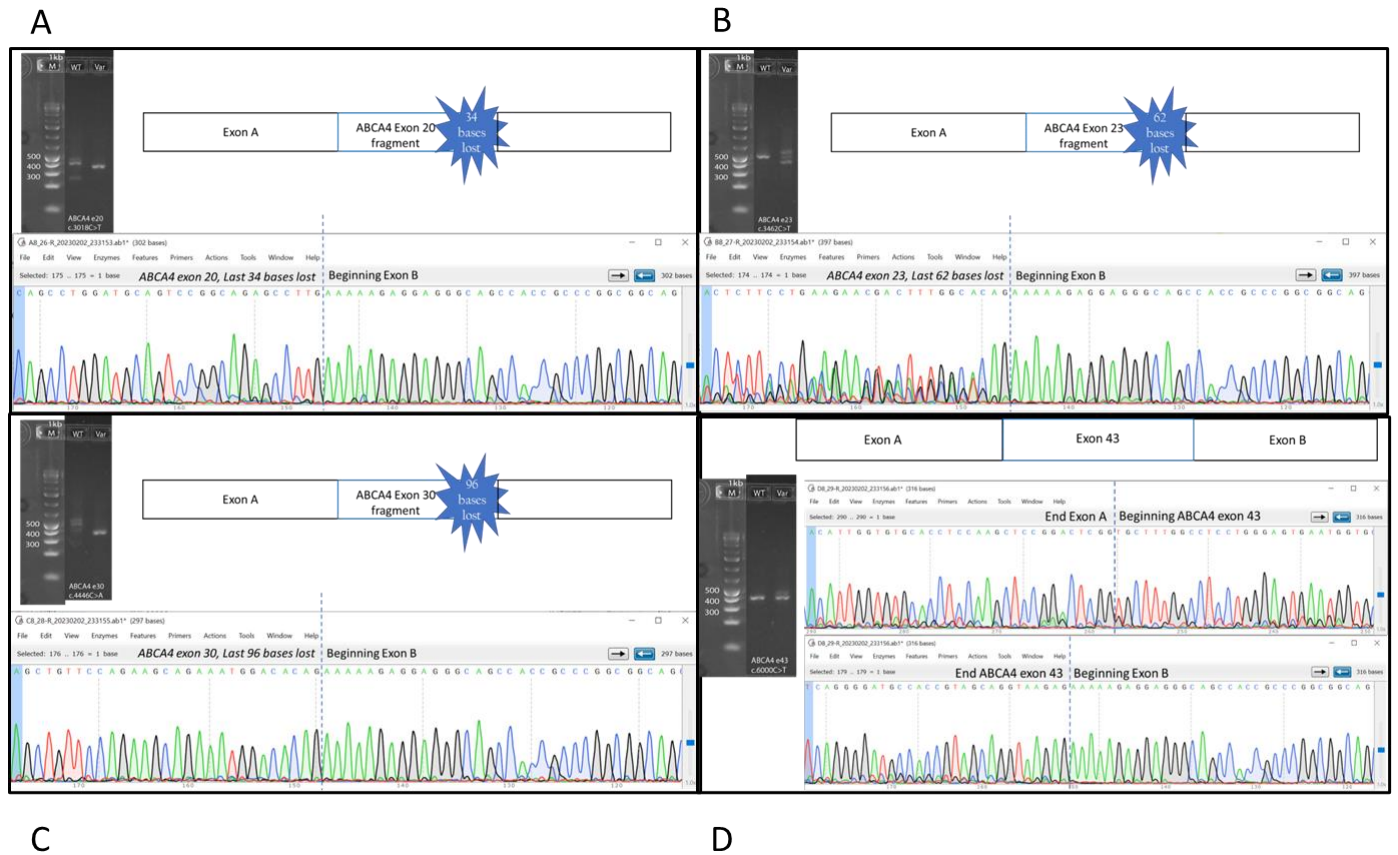*Variant Position and SpliceAI Scores*
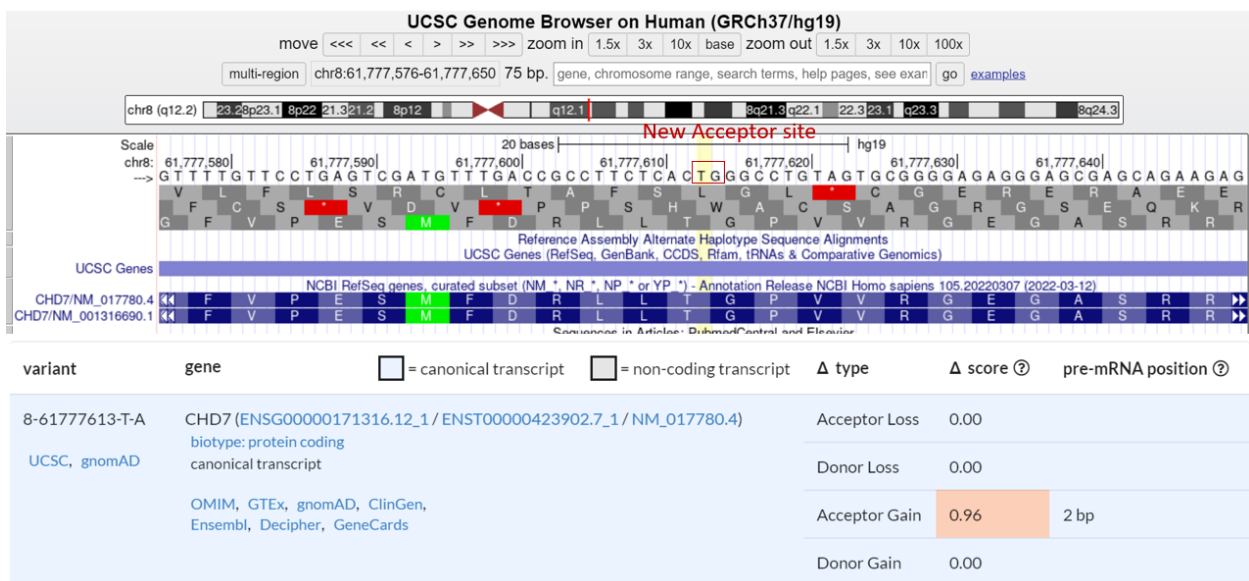
Figure C21

Minigene Outcomes
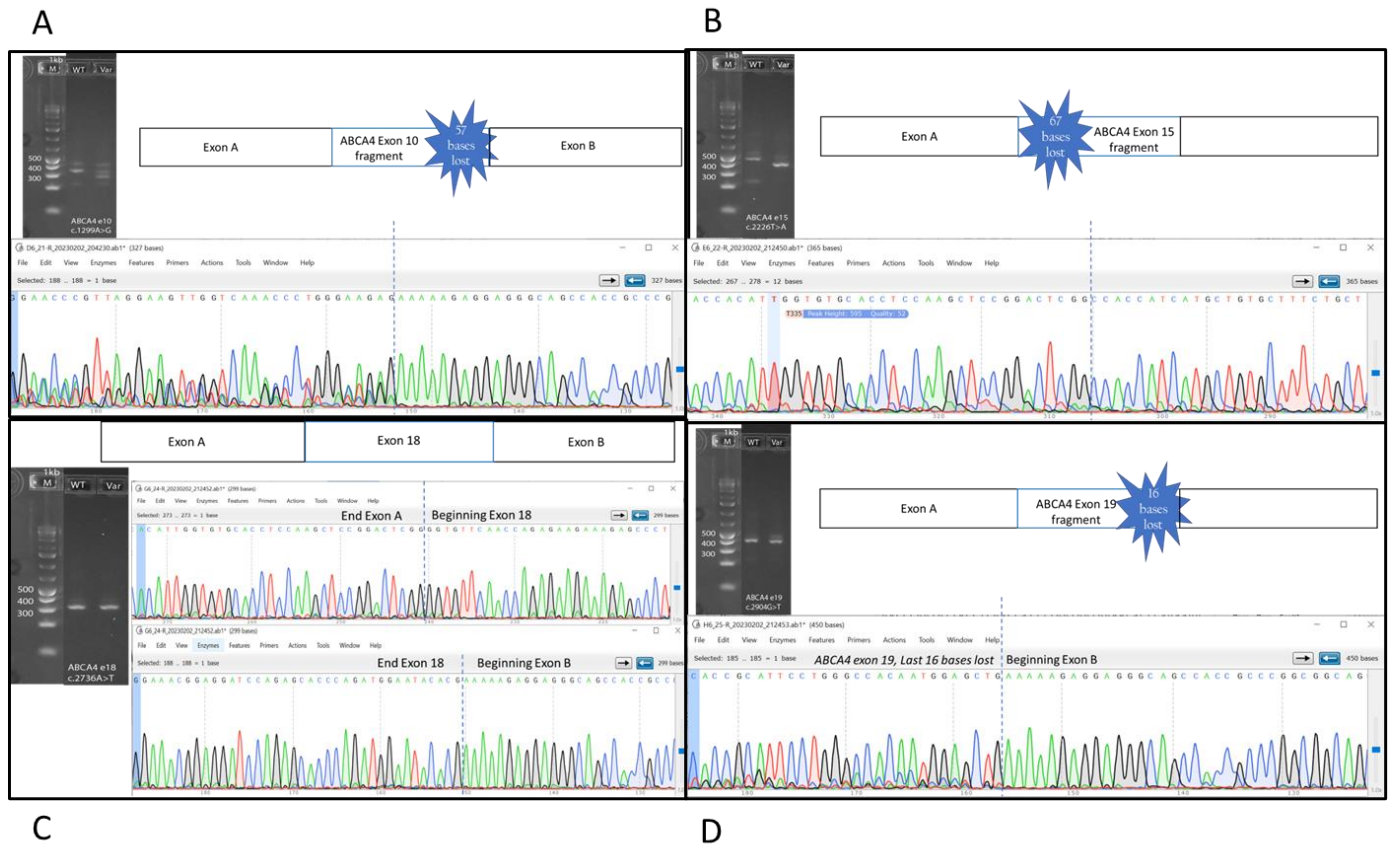
Note. Each panel includes a gel image of the wildtype and variant minigene sample on the left, a schematic of the splice outcome on the right, and the sequencing tracing on the bottom; **A**: ABCA4:c.1299A>G:p.E433=, depicts a loss of 57 bases; **B**: ABCA4:c.2226T>A:p.T742=, depicts a loss of 67 bases; **C**: ABCA4:c.2736A>T:p.G912=, shows the variant produces a normal transcript; **D**: ABCA4:c.2904G>T:p.G968=, depicts a loss of 16 bases.
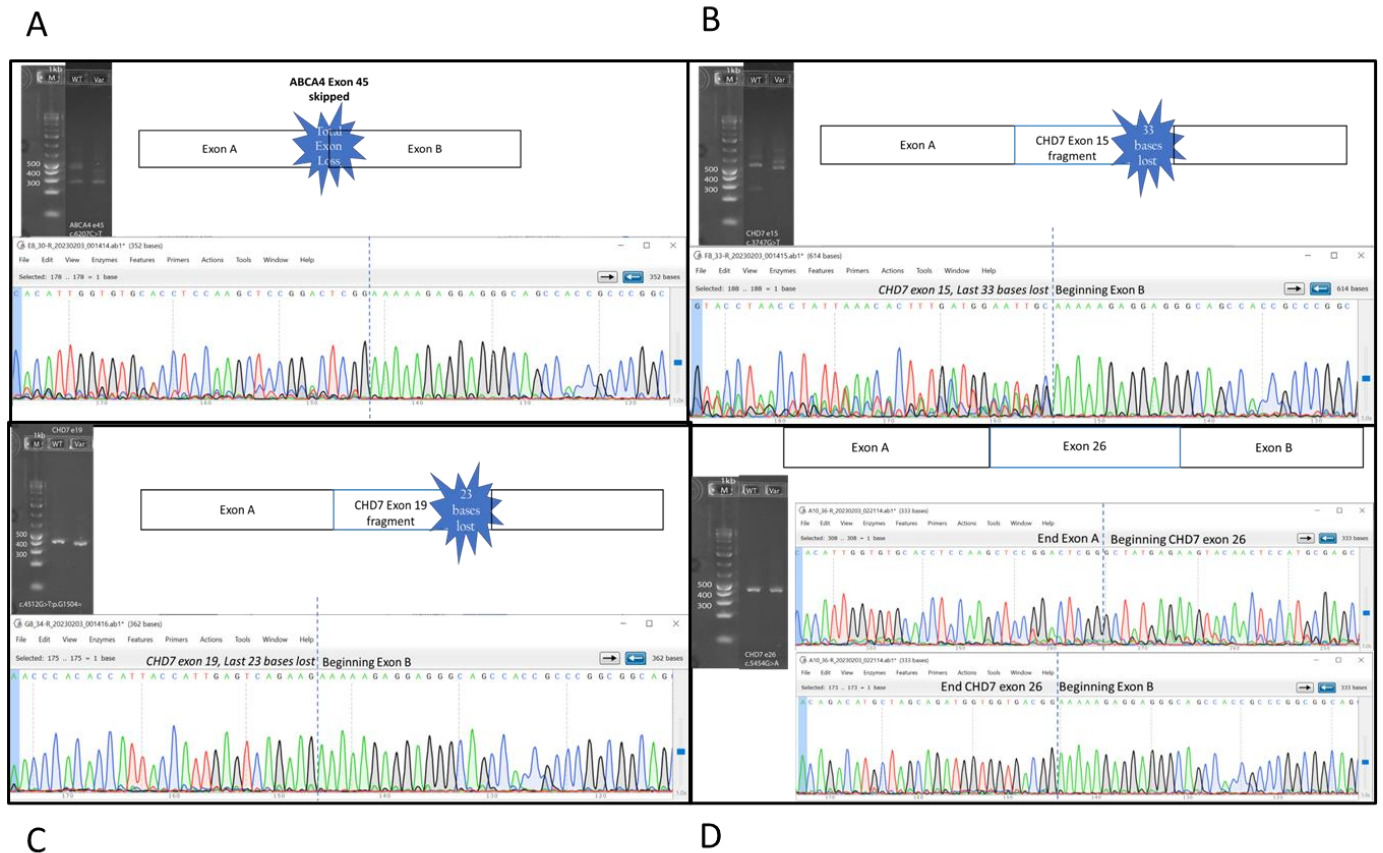
Figure C22

Minigene Outcomes

Note. Each panel includes a gel image of the wildtype and variant minigene sample on the left, a schematic of the splice outcome on the right, and the sequencing tracing on the bottom; **A**: ABCA4:c.3018C>T:p.G1006=, depicts a loss of 34 bases; **B**: ABCA4:c.3462C>T:p.G1154=, depicts a loss of 62 bases; **C**: ABCA4:c.4446C>A:p.V1482=, depicts a loss of 96 bases; **D**: ABCA4:c.6000C>T:p.G2000=, shows the variant produces a normal transcript.
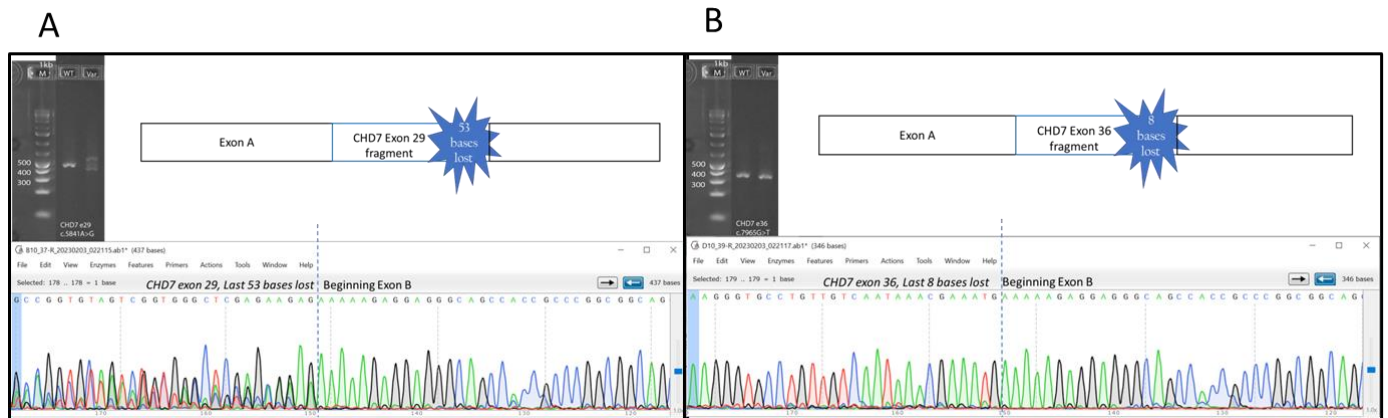
Figure C23

Minigene Outcomes

Note. Each panel includes a gel image of the wildtype and variant minigene sample on the left, a schematic of the splice outcome on the right, and the sequencing tracing on the bottom; **A**: ABCA4:c.6207C>T:p.G2069=, depicts a total loss of exon 45; **B**: ABCA4:c.3747G>T:p.R1249=, depicts a loss of 33 bases; **C**: ABCA4:c.4512G>T:p.G1504=, depicts a loss of 23 bases; **D**: ABCA4:c.5454G>A:p.L1818=, shows the variant produces a normal transcript.

Figure C24

Minigene Outcomes

Note. Each panel includes a gel image of the wildtype and variant minigene sample on the left, a schematic of the splice outcome on the right, and the sequencing tracing on the bottom; **A**: ABCA4:c.5841A>G:p.E1947=, depicts a loss of 53 bases; **B**: ABCA4:c.7965G>T:p.G2655=, depicts a loss of 8 bases.

Dr. Melissa Reeves (Ph.D., M.S., MB[CM]) is a Technical Laboratory Manager at the National Eye Institute, National Institutes of Health. She has a Bachelor of Science degree in Biology from Virginia Commonwealth University, a Master of Science degree in Genetics from George Washington University, a certification in Molecular Biology through the American Society for Clinical Pathology, and a Ph.D. in Health Related Science from Virginia Commonwealth University. Dr. Reeves has served as a clinical trial coordinator for the National Ophthalmic Genotyping and Phenotyping Network, eyeGENE®, for 15 years. She oversees the clinical laboratory operations and quality management for the NEI Ophthalmic Genomics Laboratory. She serves as an NEI Safety Committee representative for the Ophthalmic Genetics and Visual Function Branch to ensure laboratory safety in the branch and as an NEI Contracting Officer level I. She also serves on the American College of Medical Genetics and Genomics Economics of Genetic Services Committee and the board for the American Society for Clinical Laboratory Science, Virginia Chapter. Recent publications are as follows:

- Goetz, K. E., Reeves, M. J., Gagadam, S., Blain, D., Bender, C., Lwin, C., Naik, A., Tumminia, S. J., & Hufnagel, R. B. (2020). Genetic testing for inherited eye conditions in over 6,000 individuals through the eyeGENE network. *American journal of medical genetics. Part C, Seminars in medical genetics*, *184*(3), 828–837. https://doi.org/10.1002/ajmg.c.31843

- Reeves, M. J., Goetz, K. E., Guan, B., Ullah, E., Blain, D., Zein, W. M., Tumminia, S. J., & Hufnagel, R. B. (2020). Genotype-phenotype associations in a large PRPH2-related retinopathy cohort. *Human mutation*, *41*(9), 1528–1539. https://doi.org/10.1002/humu.24065

- Gao, J., D'Souza, L., Wetherby, K., Antolik, C., Reeves, M., Adams, D. R., Tumminia, S., & Wang, X. (2017). Retrospective analysis in oculocutaneous albinism patients for the 2.7 kb deletion in the *OCA2* gene revealed a co-segregation of the controversial variant, p.R305W. *Cell & bioscience*, *7*, 22. https://doi.org/10.1186/s13578-017-0149-3

- Parrish, R. S., Garafalo, A. V., Ndifor, V., Goetz, K. E., Reeves, M. J., Yim, A., Cooper, R. C., Iano-Fletcher, J., Wang, X., & Tumminia, S. J. (2016). Sample Confirmation Testing: A Short Tandem Repeat-Based Quality Assurance and Quality Control Procedure for the eyeGENE Biorepository. *Biopreservation and biobanking*, *14*(2), 149–155. https://doi.org/10.1089/bio.2015.0098

- Sullivan, L. S., Bowne, S. J., Reeves, M. J., Blain, D., Goetz, K., Ndifor, V., Vitez, S., Wang, X., Tumminia, S. J., & Daiger, S. P. (2013). Prevalence of mutations in eyeGENE probands with a diagnosis of autosomal dominant retinitis pigmentosa. *Investigative ophthalmology & visual science*, *54*(9), 6255–6261. https://doi.org/10.1167/iovs.13-12605

- Goetz, K. E., Reeves, M. J., Tumminia, S. J., & Brooks, B. P. (2012). eyeGENE(R): a novel approach to combine clinical testing and researching genetic ocular

disease. *Current opinion in ophthalmology*, *23*(5), 355–363. https://doi.org/10.1097/ICU.0b013e32835715c9